We thank the reviewers for their careful evaluation of our manuscript and constructive suggestions. Below are our point-by-point responses to the two reviewers' comments followed by the revised manuscript and supplement. Our responses are given in normal fonts and the reviewers' comments are given in italic fonts. Line numbers in red refer to the revised manuscript, while line numbers in black refer to the original manuscript under review. Changes in revised manuscript are also highlighted in red color.

Response to Reviewer #1

We thank the reviewer for evaluating our manuscript and giving constructive suggestions for improvement. Following the reviewer' suggestions, we have revised our manuscript correspondingly. Listed below are our point-by-point responses given in normal font and the reviewer's comments are given in italic font.

In this work, Li et al. investigated the reactive uptake coefficients of O3, NO3 and OH onto thin film of surrogate organic aerosols (OA) species over a troposphere-relevant temperature range. The underlying hypothesis is that the temperature induced change in phase state of the studied chemicals will impact the uptake kinetics of atmospheric oxidants onto OA and consequentially the degradation rate of OA. This was clearly shown from the measurement of uptake coefficient that took place in a temperature-controlled flow reactor with inner wall coated with the studied OA surrogate species. The phase state changes were supported by poke-flow experiments. The measured uptake coefficients onto the thin film were extended to estimate the temperature dependent particle degradation fraction (DF) for studied species/binary mixture as 200 nm particles. Atmospheric implications were drawn that the lifetimes of OA are expected to be longer against heterogeneous oxidation due to a liquid-to-solid or semi-solid to solid phase transition that slows down the reactions. The overall experimentations were well thought and designed to minimize effects that can impact the accurate determination of reaction kinetics. The results were presented in high quality and discussed in detail with appropriate reference to the literature for data interpretation and comparison. Some specific comments provided below:

1. Could authors give more background to justify the choice of canola oil, levoglucosan and glucose as OA surrogates and the choice of paired oxidant as well?

Our choices of OA surrogate compounds were motivated by the fact of examining compounds that are representative of OA and for which the phase state properties are known. The choices of gas-phase radicals and oxidants include typical species of the polluted and background atmosphere to reflect oxidation processes close to the source region and during atmospheric transport, where NO_3 is representative of nighttime oxidation processes and OH and O_3 of daytime processes.

Canola oil (CA) is a mixture of multiple saturated and unsaturated fatty acids, however, dominated by unsaturated oleic and linoleic acid. Those species are prevalent components of both marine and terrestrial organic aerosol (Kawamura et al., 2003;Schauer et al., 2002;Limbeck and Puxbaum, 1999) and constitute a major anthropogenic source of OA in urban environments from cooking (Liu et al., 2017;Allan et al., 2010;Rogge et al., 1991;Zahardis and Petrucci, 2007). Daytime photochemical aging of these compounds is simulated by studying the reaction with O_3 and OH oxidants.

Levoglucosan (LEV) is applied in this study to reflect OA from biomass burning stemming from the pyrolysis of cellulose and hemicellulose products (Schauer et al., 2001;Iinuma et al., 2007). This reflects OA from natural sources such as forest fires and anthropogenic sources such as from heating and cooking. Sugars,

such as glucose (GLU), can serve as tracers to characterize and apportion primary biogenic organic aerosols (PBOAs) (Samaké et al., 2019;Zhu et al., 2015). Previous studies, including our own, have indicated very slow oxidation reaction kinetics against O_3 (Knopf et al., 2011). To reflect urban day- and nighttime oxidation of these OA and its chemical transformation during long-range transport, we investigated the multiphase chemical kinetics involving NO_3 and OH radicals reflecting nighttime and daytime chemistry, respectively.

We will add the following sentences to the manuscript:
Line 105 (Line 108): "CA is a mixture of multiple saturated and unsaturated fatty acids, however, dominated by unsaturated oleic and linoleic acid, and serves as OA surrogate for both marine and terrestrial organic aerosol including anthropogenic emissions like cooking (Kawamura et al., 2003;Rogge et al., 1991;Schauer et al., 2002;Limbeck and Puxbaum, 1999;Liu et al., 2017).LEV serves as a surrogate for biomass burning aerosol (BBA) including natural sources such as forest fires and anthropogenic sources such as heating and cooking BBA (Schauer et al., 2001;Iinuma et al., 2007). Glucose (GLU) can serve as a tracer to characterize and apportion primary biogenic organic aerosols (PBOAs) (Samaké et al., 2019;Zhu et al., 2015). XYL and HEX are used in compounds mixtures to modify the glass transition temperature, thus, condensed-phase viscosity. O_3 and OH radicals reflect typical gas oxidants present in photochemically active regions and during long-range transport. NO_3 radicals reflect an effective oxidant participating in the nighttime chemistry of typically polluted regions (Finlayson-Pitts and Pitts Jr, 1999;Brown et al., 2006).

2. There are no clear indications on the morphologies of films before being poked. Please consider adding these images to help interpret the images including those in the SI. Are the films for all individual species and mixtures supposed to be transparent before poking?

In general, all examined films were transparent and, considering a magnification of 230, appeared to have a smooth surface. When solidifying the film substrate, we try to avoid crystallization, which would result in a poly-crystalline surface distinctly different from film images presented here. The look of the images depends on the focal point and the thickness of the substrate. We focused on the film surface (except Fig. S4, image 2) to monitor the flow of the substrate to estimate phase state. When the film is thicker than the focal depth or the focal point is further away from the film surface, the substrate holder (i.e., the surface of the silver block in the temperature-controlled cooling stage) is barely- or non-visible, e.g., Fig. 3. If the film is thinner or the focal point is further within the substrate, you may see structures which stem from scratches in the sample holder, e.g., Figs. S2 and S3. (Recall, film is on thin glass slide on top of sample holder). Hence, the morphology of the substrate before poking is the area of the substrate not affected by the poking and potential shattering. For example, in the image of Fig. 3A at 10s, the area around the dent reflects the film surface properties as imaged by the microscope. The slightly darker shades within the imaged area do not represent any surface morphology but the unfocused scratches from the silver substrate holder beneath the film. Same with figures in supplement, however, in some of those cases, one can see the scratches in the sample holder.

To clarify this issue, we add the following sentences:
Line 187 (Line 199): "Images of the film substrate are recorded at 230 magnification and the depth of field of the 10X objective is 15.9 μm."
Line 192 (Line 206): "Images were recorded with the film surface in focus to monitor the flow of the organic substrate and to probe film viscosity. Under the applied resolution, all film substrates appeared to be smooth and transparent."

Line 208 (Line 223): “The area around the dent reflects the smooth morphology of the film substrate before poking it. The slightly darker shades within the imaged area do not represent any morphology features but the unfocused scratches from the silver substrate holder beneath the film.”

Supplement, line 79 (line 79): “Structures in Figs. S2-S7 that are not in focus are from minor superficial scratches of the silver sample holder within the temperature-controlled cooling stage.”

3. Line 224, would the Tg pred agree better with Tg exp if 10%-16% residual water was accounted for in the calculation? This will help to support the argument here.

If 10%-16% residual water is considered, using Gordon-Taylor equation, the predicted $T_g^{pred,water}$ would be lower than our experimentally determined T_g^{exp}. Comparing values of $T_g^{pred,water}$ and T_g^{exp} yields for LEV 210 K and 243 K, for GLU 241 K and 273 K, for LEV/XYL 207 K and 238 K, and for GLU/HEX 216 K and 248 K, respectively. Hence, about 30 K in difference would be observed. This prediction assumes that the residual water is homogeneously distributed within the substrate. However, we suggest that this discrepancy is due to our substrate film preparation process where under slow drying (evaporation), the outermost layers of the film contain less water than the deeper layers. The outermost layers adjust quicker to the targeted phase state, potentially forming a core-shell configuration where the outer shell can display higher viscosity than the core/bulk. The focus in our poke-flow experiments is solely on the substrate surface, thus monitoring the substrate flow that is governed by the film viscosity closest representing the desired conditions. This effect will not impact the interpretation of our findings since, even in the case of a liquid substrate, the reacto-diffusive length is on the nanometer scale (Shiraiwa et al., 2011;Slade and Knopf, 2014;Lee and Wilson, 2016;George and Abbatt, 2010), much shorter than the overall depth of the substrate.

We add the following information to the text:
Line 224 (Line 243): “If 10%-16% residual water is considered while using Gordon-Taylor equation, T_g^{pred} would be roughly 30 K lower than T_g^{exp}, assuming the residual water is homogeneously distributed in the film. This discrepancy is very likely due to our substrate film preparation process where under slow drying (evaporation), the outermost layers of the film contain less water than the deeper layers. Thus, the substrate surface represents closer the experimental conditions. Furthermore, the microscope focus in our poke-flow experiments is on the substrate surface, thereby monitoring the substrate morphology that is governed by the film viscosity closest representing the desired conditions.”

4. In Section “Atmospheric implications” and “Conclusions”, author should probably note that when coupled with higher ambient relative humidity the estimated temperature dependent DF using uptake coefficient derived from dry experiments may be underestimated for hygroscopic species like levoglucosan and glucose. Some discussions in this regard and directions for future studies could be added.

The reviewer is correct. We add to the Atmospheric Implications section:
Line 466 (Line 499): “The presence of water vapor will significantly impact the phase state, in particular, of hygroscopic species such as LEV and GLU (Zobrist et al., 2008;Koop et al., 2011;Mikhailov et al., 2009), where increasing humidity yields lower condensed-phase viscosity and, in turn, faster reaction kinetics (Slade and Knopf, 2014;Slade et al., 2017;Davies and Wilson, 2015). Neglecting this effect will lead to an underestimation of DF.”

For the Conclusions section, we will add:
Line 495 (Line 540): “This study did not address the role of water vapor acting as a plasticizer concurrent to phase changes induced by temperature changes (Zobrist et al., 2008;Koop et al., 2011;Mikhailov et al., 2009). The role of humidity on amorphous phase state and resulting multiphase kinetics has been studied at room temperature (Shiraiwa et al., 2011;Slade and Knopf, 2014;Davies and Wilson, 2015;Li et al., 2018). Most of these studies suggest that increasing humidity leads to faster reactive uptake kinetics. However, at lower temperatures, diffusivity is slower leading to kinetically hindered adjustments of the condensed-phase state (Berkemeier et al., 2014;Knopf et al., 2018;Charnawskas et al., 2017;Wang et al., 2012). Future experimental studies should focus on how the coupled effects of ambient temperature and humidity on the amorphous phase state of OA particles modulate the multiphase oxidation kinetics.

Technical Notes: 1. Font types of header and numbers in Table S4-Table S6 are not consistent.
This has been corrected.

References

Allan, J. D., Williams, P. I., Morgan, W. T., Martin, C. L., Flynn, M. J., Lee, J., Nemitz, E., Phillips, G. J., Gallagher, M. W., and Coe, H.: Contributions from transport, solid fuel burning and cooking to primary organic aerosols in two UK cities, Atmos. Chem. Phys., 10, 647-668, http://doi.org/10.5194/acp-10-647-2010, 2010.

Berkemeier, T., Shiraiwa, M., Pöschl, U., and Koop, T.: Competition between water uptake and ice nucleation by glassy organic aerosol particles, Atmos. Chem. Phys., 14, 12513-12531, http://doi.org/10.5194/acp-14-12513-2014, 2014.

Brown, S. S., Ryerson, T. B., Wollny, A. G., Brock, C. A., Peltier, R., Sullivan, A. P., Weber, R. J., Dube, W. P., Trainer, M., Meagher, J. F., Fehsenfeld, F. C., and Ravishankara, A. R.: Variability in nocturnal nitrogen oxide processing and its role in regional air quality, Science, 311, 67-70, http://doi.org/10.1126/science.1120120, 2006.

Charnawskas, J. C., Alpert, P. A., Lambe, A. T., Berkemeier, T., O'Brien, R. E., Massoli, P., Onasch, T. B., Shiraiwa, M., Moffet, R. C., Gilles, M. K., Davidovits, P., Worsnop, D. R., and Knopf, D. A.: Condensed-phase biogenic-anthropogenic interactions with implications for cold cloud formation, Faraday Discuss., 200, 165-194, http://doi.org/10.1039/c7fd00010c, 2017.

Davies, J. F., and Wilson, K. R.: Nanoscale interfacial gradients formed by the reactive uptake of OH radicals onto viscous aerosol surfaces, Chem. Sci., 6, 7020-7027, http://doi.org/10.1039/c5sc02326b, 2015.

Finlayson-Pitts, B. J., and Pitts Jr, J. N.: Chemistry of the upper and lower atmosphere: theory, experiments, and applications, Academic, San Diego, 969 pp., 1999.

George, I. J., and Abbatt, J. P.: Heterogeneous oxidation of atmospheric aerosol particles by gas-phase radicals, Nat. Chem., 2, 713-722, http://doi.org/10.1038/nchem.806, 2010.

Iinuma, Y., Bruggemann, E., Gnauk, T., Muller, K., Andreae, M. O., Helas, G., Parmar, R., and Herrmann, H.: Source characterization of biomass burning particles: The combustion of selected European conifers, African hardwood, savanna grass, and German and Indonesian peat, J. Geophys. Res., 112, http://doi.org/10.1029/2006jd007120, 2007.

Kawamura, K., Ishimura, Y., and Yamazaki, K.: Four years' observations of terrestrial lipid class compounds in marine aerosols from the western North Pacific, Global Biogeochem. Cycles, 17, http://doi.org/10.1029/2001gb001810, 2003.

Knopf, D. A., Forrester, S. M., and Slade, J. H.: Heterogeneous oxidation kinetics of organic biomass burning aerosol surrogates by O_3, NO_2, N_2O_5, and NO_3, Phys. Chem. Chem. Phys., 13, 21050-21062, http://doi.org/10.1039/c1cp22478f, 2011.

Knopf, D. A., Alpert, P. A., and Wang, B.: The Role of Organic Aerosol in Atmospheric Ice Nucleation: A Review, ACS Earth Space Chem., 2, 168-202, http://doi.org/10.1021/acsearthspacechem.7b00120, 2018.
Koop, T., Bookhold, J., Shiraiwa, M., and Pöschl, U.: Glass transition and phase state of organic compounds: dependency on molecular properties and implications for secondary organic aerosols in the atmosphere, Phys. Chem. Chem. Phys., 13, 19238-19255, http://doi.org/10.1039/c1cp22617g, 2011.
Lee, L., and Wilson, K.: The reactive-diffusive Length of OH and ozone in model organic aerosols, J. Phys. Chem. A, 120, 6800-6812, http://doi.org/10.1021/acs.jpca.6b05285, 2016.
Li, Z., Smith, K. A., and Cappa, C. D.: Influence of relative humidity on the heterogeneous oxidation of secondary organic aerosol, Atmos. Chem. Phys., 18, 14585-14608, http://doi.org/10.5194/acp-18-14585-2018, 2018.
Limbeck, A., and Puxbaum, H.: Organic acids in continental background aerosols, Atmos. Environ., 33, 1847-1852, http://doi.org/10.1016/s1352-2310(98)00347-1, 1999.
Liu, T. Y., Li, Z. J., Chan, M. N., and Chan, C. K.: Formation of secondary organic aerosols from gas-phase emissions of heated cooking oils, Atmos. Chem. Phys., 17, 7333-7344, http://doi.org/10.5194/acp-17-7333-2017, 2017.
Mikhailov, E., Vlasenko, S., Martin, S. T., Koop, T., and Pöschl, U.: Amorphous and crystalline aerosol particles interacting with water vapor: conceptual framework and experimental evidence for restructuring, phase transitions and kinetic limitations, Atmos. Chem. Phys., 9, 9491-9522, http://doi.org/10.5194/acp-9-9491-2009, 2009.
Rogge, W. F., Hildemann, L. M., Mazurek, M. A., Cass, G. R., and Simonelt, B. R. T.: Souces of fine organic aerosol. 1. Charbroilers and meat cooking operations, Environ. Sci. Technol., 25, 1112-1125, http://doi.org/10.1021/es00018a015, 1991.
Samaké, A., Jaffrezo, J. L., Favez, O., Weber, S., Jacob, V., Albinet, A., Riffault, V., Perdrix, E., Waked, A., Golly, B., Salameh, D., Chevrier, F., Oliveira, D. M., Bonnaire, N., Besombes, J. L., Martins, J. M. F., Conil, S., Guillaud, G., Mesbah, B., Rocq, B., Robic, P. Y., Hulin, A., Le Meur, S., Descheemaecker, M., Chretien, E., Marchand, N., and Uzu, G.: Polyols and glucose particulate species as tracers of primary biogenic organic aerosols at 28 French sites, Atmos. Chem. Phys., 19, 3357-3374, http://doi.org/10.5194/acp-19-3357-2019, 2019.
Schauer, J. J., Kleeman, M. J., Cass, G. R., and Simoneit, B. R. T.: Measurement of emissions from air pollution sources. 3. C-1-C-29 organic compounds from fireplace combustion of wood, Environ. Sci. Technol., 35, 1716-1728, http://doi.org/10.1021/es001331e, 2001.
Schauer, J. J., Kleeman, M. J., Cass, G. R., and Simoneit, B. R. T.: Measurement of emissions from air pollution sources. 5. C-1-C-32 organic compounds from gasoline-powered motor vehicles, Environ. Sci. Technol., 36, 1169-1180, http://doi.org/10.1021/es0108077, 2002.
Shiraiwa, M., Ammann, M., Koop, T., and Pöschl, U.: Gas uptake and chemical aging of semisolid organic aerosol particles, Proc. Nat. Acad. Sci. U.S.A., 108, 11003-11008, http://doi.org/10.1073/pnas.1103045108, 2011.
Slade, J. H., and Knopf, D. A.: Multiphase OH oxidation kinetics of organic aerosol: The role of particle phase state and relative humidity, Geophys. Res. Lett., 41, 5297-5306, http://doi.org/10.1002/2014gl060582, 2014.
Slade, J. H., Shiraiwa, M., Arangio, A., Su, H., Pöschl, U., Wang, J., and Knopf, D. A.: Cloud droplet activation through oxidation of organic aerosol influenced by temperature and particle phase state, Geophys. Res. Lett., 44, 1583-1591, http://doi.org/10.1002/2016gl072424, 2017.
Wang, B. B., Lambe, A. T., Massoli, P., Onasch, T. B., Davidovits, P., Worsnop, D. R., and Knopf, D. A.: The deposition ice nucleation and immersion freezing potential of amorphous secondary organic aerosol: Pathways for ice and mixed-phase cloud formation, J. Geophys. Res., 117, http://doi.org/10.1029/2012jd018063, 2012.

Zahardis, J., and Petrucci, G. A.: The oleic acid-ozone heterogeneous reaction system: products, kinetics, secondary chemistry, and atmospheric implications of a model system - a review, Atmos. Chem. Phys., 7, 1237-1274, http://doi.org/10.5194/acp-7-1237-2007, 2007.
Zhu, C. M., Kawamura, K., and Kunwar, B.: Organic tracers of primary biological aerosol particles at subtropical Okinawa Island in the western North Pacific Rim, J. Geophys. Res., 120, 5504-5523, http://doi.org/10.1002/2015jd023611, 2015.
Zobrist, B., Marcolli, C., Pedernera, D. A., and Koop, T.: Do atmospheric aerosols form glasses?, Atmos. Chem. Phys., 8, 5221-5244, http://doi.org/10.5194/acp-8-5221-2008, 2008.

Response to Reviewer #2

We thank the reviewer for taking the time to carefully evaluate our manuscript and for the constructive comments. We feel that the comments improved the presentation of our study. Following the reviewer's suggestions, we have revised our manuscript correspondingly.

Summary

The manuscript by Li et al. used both experimental techniques and different mode simulations (including a viscosity model and a reaction kinetics model) to systematically understand the influence of temperature on the multiphase reactive process of O_3, NO_3, and OH on levoglucosan, xylitol, glucose, 1,2,3-hexanetriol, and canola oil mixtures. The authors carefully designed a flow tube reactor to measure the reactive uptake coefficient, γ, of these three gas phase species with organic thin films from 213 to 293 K. The results suggest that the phase state of the organic compounds at cooler temperatures in the upper troposphere could heavily impact the multiphase reactions and the lifetime of the organic aerosols.

The experimental section and the kinetic model sections of the manuscript are well done. The results are very important to help understand the multiphase process under low temperature regimes. The interpretation of the experimental data is a little bit unclear and overstated and should be corrected in the revision. With the following points being addressed, this manuscript is suitable to be published in Atmospheric Chemistry and Physics.

We thank the reviewer for the general positive evaluation.

Major Comments

1. The author measured the reactive uptake coefficients of several species for residence times between 2 ms to 100 ms. Is the residence time safe to extrapolate the experimentally derived reactive uptake coefficients to ambient conditions where the residence time of the particles can be much longer? Shiraiwa et al. (2011) shows that the reactive uptake coefficients of ozone can vary significantly depending on the residence time. Can the author discuss about the potentially effects of short residence times in the manuscript?

We believe there is a misunderstanding between the residence time in the flow reactor (i.e., reaction time) and the oxidant exposure. For example, at a fixed injector position, we can expose a substrate film for an hour, but the residence time of the gas oxidant is still in milliseconds. Hence, the interpretation comparing residence time with exposure time discussed in Shiraiwa et al. (2011) is misleading. We have previously discussed the relevance of the exposure time on the reaction mechanisms by applying a kinetic flux model (Arangio et al., 2015;Shiraiwa et al., 2012).

The concentrations of gas-phase oxidants applied in this study are around 10^{12}, 10^{10} and 10^{8} molecules cm^{-3} for O_3, NO_3, and OH, respectively. This corresponds to 40, 0.4 and 0.004 ppb at 293 K and 1 atm, which are representative of or close to typical atmospheric concentrations as discussed in section 2.2 entitled "Oxidant formation, detection and flow conditions". As outlined in the Supplement, application of these concentrations does not lead to a surface saturation effect on the derived kinetics. However, as outlined in Fig. 10, significant surface oxidation of OA can occur over typical exposure time periods in the atmosphere.

In the case of OH oxidation, our analysis supports that the oxidation reaction with a semi-solid or solid organic substrate is confined to the surface under applied OH concentrations for long time periods (Arangio et al., 2015). Related studies also indicate that, in the case of a liquid substrate, the reacto-diffusive length is on the order of nanometers (Slade and Knopf, 2014;George and Abbatt, 2010;Lee and Wilson, 2016;Shiraiwa et al., 2011). In the case of NO_3 oxidation of a solid substrate, we cannot rule out that under longer exposure as encountered in the atmosphere, bulk reaction processes may also play a role, thereby changing the reactivity as we have shown previously (Shiraiwa et al., 2012). In the case of O_3 oxidation of liquid and solid organic substrates, the results by Shiraiwa et al. (2011) indicate that the reactivity of O_3 oxidation decreases with exposure time. Therefore, in the cases of NO_3 and O_3 oxidation, we probably underestimate the chemical lifetime.

We add to the section "Atmospheric Implications"
Line 456 (Line 483): For OH oxidation, previous studies indicate that the oxidation reaction is confined to near the surface of a liquid or solid organic substrate, even for longer OH exposure periods at lower OH concentrations (Slade and Knopf, 2014;George and Abbatt, 2010;Lee and Wilson, 2016;Shiraiwa et al., 2011). However, whether bulk processes may significantly change the reactivity under long oxidant exposure as encountered in the atmosphere still needs to be examined. In the case of O_3 and NO_3 oxidation of organic substrates, the results by Shiraiwa et al. (2011) and Shiraiwa et al. (2012) indicate that the reactive uptake coefficients decrease with increasing exposure. Therefore, we probably underestimate the chemical lifetime.

2. The trends of the γ values as a function of temperature are really interesting and it shows strong heterogeneity among different species. The authors seem to imply in the manuscript that phase state change is the dominant reason for γ values to change (line 18, line 484-485, line 496-497). However, Shiraiwa et al. (2011&2012) demonstrate that if the organic species change their phase state from liquid to glass, the mass accommodation coefficients will change by orders of magnitude rather than just 34 times. Could the authors comment on the discrepancy between previous modeling results showing the uptake could change by orders of magnitude vs. the current experimental data showing the γ values only change up to a factor of 34?

With respect to the surface accommodation coefficient, Shiraiwa and Seinfeld (2012) present a theoretical sensitivity study on how this coefficient impacts the equilibration timescale of SOA gas-particle partitioning. Therefore, this research is not directly relevant for interpretation of our experimentally derived reactive uptake coefficients. Shiraiwa et al. (2011) discriminates between the surface and bulk mass accommodation coefficient being 1 and 10^{-5} for the entirety of their experiments including the presence of different substrate phase states. Hence, there is no change in their accommodation coefficients but after a certain exposure time period the reactive uptake coefficient is lower than the bulk mass accommodation coefficient. We cannot derive the mass accommodation coefficients directly from the experimental data, but it is reasonable to assume that the surface mass accommodation coefficient is around 1 as well. However, since our reactive uptake coefficients are greater than in the study by Shiraiwa et al. (2011), the bulk mass accommodation coefficient is likely also larger.

Regarding to the variation of the reactive uptake coefficient with the phase change, we observed about one order in magnitude change in the reactivity towards O_3 when the substrate phase state changes from liquid to solid. This is in agreement with the observations by Shiraiwa et al. (2011), Steimer et al. (2015), and Berkemeier et al. (2016), besides the direct comparison with the study by de Gouw and Lovejoy (1998). Overall, we observe very similar changes in the multiphase chemical kinetics.

With carefully designed experiments, I do believe the γ values the authors presented are accurate, but I think the data interpretation part is a little bit overstated to conclude phase state is the main reason for γ to change. The authors need to discuss more why γ values did not decrease as fast as previous modeling results (Shiraiwa et al., 2011&2012) shown when the viscosity changes. For instance, could the desorption lifetime (line 331) help increase γ values as temperature decreases? I think it is important to discuss these aspects in the paper to show that maybe both phase state and the desorption kinetics play important, but counter roles, with the role of the phase state dominating the γ value during this process.

As discussed above, the observed change in O_3 reactivity with phase state is similar to previous studies. The role of the desorption lifetime in multiphase chemical kinetics and its dependence is yet not resolved. Desorption lifetime is assumed as a constant on the order of nanoseconds in most recent modeling studies (Berkemeier et al., 2016;Arangio et al., 2015;Shiraiwa et al., 2012;Shiraiwa et al., 2011). For OH oxidation, we have discussed the importance of the desorption lifetime in Arangio et al. (2015). In this manuscript that focuses on the experimental results, we do not want to add too much speculation. Application of a kinetic flux model as in our previous studies (Shiraiwa et al., 2012;Arangio et al., 2015;Springmann et al., 2009;Kaiser et al., 2011) could assist in furthering this discussion in the future. We have included the importance of desorption lifetime and its potential counter role at several places in the manuscript including the conclusions, e.g., lines 321, 331 and 489. Although we cannot quantify the effect of the desorption lifetime on the observed kinetics, the greatest changes in reactivity commence when the substrate undergoes a phase transition.

3. The authors performed the poke-flow technique that was used in other papers to determine the glass transition temperatures of organic species. However, past literature on poke-flow technique were mostly used to determine the viscosity of the organic species and glass shattering phenomenon can indicate the viscosity is anywhere >10^{12} Pa s (Lindsay et al. 2013), but does not necessarily mean the viscosity is exactly near 10^{12} Pa s when the compound is right around glass transition. The accuracy of the glass transition temperature derived from this technique will heavily impact data interpretation in Fig. 7-9. Given that the T_g values shown in Table 1 do not match the T_g values from literature (and the author also mentioned these compounds may have water in them, so it is difficult to compare the T_g values with pure compounds from the literature), can the author provide any evidence to consistently show that the poke-flow technique can be used to derived accurate T_g values? Given there hasn't been studies before using observation on glass shattering to solely determine the glass transition temperature, maybe the author can cross compare with previous data to validate this technique (such as Koop et al. 2010, Dette et al. 2015).

First, we want to emphasize that we clearly mentioned in the manuscript at line 182 and 185, our poke-flow technique is a semi-quantitative method to probe the phase transition of applied substrate films within the investigated temperature range. We do not know any study that has probed and controlled such a large organic substrate for oxidation kinetics experiments. The poke-flow technique gives us the means to ascertain or rule out specific phase states. We do not claim that we can measure accurately the continuous viscosity change of applied substrates. Although, when looking at revised Table 1 (given below) that includes the uncertainty of literature values of T_g and T_g predictions, we achieve agreement or close agreement with those values.

We agree with the reviewer that the glass shattering phenomenon only indicates that the viscosity is >10^{12} Pa s. To minimize this uncertainty, we measure T_g as the highest temperature when shattering occurs. For example, if the GLU substrate films were poked at 276 K and 273 K, and the shattering phenomenon did not occur at 276 K but at 273 K, we know that the viscosity is smaller than 10^{12} Pa s at 276 K but larger

than 10^{12} Pa s at 273 K. Of course, if we poke the same film at 270 K, the shattering occurs, and the viscosity will probably be larger than 10^{12} Pa s at this temperature. Therefore, we assign the shattering of the substrate film a viscosity of 10^{12} Pa s at the highest determined temperature. We will make an additional remark in the manuscript to point out this uncertainty:
Line 219 (Line 236): "Viscosity greater than 10^{12} Pa s indicates the presence of a glassy phase. Thus, we ascribe the observed shattering of the substrate film a viscosity of 10^{12} Pa s, although the exact value cannot be assessed with the poke-flow technique."

We revised Table 1 and changed the main text accordingly:
We changed line 220 (Line 239):

" T_g^{pred} is derived from the Gordon Taylor equation (Gordon and Taylor, 2007) assuming no residual water in the organic mixture. Since T_g determination depends on cooling or drying rates, we do not expect agreement with literature values or predicted values. For most investigated substrates, our estimated T_g^{exp} is lower than either T_g^{lit} or T_g^{pred}. This is consistent with the notion that our substrates contain some residual water that lowers T_g."
To

" T_g^{pred} for substrate mixtures is derived from the Gordon Taylor equation (Gordon and Taylor, 2007) assuming literature T_g values and no residual water present. The uncertainties in T_g^{pred} values are derived by Gaussian error propagation. Except for the GLU substrate film, we achieve agreement or close agreement with either T_g^{lit} or T_g^{pred}. Since T_g determination depends on cooling or drying rates, we do not expect agreement with literature values or predicted values."

To address the issue of residual water, this is followed by text in response to reviewer #1 (Line 243):
"In addition, if 10%-16% residual water is considered while using Gordon-Taylor equation, T_g^{pred} would be roughly 30 K lower than T_g^{exp}, assuming the residual water is homogeneously distributed in the film. This discrepancy is very likely due to our substrate film preparation process where under slow drying (evaporation), the outermost layers of the film contain less water than the deeper layers. Thus, the substrate surface represents closer the experimental conditions. Furthermore, the microscope focus in our poke-flow experiments is on the substrate surface, thereby monitoring the substrate morphology that is governed by the film viscosity closest representing the desired conditions."

The new Table 1 reads:

Table 1. Estimated T_g of the applied substrate films. T_g^{exp} is the measured T_g using the poke-flow technique. T_g^{lit} is the literature reported T_g. T_g^{pred} is predicted T_g for mixtures by Gordon-Taylor equation using T_g^{lit} and k_{GT}. k_{GT} is solute specific constant in the Gordon-Taylor equation. *D* is fragility.

Substrate	T_g^{exp} / K	T_g^{pred} / K	T_g^{lit} / K	k_{GT}	*D*
Levoglucosan (LEV)	243 ± 4		248 ± 2 [a,h,g]	3.26[a]	14.1[b]
Xylitol (XYL)			249 ± 7 [f,g,i]	2.1[c]	8.65[b]
LEV/XYL	238 ± 3	249 ± 5			11.3[d]
Glucose (GLU)	273 ± 3		305 ± 13 [e,g,j]	3.95[e]	12.1[b]

1,2,6-Hexanetriol (HEX)			204 ± 6 [f,g,i]	0.88[e]	13.16[f]
GLU/HEX	248 ± 3	252 ± 7			12.3[d]

[a] Lienhard et al. (2012). [b] DeRieux et al. (2018). [c] Elamin et al. (2012). [d] Interpolated values based on mass fraction. [e]Zobrist et al. (2008). [f] Nakanishi et al. (2011). [g] Rothfuss (2019). [h] Tombari and Johari (2015). [i]Dorfmüller et al. (1979). [j] Diogo and Ramos (2008).

4. What is the relative humidity of the flow tube when the experiments were performed? Given the author performed the flow experiments under a variety of low temperatures, even small partial pressure of water could potential lead to relatively high humidity and alter the phase state of the organic film and increase the error bar range of the estimated viscosity. Another related question is that the poke flow measurement also was performed under "sealed room air" (line 190). The water vapor in the room air may lead to near high relative humidity at cooler temperatures. How would the authors ensure the RH levels in the flow tube and the poke flow cooling state are the same and don't lead to errors in estimating the phase state?

The reviewer is correct that miniscule amounts of water vapor could lead to high humidity levels in the flow reactor at low temperatures. All experiments were conducted under dry conditions. Extra care has been taken as described in our experimental section (section 2.2, line 141). We apply a carbon filter (Supelco, Superlcarb HC) and a Drierite cold trap cooled with liquid nitrogen or an ethanol/dry ice mixture to purify all the ultra-high purity (UHP) gases, such as N_2, He and O_2, which yields insignificant water partial pressures. The system is a vacuum system and thus leakage of room air resulting in water vapor contamination can be excluded.

Also, for the poke flow experiments, as discussed in section 2.3 line 190, the organic substrate film placed within the cooling stage is sealed against room air during the entire poking process, residing in a dry N_2 atmosphere. Only pure N_2 gas from a liquid nitrogen container is purged into the cooling stage to keep a positive pressure environment. Therefore, this measure excludes contamination of water vapor from room air.
We will change the sentence on line 190 (line 203)
"In the cooling stage the organic film sample is sealed against room air during the entire poking process."
To
"In the cooling stage, the organic film sample is sealed against room air and resides in an atmosphere of dry N_2 at positive pressure during the entire poking process."

5. The author used "slight changes in viscosity" (line 330) and "small changes in viscosity" (line 491) multiple times in the manuscript to describe viscosity change as temperature drops. However, the changes in viscosity during semi-solid phase state spans over several orders of magnitude (Figure 4) and I would not consider these changes small. In fact, these changes could be even larger than the phase state transition from liquid to semi-solid. This leads to my question when viscosity changes a few orders of magnitude from liquid to semi-solid, it seems the uptake coefficients are still the same.

We agree with this statement of the reviewer and we will re-phrase these statements. We want to clarify how we interpret the data regarding the uptake coefficients change little although viscosity changes by several orders of magnitude. Please recall our point above that the poke-flow technique is a semi-quantitative approach. However, we can, rather accurately, determine the glassy and liquid phase state

of the substrate but not the changes in between these extreme points. We observe that the greatest changes in the reactive uptake occur when the substrate phase changes from solid or semi-solid to liquid. This is evident for O_3 and OH reacting with canola oil and for NO_3 reacting with the LEV/XYL mixture and to a lesser extent for OH reacting with the GLU/HEX mixture. For those observations, without a detailed model, we cannot assign a definitive change in viscosity. Figure 4 serves as guidance only and will need further investigation. We observe that the reactive uptake does not change significantly when the substrate is in the solid and semi-solid phase regime. This is the case for NO_3 uptake by LEV and OH uptake by GLU. Literature data depicted in Fig. 4 demonstrates that LEV and GLU substrate films indeed do not transition into the liquid phase in the experimentally probed temperature range. Hence, although viscosity changes by several orders of magnitude in the semi-solid regime, the self-diffusion of organic molecules and characteristic mixing time scales are, even at lowest viscosity, similar and longer than typical experimental times, thereby contributing to a lesser impact on the reactive uptake. Therefore, the reactivity changes less in this regime than it does from a semi-solid to liquid phase.

We will change the sentence on line 330 (line 354):
"The slight increase of γ with temperature may due to the slight change in substrate viscosity (see Fig. 4), the counteracting effect of the temperature dependence of the reaction rate (Atkinson et al., 2006) and the desorption lifetime (Pöschl et al. 2007)."
to
"The slight increase of γ with temperature may be due to the combined effects of changes in substrate viscosity (see Fig. 4), the counteracting effect of the temperature dependence of the reaction rate (Atkinson et al., 2006) and the desorption lifetime (Pöschl et al., 2007). Assessment of these various impacts on the observed uptake kinetics necessitates an in-depth analysis, e.g., by application of kinetic flux modeling (Shiraiwa et al., 2012;Arangio et al., 2015)."

We change the sentence on line 491 (line 536):
"Small changes in viscosity with temperature may also play a role in the overall heterogeneous kinetics when the substrate is in a semi-solid phase state."
To
"Changes in substrate viscosity with temperature may also play a role in the overall heterogeneous kinetics when the substrate is in a semi-solid phase state."

6. The logical deductions of how phase state alters γ values are a bit confusing and somewhat contradictory in multiple parts of the manuscript. For instance, line 339 shows the largest change of γ is observed around the expected Tg for LEV/XYL film, showing a transition from semi-solid to glass regime has the maximum influence of γ. However, in the next sentence, the author made a contradictory comment (line 340-341), saying "significant change in NO_3 uptake reactivity in the investigated temperature range can be attributed to the transition of a liquid to a highly viscous or solid substrate film". The similar statement appeared in line 351-352 saying that "the lower sensitivity of γ on temperature may be due to the generally higher viscosity" of the compound studied. Again, in line 358-400 the authors state that the γ is less sensitive to temperature change when canola is in semi-solid/glass phase states. If the γ change is less obvious, then why would the author observe the largest change of γ around Tg for LEV/XYL film?

We agree with the reviewer's assessment that our statements can cause confusion. In general, we meant that the largest changes in γ are observed above the expected T_g (e.g., line 339). This may have caused confusion at subsequent instances. We change those sentences accordingly:

Line 339 (Line 364): “The largest change of γ is observed around the expected T_g (Fig. 8b). Therefore, the significant change in NO_3 uptake reactivity in the investigated temperature range can be attributed to the transition of a liquid to a highly viscous or solid substrate film.”
Is changed to
“The largest change of γ is observed above the expected T_g (Fig. 8b). Therefore, the significant change in NO_3 uptake reactivity in the investigated temperature range can be attributed to the transition of a solid or highly viscous to a liquid substrate film.”

Line 338: To avoid repetition, we delete “The observed change in uptake kinetics is attributed to the phase change of the film substrate. ”

Line 351 (Line 375): “Therefore, the lower sensitivity of γ on temperature may be due to the generally higher viscosity compared to a glycerol substrate.”
Is changed to
“We hypothesize that the lesser change in γ with temperature for the LEV/XYL substrate compared to a GLY substrate (Gross et al. 2009), may be due to the viscosity difference between both substrates.”

Line 349: To avoid repetition, we delete “The reason for this difference may lie in the higher viscosity of the LEV/XYL substrate within this temperature range. ”

Line 390 (Line 416): “The major change in γ matches the expected phase change of the GLU/HEX mixture.”
Is changed to
“The major change in γ occurs above the expected T_g of the GLU/HEX mixture.”

Line 396 (Line 422): “γ increases by a factor of ~2.4 between 273 K and 293 K, where the viscosity of canola oil changes from 0.185 to 0.079 Pa s (Fasina et al., 2006).”
Is changed to
“Above the melting point temperature, γ increases by a factor of ~2.4 between 273 K and 293 K, where the viscosity of canola oil changes from 0.185 to 0.079 Pa s (Fasina et al., 2006).”

The authors also compared the γ change with the same amount of temperature change (25 K) at higher temperature regimes (liquid) and lower temperature regimes (semi-solid/solid) in the manuscript. Results show that that γ changes more significantly at higher temperature regimes (liquid). My question is, would the statement still be correct when comparing viscosity change instead of temperature change? I.e., will γ still change more significantly when viscosity changes the same orders of magnitude from liquid to semi-solid vs. semi-solid to glass?

We could plot reactive uptake coefficients as a function of viscosity using data of Fig. 4. However, the viscosity data represents only estimates and as such we refrain from this exercise. In general, we would expect a greater sensitivity of γ on temperature and thus viscosity in the liquid phase regime. The lower the viscosity, the faster the diffusivity and in turn more reactive sites are available. In the semi-solid and solid phase regime, the sensitivity of γ is likely lower, since if the viscosity is sufficiently low and characteristic diffusion time scales are longer than experimental time scales, no difference in reactivity due to phase or viscosity changes may be observed.

We add the following sentences to the section “Conclusions”:

Line 478 (Line 520): “Furthermore, once in the liquid phase, as temperature increases viscosity decreases and diffusivity increases, leading to potentially strong increases in reactivity.”

Line 481 (Line 524): “Although viscosity in the semi-solid phase regime can change substantially with temperature, viscosity can still be too high to allow for significant bulk processes to play a role.”

7. The reactive uptake data as a function of temperature from this manuscript is very insightful since there have not been such data available at low temperature. Results also show that change of γ as a function of temperature is drastically different when it comes to different organic species. For instance, OH oxidation of GLU/HEX mix and NO3 oxidation of LEV is not sensitive to temperature while OH and O3 oxidation oxidations of canola oil are more sensitive to temperature change. Can the author discuss further in the manuscript why different species exhibit difference in γ value changes? Given the strong heterogeneity of how the γ values of different compounds respond to temperature change, can the author still make the conclusions that “chemical reactivity of organic matter towards atmospheric oxidants can vary significantly in response to ambient temperature”, as the ambient OA may have a different response of γ towards temperature than the organic surrogate compounds used in this study?

In response to “*. Can the author discuss further in the manuscript why different species exhibit difference in γ value changes?”.* We have not discussed this point in our conclusion section. However, in the discussion section, we explored the differences in reactivity of the examined gas-substrate systems. Based on gas-phase reaction kinetics, we expect different reaction pathways for the systems studied. For example, O_3 will preferably react with a double bond, and OH and NO_3 abstract a hydrogen. As deduced from gas-phase chemistry, different reaction systems will show different reaction rates and different dependencies with temperature. See for example the decrease in reactivity with increasing temperature for the reaction of glucose with OH. We will add these points in the atmospheric implication section. In addition to this, we have to deal with the effect of phase state on reactivity (analogously to pressure dependence of gas-phase kinetics). For each substrate, the viscosity variation with temperature change is different, and thus the diffusion coefficients of organic molecules and gas oxidants can be quite different.

Regarding the second point of the reviewer. Yes, it still holds that “*chemical reactivity of organic matter towards atmospheric oxidants can vary significantly in response to ambient temperature”*. If we assume multiphase and multicomponent particles with complex composition and morphology (Laskin et al., 2016;Laskin et al., 2019), which can potentially lead to matrix effects and phase separation (Lignell et al., 2014;Lee and Wilson, 2016;Charnawskas et al., 2017;Bertram et al., 2011), clearly, the applied single and binary substrate films are insufficient to describe these scenarios. However, OA can only cycle between solid and liquid phase states, and the temperature and humidity under which these phase changes occur will depend on organic compounds and the presence of the plasticizer (i.e., water, sulfates, etc.) (Mikhailov et al., 2009;Virtanen et al., 2010;Koop et al., 2011;Reid et al., 2018). For example, Shiraiwa et al. (2017) estimates that the majority of SOA particles transition from liquid to solid with increasing altitude (and decreasing temperature) independent of the particles’ chemical complexity. Our multiphase chemistry experiments cover a broad temperature range and corresponding range of phase states typically encountered in the atmosphere and thus can provide useful estimates and atmospheric implications. We agree with the reviewer and we will add the issue of heterogeneity to our conclusions section.

We add to the section “Atmospheric Implications”:
Line 466 (Line 502):

"This discussion neglects the chemical complexity of ambient OA where different condensed-phase species can result in different reactivities and reaction pathways (Zhang et al., 2015;Surratt et al., 2010;Ziemann and Atkinson, 2012;Knopf et al., 2005;Davies and Wilson, 2015). Those in turn can change the multiphase kinetics and its dependency on temperature and particle phase state. Furthermore, heterogeneous particle composition and morphology can result in matrix effects or liquid-liquid phase separation, where, e.g., more reactive organic species are shielded by less reactive species (Lignell et al., 2014;Lee and Wilson, 2016;Charnawskas et al., 2017;Bertram et al., 2011). Those effects were not assessed in this study but necessitate additional experimental investigations.

In the section "Conclusions" we add:
Line 497 (Line 549):
"Ambient OA, however, display greater chemical and morphological complexity (Laskin et al., 2016;Laskin et al., 2019), and as such we expect varying multiphase reaction pathways having different reactivity towards atmospheric gas-phase oxidants which will translate into different reactivity dependencies on temperature and phase state. Despite this caveat, due to lower temperatures at higher altitudes, we can expect OA particles during transport in the free troposphere to have significantly longer lifetimes with respect to chemical degradation."

Minor Comments

1. Line 287: The equation doesn't seem to be right. Why would the diffusion coefficient to the left side of the equation be in the numerator, but the diffusion coefficients to the right side of the equation be in the denominator? Could the authors please double check?

Thank you for pointing this out. It is a typo; we forgot to take the "inverse" and is corrected as below (line 311):

$$D_{\mathrm{X}} = \left(\frac{P_{\mathrm{He}}}{D_{\mathrm{X-He}}} + \frac{P_{\mathrm{O_2}}}{D_{\mathrm{X-O_2}}}\right)^{-1}$$

2. The literature citation in the introduction part is good overall, but missed some recent important publications that are highly relevant to this study. Please include those citations for a more comprehensive introduction.

The reviewer points out many nice and important publications to be cited in the introduction. We really appreciate these suggestions and will include some of those articles. However, there are several that, although important studies, we will not include. The reason is that we want to keep the focus on relevant studies that discuss the oxidation kinetics between the investigated gaseous oxidants (i.e., O_3, NO_3 and OH) and organic substrates. This already resulted in 137 references. To not further distract the reader, we reference studies on SOA formation, gas-particle partitioning, photochemical aging studies, or reactive uptake studies of other gas species only in a very limited manner. Some of the not directly relevant studies are covered by the referenced review articles.

Line 40 (Line40): please add the following two papers that are relevant. Murray, B. J., T. W. Wilson, S. Dobbie, Z. Cui, S. M. R. K. Al-Jumur, O. Mohler, M. Schnaiter, R. Wagner, S. Benz, M. Niemand, H. Saathoff, V. Ebert, S. Wagner and B. Karcher (2010). "Heterogeneous nucleation of ice particles on glassy aerosols under cirrus conditions." Nature Geosci 3(4): 233-237.

We will add the cited Murray et al. (2010) study and the study by Wang et al. (2012) showing the ice nucleation ability of glassy SOA or SOA surrogate particles.

Pöschl, U. and M. Shiraiwa (2015). "Multiphase Chemistry at the Atmosphere–Biosphere Interface Influencing Climate and Public Health in the Anthropocene." Chemical Reviews 115(10): 4440-4475.

We have already cited this paper on line 31, line 53 and line 487 in the manuscript. We do not feel we need to add it to this list.

Line 42 (Line 42): please add the following two papers that are relevant.
Renbaum-Wolff, L., J. W. Grayson, A. P. Bateman, M. Kuwata, M. Sellier, B. J. Murray, J. E. Shilling, S. T. Martin and A. K. Bertram (2013). "Viscosity of α-pinene secondary organic material and implications for particle growth and reactivity." Proceedings of the National Academy of Sciences 110(20): 8014-8019.

This paper has been cited in line 185. We will also add this reference on line 42.

Kidd, C., V. Perraud, L. M. Wingen and B. J. Finlayson-Pitts (2014). "Integrating phase and composition of secondary organic aerosol from the ozonolysis of α-pinene." Proceedings of the National Academy of Sciences 111(21): 7552-7557.

We will add this reference.

Line 44-45 (Line 45): please include the following two papers that are relevant.
Dette, H. P. and T. Koop (2015). "Glass Formation Processes in Mixed Inorganic/Organic Aerosol Particles." The Journal of Physical Chemistry A 119(19): 4552-4561.

Zhang, Y., L. Nichman, P. Spencer, J. I. Jung, A. Lee, B. K. Heffernan, A. Gold, Z. Zhang, Y. Chen, M. R. Canagaratna, J. T. Jayne, D. R. Worsnop, T. B. Onasch, J. D. Surratt, D. Chandler, P. Davidovits and C. E. Kolb (2019). "The Cooling Rate- and Volatility-Dependent Glass-Forming Properties of Organic Aerosols Measured by Broadband Dielectric Spectroscopy." Environmental Science & Technology 53(21): 12366-12378.

We will include these two references.

Line 47 (Line 47-48): please include the following three papers that are relevant
Rothfuss, N. E. and M. D. Petters (2016). "Coalescence-based assessment of aerosol phase state using dimers prepared through a dual-differential mobility analyzer technique." Aerosol Science and Technology 50(12): 1294-1305.

Zhang, Y., M. S. Sanchez, C. Douet, Y. Wang, A. P. Bateman, Z. Gong, M. Kuwata, L. Renbaum-Wolff, B. B. Sato, P. F. Liu, A. K. Bertram, F. M. Geiger and S. T. Martin (2015). "Changing shapes and implied viscosities of suspended submicron particles." Atmos. Chem. Phys. 15(14): 7819-7829.

Jarvinen, E., K. Ignatius, L. Nichman, T. B. Kristensen, C. Fuchs, C. R. Hoyle, N. Hoppel, J. C. Corbin, J. Craven, J. Duplissy, S. Ehrhart, I. El Haddad, C. Frege, H. Gordon, T. Jokinen, P. Kallinger, J. Kirkby, A. Kiselev, K. H. Naumann, T. Petaja, T. Pinterich, A. S. H. Prevot, H. Saathoff, T. Schiebel, K. Sengupta, M. Simon, J. G. Slowik, J. Trostl, A. Virtanen, P. Vochezer, S. Vogt, A. C. Wagner, R. Wagner, C. Williamson, P. M. Winkler,

C. Yan, U. Baltensperger, N. M. Donahue, R. C. Flagan, M. Gallagher, A. Hansel, M. Kulmala, F. Stratmann, D. R. Worsnop, O. Mohler, T. Leisner and M. Schnaiter (2016). "Observation of viscosity transition in α-pinene secondary organic aerosol." Atmos. Chem. Phys. 16(7): 4423-4438.

Here, we only cite studies to show, in general, that the amorphous phase state is modulated by temperature and humidity. There, is no need to cite the suggested very specific studies. In fact, we could just cite only Koop et al. (2011). Hence, we will not include these references.

Line 51 (Line 51-52): please add the following two relevant papers:
Shiraiwa, M. and J. H. Seinfeld (2012). "Equilibration timescale of atmospheric secondary organic aerosol partitioning." Geophysical Research Letters 39(24): L24801.
Renbaum-Wolff, L., J. W. Grayson, A. P. Bateman, M. Kuwata, M. Sellier, B. J. Murray, J. E. Shilling, S. T. Martin and A. K. Bertram (2013). "Viscosity of α-pinene secondary organic material and implications for particle growth and reactivity." Proceedings of the National Academy of Sciences 110(20): 8014-8019.

Shiraiwa and Seinfeld (2012) are referenced in the subsequent sentence. We will move the reference to this place. We will add Renbaum-Wolff et al. (2013).

Line 53 (Line 54-55): please include the following two papers that are relevant:
Gaston, C. J., J. A. Thornton and N. L. Ng (2014). "Reactive uptake of N2O5 to internally mixed inorganic and organic particles: the role of organic carbon oxidation state and inferred organic phase separations." Atmos. Chem. Phys. 14(11): 5693-5707.
Zhang, Y., Y. Chen, A. T. Lambe, N. E. Olson, Z. Lei, R. L. Craig, Z. Zhang, A. Gold, T. B. Onasch, J. T. Jayne, D. R. Worsnop, C. J. Gaston, J. A. Thornton, W. Vizuete, A. P. Ault and J.D. Surratt (2018). "Effect of Aerosol-Phase State on Secondary Organic Aerosol Formation from the Reactive Uptake of Isoprene-Derived Epoxydiols (IEPOX)." Environmental Science & Technology Letters 5(3): 167-174.

We will add those two references.

Line 55 (Line 57): Please add the following paper that is relevant:
Riedel, T. P., Y.-H. Lin, S. H. Budisulistiorini, C. J. Gaston, J. A. Thornton, Z. Zhang, W. Vizuete, A. Gold and J. D. Surratt (2015). "Heterogeneous Reactions of Isoprene-Derived Epoxides: Reaction Probabilities and Molar Secondary Organic Aerosol Yield Estimates." Environmental Science & Technology Letters 2(2): 38-42.

No further citation is need here. We just refer to the definition of the reactive uptake coefficient. Stephen Schwartz developed the mathematical groundwork for the resistor model and Pöschl et al. (2007) introduced the kinetic flux model approach which is consistent with the resistor model.

Line 61 (Line 64): please include the following citations that are highly relevant to the paper:
Pajunoja, A., W. Hu, Y. J. Leong, N. F. Taylor, P. Miettinen, B. B. Palm, S. Mikkonen, D. R. Collins, J. L. Jimenez and A. Virtanen (2016). "Phase state of ambient aerosol linked with water uptake and chemical aging in the southeastern US." Atmos. Chem. Phys. 16(17): 11163-11176.

We will add this reference.

Gaston, C. J., J. A. Thornton and N. L. Ng (2014). "Reactive uptake of N2O5 to internally mixed inorganic and organic particles: the role of organic carbon oxidation state and inferred organic

phase separations." Atmos. Chem. Phys. 14(11): 5693-5707.

Here, we want to place the focus on studies that specifically target multiphase oxidation reactions involving O_3, NO_3, and OH and discuss reaction rates. We cannot include all gas uptake experiments (please see UIPAC reviews on those, e.g., by Ammann et al. (2013) and Crowley et al. (2013) or reviews by Kolb et al. (2010), Davidovits et al. (2006), and other colleagues), gas-partitioning, SOA formation, or photochemical aging studies. Also, those studies are not directly comparable and relevant to the experiments presented here. For these reasons, we do not add this work here but in line 53.

Houle, F. A., A. A. Wiegel and K. R. Wilson (2018). "Predicting Aerosol Reactivity Across Scales: from the Laboratory to the Atmosphere." Environmental Science & Technology 52(23): 13774-13781.

Here we focus experimental studies involving RH effects on kinetics, and thus will not include this article at this place. We already cited this study on line 487 in the conclusion part while mentioning detailed modelling studies.

Zhang, Y., Y. Chen, A. T. Lambe, N. E. Olson, Z. Lei, R. L. Craig, Z. Zhang, A. Gold, T. B. Onasch, J. T. Jayne, D. R. Worsnop, C. J. Gaston, J. A. Thornton, W. Vizuete, A. P. Ault and J. D. Surratt (2018). "Effect of Aerosol-Phase State on Secondary Organic Aerosol Formation from the Reactive Uptake of Isoprene-Derived Epoxydiols (IEPOX)." Environmental Science & Technology Letters 5(3): 167-174.

As discussed above, we keep the main focus on determination of reaction kinetics and on the oxidants examined in this study. For these reasons, we do not add this work.

Riva, M., et al. (2019). "Increasing Isoprene Epoxydiol-to-Inorganic Sulfate Aerosol (IEPOX:Sulfinorg) Ratio Results in Extensive Conversion of Inorganic Sulfate to Organosulfur Forms: Implications for Aerosol Physicochemical Properties." Environmental Science & Technology 53(15): 8682-8694.

As discussed above, we keep the main focus on determination of reaction kinetics and on the oxidants examined in this study. For these reasons, we do not add this work.

Zhang, Y., Y. Chen, Z. Lei, N. E. Olson, M. Riva, A. R. Koss, Z. Zhang, A. Gold, J. T. Jayne, D. R. Worsnop, T. B. Onasch, J. H. Kroll, B. J. Turpin, A. P. Ault and J. D. Surratt (2019). "Joint Impacts of Acidity and Viscosity on the Formation of Secondary Organic Aerosol from Isoprene Epoxydiols (IEPOX) in Phase Separated Particles." ACS Earth and Space Chemistry 3(12): 2646-2658.

As discussed above, we keep the main focus on determination of reaction kinetics and on the oxidants examined in this study. For these reasons, we do not add this work.

DeRieux, W.-S. W., P. S. J. Lakey, Y. Chu, C. K. Chan, H. S. Glicker, J. N. Smith, A. Zuend and M. Shiraiwa (2019). "Effects of Phase State and Phase Separation on Dimethylamine Uptake of Ammonium Sulfate and Ammonium Sulfate–Sucrose Mixed Particles." ACS Earth and Space Chemistry 3(7): 1268-1278.

As discussed above, we keep the main focus on determination of reaction kinetics and on the oxidants examined in this study. For these reasons, we do not add this work.

Line 64 (Line 66): please include the following citation that is relevant:
Arangio, A. M., J. H. Slade, T. Berkemeier, U. Pöschl, D. A. Knopf and M. Shiraiwa (2015). "Multiphase chemical kinetics of OH radical uptake by molecular organic markers of biomass burning aerosols: humidity and temperature dependence, surface reaction, and bulk diffusion." The Journal of Physical Chemistry A 119(19): 4533-4544.

We will add this reference.

Line 70-73: there are other works that also analyzed the effects of phase states on OH oxidation that should be included:
Houle, F. A., A. A. Wiegel and K. R. Wilson (2018a). "Predicting Aerosol Reactivity Across Scales: from the Laboratory to the Atmosphere." Environmental Science & Technology 52(23): 13774-13781.
Houle, F. A., A. A. Wiegel and K. R. Wilson (2018b). "Changes in Reactivity as Chemistry Becomes Confined to an Interface. The Case of Free Radical Oxidation of C30H62 Alkane by OH." The Journal of Physical Chemistry Letters 9(5): 1053-1057.

In this text section we only reference studies that investigate the effect of RH on phase state and reaction kinetics. The cited articles do not discuss this effect.
However, as discussed above, we already cited Houle et al. (2018a) in our conclusion section (Line 532).
We will also cite Houle et al. (2018b) on line 52 (line 55) in the introduction section.

3. The measured Tg values of a few species listed in Table 1 are lower than the value measured by other literature. The author explains that was due to water remaining in the organic compound which lowers the glass transition temperature. If that is the case, it is a bit misleading to still associate the experimentally derived glass transition temperatures with the name of the pure compounds. Maybe the author should add information to highlight that the experimental derived Tg values in Table 1 refers to the mixture of water and organic species.

Please see our response above, revised table, and response to reviewer #1.

4. n-Hexadecane in Table 2 was never mentioned in the main text. Please call out the name. Also, in Table2, a comma should be added between reference number and the γ values

Thank you for pointing this out. Table 2 has been corrected by adding commas.
The literature n-hexadecane results are part of our discussion of LEV and LEV/XYL substrate films, and we now include it. We change the sentence on line 363 (line 387)
"Also, γ of solid LEV and LEV/XYL is similar to NO_3 uptake by solid alkane substrates and monolayers (Knopf et al., 2011;Gross and Bertram, 2009;Moise et al., 2002)."
to
"Also, γ of solid LEV and LEV/XYL is similar to NO_3 uptake by solid alkane substrates and monolayers, e.g. n-hexadecane given in Table 2 (Knopf et al., 2006;Knopf et al., 2011;Gross and Bertram, 2009;Moise et al., 2002)."

References

Allan, J. D., Williams, P. I., Morgan, W. T., Martin, C. L., Flynn, M. J., Lee, J., Nemitz, E., Phillips, G. J., Gallagher, M. W., and Coe, H.: Contributions from transport, solid fuel burning and cooking to primary organic aerosols in two UK cities, Atmos. Chem. Phys., 10, 647-668, http://doi.org/10.5194/acp-10-647-2010, 2010.

Ammann, M., Cox, R. A., Crowley, J. N., Jenkin, M. E., Mellouki, A., Rossi, M. J., Troe, J., and Wallington, T. J.: Evaluated kinetic and photochemical data for atmospheric chemistry: Volume VI - heterogeneous reactions with liquid substrates, Atmos. Chem. Phys., 13, 8045-8228, http://doi.org/10.5194/acp-13-8045-2013, 2013.
Arangio, A. M., Slade, J. H., Berkemeier, T., Pöschl, U., Knopf, D. A., and Shiraiwa, M.: Multiphase chemical kinetics of OH radical uptake by molecular organic markers of biomass burning aerosols: humidity and temperature dependence, surface reaction, and bulk diffusion, J. Phys. Chem. A, 119, 4533-4544, http://doi.org/10.1021/jp510489z, 2015.
Atkinson, R., Baulch, D. L., Cox, R. A., Crowley, J. N., Hampson, R. F., Hynes, R. G., Jenkin, M. E., Rossi, M. J., and Troe, J.: Evaluated kinetic and photochemical data for atmospheric chemistry: Volume II - gas phase reactions of organic species, Atmos. Chem. Phys., 6, 3625-4055, http://doi.org/10.5194/acp-6-3625-2006, 2006.
Berkemeier, T., Shiraiwa, M., Pöschl, U., and Koop, T.: Competition between water uptake and ice nucleation by glassy organic aerosol particles, Atmos. Chem. Phys., 14, 12513-12531, http://doi.org/10.5194/acp-14-12513-2014, 2014.
Berkemeier, T., Steimer, S. S., Krieger, U. K., Peter, T., Pöschl, U., Ammann, M., and Shiraiwa, M.: Ozone uptake on glassy, semi-solid and liquid organic matter and the role of reactive oxygen intermediates in atmospheric aerosol chemistry, Phys. Chem. Chem. Phys., 18, 12662-12674, http://doi.org/10.1039/c6cp00634e, 2016.
Bertram, A. K., Martin, S. T., Hanna, S. J., Smith, M. L., Bodsworth, A., Chen, Q., Kuwata, M., Liu, A., You, Y., and Zorn, S. R.: Predicting the relative humidities of liquid-liquid phase separation, efflorescence, and deliquescence of mixed particles of ammonium sulfate, organic material, and water using the organic-to-sulfate mass ratio of the particle and the oxygen-to-carbon elemental ratio of the organic component, Atmos. Chem. Phys., 11, 10995-11006, http://doi.org/10.5194/acp-11-10995-2011, 2011.
Brown, S. S., Ryerson, T. B., Wollny, A. G., Brock, C. A., Peltier, R., Sullivan, A. P., Weber, R. J., Dube, W. P., Trainer, M., Meagher, J. F., Fehsenfeld, F. C., and Ravishankara, A. R.: Variability in nocturnal nitrogen oxide processing and its role in regional air quality, Science, 311, 67-70, http://doi.org/10.1126/science.1120120, 2006.
Charnawskas, J. C., Alpert, P. A., Lambe, A. T., Berkemeier, T., O'Brien, R. E., Massoli, P., Onasch, T. B., Shiraiwa, M., Moffet, R. C., Gilles, M. K., Davidovits, P., Worsnop, D. R., and Knopf, D. A.: Condensed-phase biogenic-anthropogenic interactions with implications for cold cloud formation, Faraday Discuss., 200, 165-194, http://doi.org/10.1039/c7fd00010c, 2017.
Crowley, J. N., Ammann, M., Cox, R. A., Hynes, R. G., Jenkin, M. E., Mellouki, A., Rossi, M. J., Troc, J., and Wallington, T. J.: Evaluated kinetic and photochemical data for atmospheric chemistry: Volume V - heterogeneous reactions on solid substrates (vol 10, pg 9059, 2010), Atmos. Chem. Phys., 13, 7359-7359, http://doi.org/10.5194/acp-13-7359-2013, 2013.
Davidovits, P., Kolb, C. E., Williams, L. R., Jayne, J. T., and Worsnop, D. R.: Mass accommodation and chemical reactions at gas-liquid interfaces, Chem. Rev., 106, 1323-1354, http://doi.org/10.1021/cr040366k, 2006.
Davies, J. F., and Wilson, K. R.: Nanoscale interfacial gradients formed by the reactive uptake of OH radicals onto viscous aerosol surfaces, Chem. Sci., 6, 7020-7027, http://doi.org/10.1039/c5sc02326b, 2015.
de Gouw, J. A., and Lovejoy, E. R.: Reactive uptake of ozone by liquid organic compounds, Geophys. Res. Lett., 25, 931-934, http://doi.org/10.1029/98gl00515, 1998.
Diogo, H. P., and Ramos, J. J. M.: Slow molecular mobility in the crystalline and amorphous solid states of glucose as studied by thermally stimulated depolarization currents (TSDC), Carbohydr. Res., 343, 2797-2803, http://doi.org/10.1016/j.carres.2008.07.002, 2008.

Dorfmüller, T., Dux, H., Fytas, G., and Mersch, W.: A light scattering study of the molecular motion in hexanetriol 1,2,6, J. Chem. Phys., 71, 366-375, http://doi.org/10.1063/1.438079, 1979.
Fasina, O. O., Hallman, H., Craig-Schmidt, M., and Clements, C.: Predicting temperature-dependence viscosity of vegetable oils from fatty acid composition, J. Am. Oil Chem. Soc., 83, 899-903, http://doi.org/10.1007/s11746-006-5044-8, 2006.
Finlayson-Pitts, B. J., and Pitts Jr, J. N.: Chemistry of the upper and lower atmosphere: theory, experiments, and applications, Academic, San Diego, 969 pp., 1999.
George, I. J., and Abbatt, J. P.: Heterogeneous oxidation of atmospheric aerosol particles by gas-phase radicals, Nat. Chem., 2, 713-722, http://doi.org/10.1038/nchem.806, 2010.
Gordon, M., and Taylor, J. S.: Ideal copolymers and the second-order transitions of synthetic rubbers. i. non-crystalline copolymers, J. Appl. Chem., 2, 493-500, http://doi.org/10.1002/jctb.5010020901, 2007.
Gross, S., and Bertram, A. K.: Products and kinetics of the reactions of an alkane monolayer and a terminal alkene monolayer with NO_3 radicals, J. Geophys. Res., 114, http://doi.org/10.1029/2008jd010987, 2009.
Houle, F. A., Wiegel, A. A., and Wilson, K. R.: Predicting Aerosol Reactivity Across Scales: from the Laboratory to the Atmosphere, Environ. Sci. Technol., 52, 13774-13781, http://doi.org/10.1021/acs.est.8b04688, 2018a.
Houle, F. A., Wiegel, A. A., and Wilson, K. R.: Changes in Reactivity as Chemistry Becomes Confined to an Interface. The Case of Free Radical Oxidation of $C_{30}H_{62}$ Alkane by OH, J. Phys. Chem. Lett., 9, 1053-1057, http://doi.org/10.1021/acs.jpclett.8b00172, 2018b.
Iinuma, Y., Bruggemann, E., Gnauk, T., Muller, K., Andreae, M. O., Helas, G., Parmar, R., and Herrmann, H.: Source characterization of biomass burning particles: The combustion of selected European conifers, African hardwood, savanna grass, and German and Indonesian peat, J. Geophys. Res., 112, http://doi.org/10.1029/2006jd007120, 2007.
Kaiser, J. C., Riemer, N., and Knopf, D. A.: Detailed heterogeneous oxidation of soot surfaces in a particle-resolved aerosol model, Atmos. Chem. Phys., 11, 4505-4520, http://doi.org/10.5194/acp-11-4505-2011, 2011.
Kawamura, K., Ishimura, Y., and Yamazaki, K.: Four years' observations of terrestrial lipid class compounds in marine aerosols from the western North Pacific, Global Biogeochem. Cycles, 17, http://doi.org/10.1029/2001gb001810, 2003.
Knopf, D. A., Anthony, L. M., and Bertram, A. K.: Reactive uptake of O_3 by multicomponent and multiphase mixtures containing oleic acid, J. Phys. Chem. A, 109, 5579-5589, http://doi.org/10.1021/jp0512513, 2005.
Knopf, D. A., Mak, J., Gross, S., and Bertram, A. K.: Does atmospheric processing of saturated hydrocarbon surfaces by NO3 lead to volatilization?, Geophys. Res. Lett., 33, L17816, http://doi.org/10.1029/2006gl026884, 2006.
Knopf, D. A., Forrester, S. M., and Slade, J. H.: Heterogeneous oxidation kinetics of organic biomass burning aerosol surrogates by O_3, NO_2, N_2O_5, and NO_3, Phys. Chem. Chem. Phys., 13, 21050-21062, http://doi.org/10.1039/c1cp22478f, 2011.
Knopf, D. A., Alpert, P. A., and Wang, B.: The Role of Organic Aerosol in Atmospheric Ice Nucleation: A Review, ACS Earth Space Chem., 2, 168-202, http://doi.org/10.1021/acsearthspacechem.7b00120, 2018.
Kolb, C. E., Cox, R. A., Abbatt, J. P. D., Ammann, M., Davis, E. J., Donaldson, D. J., Garrett, B. C., George, C., Griffiths, P. T., Hanson, D. R., Kulmala, M., McFiggans, G., Pöschl, U., Riipinen, I., Rossi, M. J., Rudich, Y., Wagner, P. E., Winkler, P. M., Worsnop, D. R., and O'Dowd, C. D.: An overview of current issues in the uptake of atmospheric trace gases by aerosols and clouds, Atmos. Chem. Phys., 10, 10561-10605, http://doi.org/10.5194/acp-10-10561-2010, 2010.

Koop, T., Bookhold, J., Shiraiwa, M., and Pöschl, U.: Glass transition and phase state of organic compounds: dependency on molecular properties and implications for secondary organic aerosols in the atmosphere, Phys. Chem. Chem. Phys., 13, 19238-19255, http://doi.org/10.1039/c1cp22617g, 2011.
Laskin, A., Gilles, M. K., Knopf, D. A., Wang, B. B., and China, S.: Progress in the Analysis of Complex Atmospheric Particles, in: Annual Review of Analytical Chemistry, Vol 9, edited by: Bohn, P. W., and Pemberton, J. E., Annu. Rev. Anal. Chem., 117-143, http://doi.org/10.1146/annurev-anchem-071015-041521, 2016.
Laskin, A., Moffet, R. C., and Gilles, M. K.: Chemical Imaging of Atmospheric Particles, Acc. Chem. Res., 52, 3419-3431, http://doi.org/10.1021/acs.accounts.9b00396, 2019.
Lee, L., and Wilson, K.: The reactive-diffusive Length of OH and ozone in model organic aerosols, J. Phys. Chem. A, 120, 6800-6812, http://doi.org/10.1021/acs.jpca.6b05285, 2016.
Li, Z., Smith, K. A., and Cappa, C. D.: Influence of relative humidity on the heterogeneous oxidation of secondary organic aerosol, Atmos. Chem. Phys., 18, 14585-14608, http://doi.org/10.5194/acp-18-14585-2018, 2018.
Lignell, H., Hinks, M. L., and Nizkorodov, S. A.: Exploring matrix effects on photochemistry of organic aerosols, Proc. Nat. Acad. Sci. U.S.A., 111, 13780-13785, http://doi.org/10.1073/pnas.1322106111, 2014.
Limbeck, A., and Puxbaum, H.: Organic acids in continental background aerosols, Atmos. Environ., 33, 1847-1852, http://doi.org/10.1016/s1352-2310(98)00347-1, 1999.
Liu, T. Y., Li, Z. J., Chan, M. N., and Chan, C. K.: Formation of secondary organic aerosols from gas-phase emissions of heated cooking oils, Atmos. Chem. Phys., 17, 7333-7344, http://doi.org/10.5194/acp-17-7333-2017, 2017.
Mikhailov, E., Vlasenko, S., Martin, S. T., Koop, T., and Pöschl, U.: Amorphous and crystalline aerosol particles interacting with water vapor: conceptual framework and experimental evidence for restructuring, phase transitions and kinetic limitations, Atmos. Chem. Phys., 9, 9491-9522, http://doi.org/10.5194/acp-9-9491-2009, 2009.
Moise, T., Talukdar, R. K., Frost, G. J., Fox, R. W., and Rudich, Y.: Reactive uptake of NO_3 by liquid and frozen organics, J. Geophys. Res., 107, http://doi.org/10.1029/2001jd000334, 2002.
Murray, B. J., Wilson, T. W., Dobbie, S., Cui, Z. Q., Al-Jumur, S., Mohler, O., Schnaiter, M., Wagner, R., Benz, S., Niemand, M., Saathoff, H., Ebert, V., Wagner, S., and Karcher, B.: Heterogeneous nucleation of ice particles on glassy aerosols under cirrus conditions, Nat. Geosci., 3, 233-237, http://doi.org/10.1038/ngeo817, 2010.
Pöschl, U., Rudich, Y., and Ammann, M.: Kinetic model framework for aerosol and cloud surface chemistry and gas-particle interactions–Part 1: General equations, parameters, and terminology, Atmos. Chem. Phys., 7, 5989-6023, http://doi.org/acp-7-5989-2007, 2007.
Renbaum-Wolff, L., Grayson, J. W., Bateman, A. P., Kuwata, M., Sellier, M., Murray, B. J., Shilling, J. E., Martin, S. T., and Bertram, A. K.: Viscosity of alpha-pinene secondary organic material and implications for particle growth and reactivity, Proc. Nat. Acad. Sci. U.S.A., 110, 8014-8019, http://doi.org/10.1073/pnas.1219548110, 2013.
Rogge, W. F., Hildemann, L. M., Mazurek, M. A., Cass, G. R., and Simonelt, B. R. T.: Souces of fine organic aerosol. 1. Charbroilers and meat cooking operations, Environ. Sci. Technol., 25, 1112-1125, http://doi.org/10.1021/es00018a015, 1991.
Rothfuss, N. E.: Toward Better Characterization of the Viscosity of Organic Aerosol, 2019.
Samaké, A., Jaffrezo, J. L., Favez, O., Weber, S., Jacob, V., Albinet, A., Riffault, V., Perdrix, E., Waked, A., Golly, B., Salameh, D., Chevrier, F., Oliveira, D. M., Bonnaire, N., Besombes, J. L., Martins, J. M. F., Conil, S., Guillaud, G., Mesbah, B., Rocq, B., Robic, P. Y., Hulin, A., Le Meur, S., Descheemaecker, M., Chretien, E., Marchand, N., and Uzu, G.: Polyols and glucose particulate species as tracers of primary biogenic

organic aerosols at 28 French sites, Atmos. Chem. Phys., 19, 3357-3374, http://doi.org/10.5194/acp-19-3357-2019, 2019.
Schauer, J. J., Kleeman, M. J., Cass, G. R., and Simoneit, B. R. T.: Measurement of emissions from air pollution sources. 3. C-1-C-29 organic compounds from fireplace combustion of wood, Environ. Sci. Technol., 35, 1716-1728, http://doi.org/10.1021/es001331e, 2001.
Schauer, J. J., Kleeman, M. J., Cass, G. R., and Simoneit, B. R. T.: Measurement of emissions from air pollution sources. 5. C-1-C-32 organic compounds from gasoline-powered motor vehicles, Environ. Sci. Technol., 36, 1169-1180, http://doi.org/10.1021/es0108077, 2002.
Shiraiwa, M., Ammann, M., Koop, T., and Pöschl, U.: Gas uptake and chemical aging of semisolid organic aerosol particles, Proc. Nat. Acad. Sci. U.S.A., 108, 11003-11008, http://doi.org/10.1073/pnas.1103045108, 2011.
Shiraiwa, M., Pöschl, U., and Knopf, D. A.: Multiphase Chemical Kinetics of NO_3 Radicals Reacting with Organic Aerosol Components from Biomass Burning, Environ. Sci. Technol., 46, 6630-6636, http://doi.org/10.1021/es300677a, 2012.
Shiraiwa, M., and Seinfeld, J. H.: Equilibration timescale of atmospheric secondary organic aerosol partitioning, Geophys. Res. Lett., 39, L24801 http://doi.org/10.1029/2012gl054008, 2012.
Slade, J. H., and Knopf, D. A.: Multiphase OH oxidation kinetics of organic aerosol: The role of particle phase state and relative humidity, Geophys. Res. Lett., 41, 5297-5306, http://doi.org/10.1002/2014gl060582, 2014.
Slade, J. H., Shiraiwa, M., Arangio, A., Su, H., Pöschl, U., Wang, J., and Knopf, D. A.: Cloud droplet activation through oxidation of organic aerosol influenced by temperature and particle phase state, Geophys. Res. Lett., 44, 1583-1591, http://doi.org/10.1002/2016gl072424, 2017.
Springmann, M., Knopf, D. A., and Riemer, N.: Detailed heterogeneous chemistry in an urban plume box model: reversible co-adsorption of O_3, NO_2, and H_2O on soot coated with benzo[a]pyrene, Atmos. Chem. Phys., 9, 7461-7479, http://doi.org/10.5194/acp-9-7461-2009, 2009.
Steimer, S. S., Berkemeier, T., Gilgen, A., Krieger, U. K., Peter, T., Shiraiwa, M., and Ammann, M.: Shikimic acid ozonolysis kinetics of the transition from liquid aqueous solution to highly viscous glass, Phys. Chem. Chem. Phys., 17, 31101-31109, http://doi.org/10.1039/c5cp04544d, 2015.
Surratt, J. D., Chan, A. W. H., Eddingsaas, N. C., Chan, M. N., Loza, C. L., Kwan, A. J., Hersey, S. P., Flagan, R. C., Wennberg, P. O., and Seinfeld, J. H.: Reactive intermediates revealed in secondary organic aerosol formation from isoprene, Proc. Nat. Acad. Sci. U.S.A., 107, 6640-6645, http://doi.org/10.1073/pnas.0911114107, 2010.
Tombari, E., and Johari, G. P.: Structural fluctuations and orientational glass of levoglucosan-High stability against ordering and absence of structural glass, J. Chem. Phys., 142, http://doi.org/10.1063/1.4913759, 2015.
Wang, B. B., Lambe, A. T., Massoli, P., Onasch, T. B., Davidovits, P., Worsnop, D. R., and Knopf, D. A.: The deposition ice nucleation and immersion freezing potential of amorphous secondary organic aerosol: Pathways for ice and mixed-phase cloud formation, J. Geophys. Res., 117, http://doi.org/10.1029/2012jd018063, 2012.
Zahardis, J., and Petrucci, G. A.: The oleic acid-ozone heterogeneous reaction system: products, kinetics, secondary chemistry, and atmospheric implications of a model system - a review, Atmos. Chem. Phys., 7, 1237-1274, http://doi.org/10.5194/acp-7-1237-2007, 2007.
Zhang, X., McVay, R. C., Huang, D. D., Dalleska, N. F., Aumont, B., Flagan, R. C., and Seinfeld, J. H.: Formation and evolution of molecular products in alpha-pinene secondary organic aerosol, Proc. Nat. Acad. Sci. U.S.A., 112, 14168-14173, http://doi.org/10.1073/pnas.1517742112, 2015.
Zhu, C. M., Kawamura, K., and Kunwar, B.: Organic tracers of primary biological aerosol particles at subtropical Okinawa Island in the western North Pacific Rim, J. Geophys. Res., 120, 5504-5523, http://doi.org/10.1002/2015jd023611, 2015.

Ziemann, P. J., and Atkinson, R.: Kinetics, products, and mechanisms of secondary organic aerosol formation, Chem. Soc. Rev., 41, 6582-6605, http://doi.org/10.1039/c2cs35122f, 2012.
Zobrist, B., Marcolli, C., Pedernera, D. A., and Koop, T.: Do atmospheric aerosols form glasses?, Atmos. Chem. Phys., 8, 5221-5244, http://doi.org/10.5194/acp-8-5221-2008, 2008.

Heterogeneous oxidation of amorphous organic aerosol surrogates by O_3, NO_3, and OH at typical tropospheric temperatures

Jienan Li, Seanna M. Forrester, Daniel A. Knopf

School of Marine and Atmospheric Sciences, Stony Brook University, Stony Brook, NY 11794-5000, USA

Correspondence to: Daniel A. Knopf (Daniel.knopf@stonybrook.edu)

Abstract. Typical tropospheric temperatures render possible phase states of amorphous organic aerosol (OA) particles to solid, semi-solid and liquid. This will affect the multiphase oxidation kinetics involving the organic condensed phase and gaseous oxidants and radicals. To quantify this effect, we determined the reactive uptake coefficients (γ) of O_3, NO_3 and OH by substrate films composed of single and binary OA surrogate species under dry conditions for temperatures from 213 to 313 K. A temperature-controlled coated-wall flow reactor coupled to a chemical ionization mass spectrometer was applied to determine γ with consideration of gas diffusion transport limitation and gas flow entrance effects, which can impact heterogeneous reaction kinetics. The phase state of the organic substrates was probed via the poke-flow technique, allowing the estimation of the substrates' glass transition temperatures. γ values for O_3 and OH uptake to a canola oil substrate, NO_3 uptake to a levoglucosan and a levoglucosan/xylitol substrate, and OH uptake to a glucose and glucose/1,2,6-hexanetriol substrate have been determined as a function of temperature. We observed the greatest changes in γ with temperature for substrates that experienced the largest changes in viscosity as a result of a solid-to-liquid phase transition. Organic substrates that maintain a semi-solid or solid phase state and as such a relatively higher viscosity, do not display large variations in heterogeneous reactivity. From 213 K to 293 K, γ values of O_3 with canola oil, of NO_3 with a levoglucosan/xylitol mixture, and of OH with a glucose/1,2,6-hexanetriol mixture and canola oil, increase by about a factor of 34, 3, 2 and 5, respectively, due to a solid-to-liquid phase transition of the substrate. These results demonstrate that the surface and bulk lifetime of the OA surrogate species can significantly increase due to the slowed heterogeneous kinetics when OA species are solid or highly viscous in the middle and upper troposphere. This experimental study will further our understanding of the chemical evolution of OA particles with subsequent important consequences for source apportionment, air quality, and climate.

1 Introduction

Organic aerosol (OA) particles are ubiquitous and can represent 20%-90% of the mass fraction of the submicron aerosol (particles $\leq$ 1 μm in diameter) in the atmosphere. The significance of OA has long been established, influencing air quality, human health, cloud formation process and the radiative budget, on a regional and global scale, and thus climate (Hallquist et al., 2009;Jimenez et al., 2009;Seinfeld and Pandis, 2016;Stocker et al., 2013;Knopf et al., 2018;Abbatt et al., 2019;Shiraiwa et

al., 2017b;Kanakidou et al., 2005;Pachauri et al., 2014;Pöschl and Shiraiwa, 2015). Characterizing these impacts crucially depends on our ability to determine and quantify aerosol sources and strengths (Bai et al., 2013;Robinson et al., 2006;McFiggans et al., 2019;Hopke, 2016) and to understand the physical and chemical transformation of aerosol particles during atmospheric transport by multiphase chemical processes (George and Abbatt, 2010;Rudich et al., 2007;Laskin et al., 2015;Springmann et al., 2009;Kaiser et al., 2011;Ervens et al., 2011;Zhou et al., 2019;Moise et al., 2015). Gas-to-particle, also termed heterogeneous, reactions can involve organic components in the condensed phase and gas-phase oxidants such as O_3, NO_3, and OH. These reactions, which can include multiple phases, change the physicochemical properties of particles including composition, density, and hygroscopicity, thereby defining their chemical lifetime, optical properties, and ice nucleating ability (Jimenez et al., 2009;Kroll et al., 2015;Katrib et al., 2005b;Knopf et al., 2018;Slade et al., 2017;Robinson et al., 2007;Shiraiwa et al., 2017a;Moise et al., 2015;Shiraiwa et al., 2012;Murray et al., 2010;Wang et al., 2012).

It is now well established that OA can exhibit amorphous phase states (Mikhailov et al., 2009;Virtanen et al., 2010;Koop et al., 2011;Reid et al., 2018;Renbaum-Wolff et al., 2013;Kidd et al., 2014). Depending on the viscosity and microstructure, the amorphous phases can be classified as glasses, rubbers, gels, or ultra-viscous liquids (Mikhailov et al., 2009;Riemer et al., 2019). The glass transition temperature, T_g, is a characteristic parameter to describe the viscosity of a liquid on the order of 10^{12} Pa s (Koop et al., 2011;Angell, 1995;Zobrist et al., 2011;Dette and Koop, 2015;Zhang et al., 2019). At this temperature, the molecular motion of the species is so slow that it can be considered a solid. The phase state of OA can be modulated by particle composition and environmental conditions such as relative humidity (RH) and temperature (Koop et al., 2011;Zobrist et al., 2008;Shiraiwa et al., 2017a;Petters et al., 2019). Particle viscosity will influence the diffusion of atmospheric oxidants and other small gas molecules (e.g., O_3, OH, NO_3, H_2O) entering the organic matrix (Price et al., 2015;Zobrist et al., 2011;Slade et al., 2017;Davies and Wilson, 2016;Moridnejad and Preston, 2016) as well as the transport and mixing of the condensed-phase organic species (Rothfuss and Petters, 2017;Marsh et al., 2018;Lienhard et al., 2015;Abramson et al., 2013;Chenyakin et al., 2017;Kiland et al., 2019;Shiraiwa and Seinfeld, 2012;Renbaum-Wolff et al., 2013). Therefore, it can be expected that the particle phase state will significantly affect the rate of multiphase chemical kinetics (Slade and Knopf, 2014;Kolesar et al., 2014;Knopf et al., 2005;Katrib et al., 2005a;Pöschl and Shiraiwa, 2015;Davies and Wilson, 2015;Gaston et al., 2014;Zhang et al., 2018;Houle et al., 2018b). The heterogeneous reaction kinetics are often expressed by the reactive uptake coefficient (γ), which represents the fraction of gas collisions with a substrate surface that yield uptake or reaction (Pöschl et al., 2007;Schwartz, 1986).

As has been demonstrated for heterogeneous ozonolysis reactions, the composition of the condensed phase can alter the phase state, thereby, significantly altering the reactive uptake kinetics (Knopf et al., 2005;Hearn et al., 2005;de Gouw and Lovejoy, 1998;Ziemann, 2005). In general, the solid condensed phase showed significantly lower γ_{O_3} values compared to the ozonolysis of the liquid phase. Recent experimental studies focused on how relative humidity (RH) influences the reactive uptake of gas oxidants via its impact on the phase state of the organic species (Berkemeier et al., 2016;Steimer et al., 2015;Shiraiwa et al., 2011;Slade and Knopf, 2014;Li et al., 2018;Davies and Wilson, 2015;Hu et al., 2016;Marshall et al., 2018;Pajunoja et al., 2016). The heterogeneous oxidation of a typical component of biomass burning aerosol (BBA) particles,

levoglucosan (LEV) by OH yielded γ values in the range from 0.008 to 1 with implications for the lifetime of LEV ranging from weeks at dry conditions (Slade and Knopf, 2013;Kessler et al., 2010;Slade and Knopf, 2014;Arangio et al., 2015) to a couple of days when LEV is in a more liquid-like state in response to ambient RH (Yang et al., 2013;Bai et al., 2013;Slade and Knopf, 2014). The general conclusion is that at lower RH, the reactive uptake can be dominated by surface reactions when the condensed phase is in a solid state, whereas at higher RH, the condensed phase can be semi-solid or liquid and the oxidation process can commence at the surface and in the bulk. For the latter scenario, the gaseous oxidants can access greater depths of the condensed phase, and the oxidized organic species at the surface can be readily replenished by unreacted molecules from the bulk (Arangio et al., 2015;Slade and Knopf, 2014). Davies and Wilson (2015) investigated how the viscosity change of citric acid, due to changes in water content, governs the reactive uptake of OH radicals. They observed that the depletion of citric acid and the formation of reaction products are confined near the aerosol-gas interface on the order of 8 nm at 20% RH, and the reaction depth increases to ~50 nm at 50% RH. Recently, Li et al. (2018) observed that the heterogeneous aging of SOA by OH radicals at 89% RH and 25% RH resulted in ~60% and 20% loss of particle mass, respectively. The authors concluded that this difference in particle mass degradation is attributed to a larger OH uptake coefficient and/or larger fragmentation probability at higher RH.

The temperature in the troposphere ranges approximately from 200 K to 300 K (Wallace and Hobbs, 2006), with subsequent impact on the OA phase state (Shiraiwa et al., 2017a;Koop et al., 2011) and multiphase reaction kinetics. However, only a few laboratory studies investigated the temperature dependence of heterogeneous oxidation reactions while considering the phase transition of organic substrates and aerosol particles (de Gouw and Lovejoy, 1998;Edebeli et al., 2019;Gross et al., 2009;Knopf et al., 2005;Moise and Rudich, 2002;Slade et al., 2017;Moise and Rudich, 2000;Moise et al., 2002). Moise and Rudich (2002) demonstrated that the uptake of ozone by oleic and linoleic acid is a strong function of temperature, where γ decreases by about an order of magnitude with decreasing temperature when both substrates transformed from a liquid to a solid state. Similarly, Gross et al. (2009) observed a decrease of 70% to 90% for γ of NO_3, as oleic acid, diethyl sebacate, and conjugated linoleic acid substrates solidified as the temperature decreased from 302 K to 263 K. The authors suggested that the net liquid phase reaction involves both a surface reaction and a bulk reaction, whereas solidification of the substrate greatly minimizes the significance of any bulk reactions. This is in line with results of a kinetic flux model applied to NO_3 exposure studies of solid LEV and abietic acid substrates, further indicating that under shorter time scales reactive uptake was dominated by surface reaction, whereas for times scales greater than ~100 s, even for a solid organic substrate, bulk processes can impact the overall reactive uptake kinetics (Shiraiwa et al., 2012) Very recently, Edebeli et al. (2019) investigated the temperature dependence of bromide oxidation by ozone in a citric acid/bromide mixture and observed that γ decreases from 2×10^{-6} at 289 K to 0.5×10^{-6} at 245 K. Their analysis indicated that the humidity-driven acceleration in uptake reactivity decreased due to the increased viscosities of the citric acid/bromide mixture and decreased diffusivity of ozone as the temperature was lowered. The effect of temperature on uptake kinetics via its impact on the condensed phase state has also been highlighted in a recent modeling study (Mu et al., 2018), which showed that low temperature conditions can substantially increase the lifetime of PAHs against O_3 and enhance their dispersion through both the planetary boundary layer and the free troposphere. Temperature

also impacts the other processes involved in multiphase kinetics (Schwartz, 1986;Pöschl et al., 2007) including the collision flux of gas-phase species, the desorption rate and surface and bulk reaction rates, both typically expressed by an Arrhenius factor (Laidler et al., 1940;Pöschl et al., 2007;Baetzold and Somorjai, 1976). Clearly, the temperature dependency of the reaction kinetics and the role of the condensed phase state pose a challenge for detangling the underlying physicochemical processes governing multiphase chemical kinetics of OA under typical tropospheric conditions.

To add to our understanding of multiphase chemical kinetics at low temperatures, we determined the reactive uptake of O_3, NO_3 and OH by OA surrogates for temperatures ranging from 213 K to 293 K under dry conditions. We employed a chemical ionization mass spectrometer coupled to a coated-wall flow-tube reactor. As OA proxies, we applied substrates of canola oil (CA), levoglucosan (LEV), a levoglucosan/xylitol mixture (LEV/XYL), glucose (GLU), and a glucose/1,2,6-hexanetriol mixture (GLU/HEX). CA is a mixture of multiple saturated and unsaturated fatty acids, however, dominated by unsaturated oleic and linoleic acid, and serves as OA surrogate for both marine and terrestrial organic aerosol including anthropogenic emissions like cooking (Kawamura et al., 2003;Schauer et al., 2002;Limbeck and Puxbaum, 1999;Liu et al., 2017;Rogge et al., 1991). LEV serves as a surrogate for biomass burning aerosol (BBA) including natural sources such as forest fires and anthropogenic sources such as heating and cooking BBA (Schauer et al., 2001;Iinuma et al., 2007). GLU can serve as a tracer to characterize and apportion primary biogenic organic aerosols (PBOAs) (Zhu et al., 2015;Samaké et al., 2019). XYL and HEX are used in compounds mixtures to modify the glass transition temperature, thus, condensed-phase viscosity. O_3 and OH radicals reflect typical gas oxidants present in photochemically active regions and during long-range transport. NO_3 radicals reflect an effective oxidant participating in the nighttime chemistry of typically polluted regions (Finlayson-Pitts and Pitts Jr, 1999;Brown et al., 2006). Some of the examined substrates undergo a phase transition from liquid to solid in the probed temperature regime with subsequent consequences for the heterogeneous uptake kinetics. The substrate's phase state was qualitatively verified by conducting film poke-flow experiments. The results of our reactive uptake experiments emphasize the importance of the temperature-induced phase changes of the OA surrogates when describing the chemical degradation of OA during atmospheric transport.

2 Experimental methods

2.1 Apparatus

The experimental system is based on our previous setups (Slade and Knopf, 2013;Knopf et al., 2011;Knopf et al., 2005) and includes a temperature-controlled coated-wall flow reactor and a custom-built chemical ionization mass spectrometer (CIMS), as shown in Fig. 1. It consists of three parts: gas-phase oxidant generation, multiphase chemical reaction, and oxidant detection. The gas-phase oxidant (O_3, NO_3, or OH) enters the coated-wall flow reactor via a movable injector, where it can react with the organic substrate film coating on the inner wall of a rotating tube. The changes in oxidant concentration are measured by CIMS via soft ionization in the chemical ionization region.

The uptake measurements are conducted in a temperature range of 213 to 313 K. The axial temperature variation in the flow reactor is smaller than 1 K for all our experimental conditions, which is determined with a thermocouple that is fixed at the tip of the injector, as discussed in the Supplement S1. The rotating tube fits snuggly inside the flow tube that is enclosed by a cooling jacket for temperature control. The rotating speed of the substrate tube is set to ~5-10 rpm to keep the liquid film evenly distributed on its inner surface. The pressure in flow reactor ranges from 2 to 5 hPa depending on the applied oxidant gases.

For OH radical uptake experiments, an additional rotatory pump is directly connected to the flow reactor. The pump is used to lower the flow reactor pressure to < 2.5 hPa, thus minimizing gas transport limitation due to diffusion (Knopf et al., 2015;Zasypkin et al., 1997) while simultaneously maintaining a high flow rate. Two sizes of rotating glass cylinders with diameters of 1.75 cm and 1.2 cm are used in these uptake experiments. The latter one is designed specifically for OH heterogeneous reactions to avoid limitation of gas transport by diffusion. For O_3 and NO_3 uptake experiments, gas transport limitations due to diffusion can be neglected under applied flow conditions because of a slower reactive uptake.

The pseudo-first-order loss of the oxidant species to the organic substrate is determined by monitoring the loss of the gaseous oxidants as the injector is pulled back in 1 or 2 cm increments until reaching 10 cm. The flow rate of gas oxidants in the movable injector ranges from 2 to 100 $cm^3\,min^{-1}$ STP (standard temperature and pressure). The flow rate of the carrier gas He in the flow reactor ranges from 30 to 900 $cm^3\,min^{-1}$ STP. As a result, the residence time varies two orders of magnitude in these experiments, ranging from ~2 ms for OH uptake to 100 ms for O_3 uptake. The Reynolds number (Re) for all experiments is below 20, indicating laminar flow conditions. Care has been taken to ensure a carrier-to-injector gas velocity ratio of >1.33, in order to avoid the disruption of the gas flow by a fast gas flow exiting the injector, as pointed out by Davis (2008). This condition is also a necessity to accurately account for the gas flow entrance effect, which is important for fast uptake kinetics, as further discussed in the Appendix. The γ value at each temperature reported in this study is derived from at least 6 reactive uptakes, with a freshly prepared organic substrate employed for each.

2.2 Oxidant formation, detection and flow conditions

A carbon filter (Supelco, Superlcarb HC) and a Drierite cold trap cooled with liquid nitrogen or an ethanol/dry ice mixture are used to purify ultra-high purity (UHP) gases of N_2, He and O_2. O_3 is generated by introducing a flow of O_2 through a UV source (Jelight, model #600) prior to the injector. The flow rate of the O_2/O_3 mixture ranged between 2 - 7 $cm^3\,min^{-1}$ (STP). A carrier He gas flow of 30-85 $cm^3\,min^{-1}$ (STP) enters the flow reactor, mixes with the injector O_2/O_3 gas flow, and results in a laminar flow with Re < 3. O_3 is detected as O_3^- after charge transfer reaction with SF_6^-. SF_6^- is generated by passing a minor amount of SF_6 in N_2(g) through a ^{210}Po source. The O_3 concentrations ranged between 1.5×10^{11} - 2.1×10^{12} molecules cm^{-3}, reflecting typical atmospheric concentrations (Wallace and Hobbs, 2006;Finlayson-Pitts and Pitts Jr, 1999).

NO_3 is generated by thermal dissociation of N_2O_5 gas at 433 K in a glass oven prior to the injector, as previously (Knopf et al., 2006;Knopf et al., 2011). N_2O_5 is generated via reaction of NO_2 and O_3 and stored as pure N_2O_5 crystals in a glass container at 193 K. A gas flow of N_2O_5 in He of about 12-18 $cm^3\,min^{-1}$ STP is further diluted by 100-120 $cm^3\,min^{-1}$ (STP)

He(g) flow before entering the injector. The flow reactor carrier gas is composed of He and O_2 at ~500 and ~100 $cm^3\,min^{-1}$ (STP), respectively. This results in laminar flow conditions (Re < 10). NO_3 is detected as NO_3^- after chemical ionization by I^-. NO_3 concentrations are obtained via titration of a known amount of NO, resulting in 8×10^9 to 7×10^{11} molecules cm^{-3}, representing typical atmospheric NO_3 nighttime concentrations (Finlayson-Pitts and Pitts Jr, 1999;Brown et al., 2006).

OH radicals are produced following previously established methods (Bertram et al., 2001;Slade and Knopf, 2014) via the reaction of H atoms with O_2. A 2.45 GHz Evenson microwave cavity powered by a microwave generator is utilized to maintain an H plasma. The H atoms are formed by flowing a mixture of H_2(g) (1-2 $cm^3\,min^{-1}$, STP) and He(g) (40-80 $cm^3\,min^{-1}$, STP) through a 1/4" OD (outer diameter). Pyrex tube that runs through the center of the microwave cavity. The generated H atoms then pass through a 1/8" OD. Pyrex tube directed down the center of a 1/4" OD Pyrex injector where OH production occurs with H radicals reacting with O_2(g) at 2-22 $cm^3\,min^{-1}$ (STP). Complete reaction to OH is ensured by monitoring the formation of OH^- via charge transfer with SF_6^- in the CIMS. At colder flow reactor temperatures, the usable injector length is shortened to avoid artifacts in OH concentration due to temperature gradients in the injector tube which can impact OH formation (Atkinson et al., 2004). A He gas flow of 700-900 $cm^3\,min^{-1}$ (STP) enters the flow reactor and further mixes with the injector flow, yielding a laminar gas flow with Re < 20. Employed OH concentrations ranged between 5×10^7 and 1×10^9 molecule cm^{-3}, which are higher than typical background OH concentrations of 10^6 molecule cm^{-3} (Finlayson-Pitts and Pitts Jr, 1999).

2.3 Substrate film preparation and characterization

The film substrate preparation method when using a coated-wall flow reactor has been discussed in detail in previous studies (Knopf et al., 2011;Slade and Knopf, 2013). Canola oil is liquid and thus can be directly applied on the inner surface of the rotating tube. The other organic substrates, i.e., LEV, LEV/XYL mixture, GLU and GLU/HEX mixture, are first dissolved in water and then 1-2 ml of the aqueous solution is evenly distributed inside the rotating glass tube. The concentration of the LEV solution is 5% (w/w) due to its relatively lower solubility, and all other solutions are 10% (w/w). The organic mass ratios of the LEV/XYL and GLU/HEX films are 1:1 and 4:1, respectively. As outlined further below, these mass ratios were chosen to set the expected glass transition temperature within the examined temperature range. During the entire process, a dry He or N_2 purging gas flow is applied to avoid contamination by room air. The glass tube is rotating in the flow reactor until a smooth coating is established. To dry the substrate, the substrate is exposed to rough vacuum conditions (1~2 hPa) resulting in the evaporation of water. Surface solidification of single-component saccharide films may result in trapping of condensed-phase water and thus impacting the film composition and its viscosity. The remaining water content for all substrate films after the drying process were determined to be 13%-16% (w/w) by measuring the mass change of the organic substrate films before and after the drying process with an ultra-microbalance (Mettler Toledo XP2U), as detailed in Supplement S2. The thickness of the applied organic film is estimated to be around 50-100 μm. We assume a smooth surface morphology and use the geometric surface area of the film to derive γ.

The phase state of the applied organic substrates at different temperatures can be qualitatively verified by using the poking experiments outlined below. The “poke-flow” technique has been applied to quantitatively estimate the viscosity of amorphous

organic particles (Murray et al., 2012) including secondary organic material (SOM) produced by α-pinene ozonolysis (Renbaum-Wolff et al., 2013). A similar setup is used here to qualitatively investigate the phase state of applied amorphous substrates at different temperatures ranging from 213 to 313 K. A temperature-controlled cooling stage (Linkam BSC 196) is coupled to an optical microscope (Olympus BX51) (Fig. 2). Images of the film substrate are recorded at 230 magnification and the depth of field of the 10X objective is 15.9 µm. The organic film substrate, generated from a volume of 2 µl liquid applied to a glass slide, is first placed into the flow reactor, undergoing the same preparation method as the substrate films employed for reactive uptake experiments. This results in a film with a thickness of about 50-100 µm. The substrate film is then moved into the poke-flow experiment. In the cooling stage, the organic substrate film is sealed against room air and resides in an atmosphere of dry N_2 at positive pressure during the entire poking process. After poking with a needle, the phase states and flow characteristics of the organic substrate films at different temperatures are determined under the microscope as a function of time. Images are recorded with the film surface in focus to monitor the flow of the organic substrate and to probe film viscosity. Under the applied resolution, all film substrates appeared to be smooth and transparent. The calibration of the cooling stage was performed via measurements of the melting points of octane (216.35 K), decane (243.5 K) and water (273.15 K). Before each experiment, the temperature was verified by measuring the melting temperature of three 2 µL water droplets (273.15 K). The difference to the expected melting temperature difference is always smaller than 1 °C. We measured T_g with at least five independently prepared substrate films.

2.4 Chemicals

Listed below are the chemicals we used in our study, and corresponding purities and manufactures. N_2 (ultra-high purity, UHP), O_2 (UHP), H_2 (UHP) and He (UHP) were purchased from Airgas East. SF_6 (99.998%) was acquired from Praxair. NO_2 (99.5%) was purchased from Mathenson. 1,6-anhydro-b-D-glucopyranose (99%) was purchased from Acros Organics. Glucose (99%) and xylitol (99%) were acquired from Alfa Aesar. 1,2,6-Hexanetriol (96%) and iodomethane (99%) were purchased from Sigma-Aldrich. Purity of canola oil was not determined. Millipore water (resistivity >18.2 MΩ cm) was applied to prepare aqueous solutions for generation of organic substrates.

3 Results and Discussion

3.1 Characterization of substrate phase state

Images of the film surfaces in Fig. 3 show the flow characteristics and the morphologies of a GLU/HEX substrate mixture when subject to poking by a needle. In the experiment at T = 293 K (Fig. 3A), the film surface is deformed after being poked, leaving a black dent. The area around the dent reflects the smooth morphology of the film substrate before poking it. The slightly darker shades within the imaged area do not represent any morphology features but the unfocused scratches from the silver substrate holder beneath the film. The film flowed at an observable rate to restore a smooth surface, minimizing the

surface energy of the system (Fig. 3A). At 273 K, the same deformed film did not show observable changes within 30 minutes (Fig. 3B). Only after 8 hours, minor changes in film morphology can be identified, clearly demonstrating greater substrate viscosity at this temperature compared to 293 K. At 253 K, the notch by poking on the surface maintains its shape for 8 hours, indicative of a semi-solid phase state (Fig. 3C). At T = 233 K, which is below the predicted T_g = 248 K, the surface shattered when poked with a needle (Fig. 3D). Furthermore, over the experimental observation time of 8 h, no restorative flow was observed at 233 K. The fragments have clear glass-like cracks, and no smoothing of the edges was observed over the course of the experiment. Based on our poke-flow experiments as shown in Figure S2-S7, the applied GLU and LEV substrates remain in a solid or semi-solid phase state within the temperature range of 213 K to 313 K. However, the mixtures of GLU/HEX and LEV/XYL exist as liquids at 293 K and experience a glass phase transition with decreasing temperature.

By monitoring the substrate surface morphology, we can estimate T_g of the applied substrates as the highest temperature when shattering occurs. Viscosity greater than 10^{12} Pa s indicates the presence of a glassy phase. Thus, we ascribe the observed shattering of the substrate film a viscosity of 10^{12} Pa s, although the exact value cannot be assessed with the poke-flow technique. All images of the poke-flow experiment are documented in Figs. S2-S7 in the Supplement S3. Table 1 gives the estimated T_g^{exp} values of applied substrates compared to literature T_g^{lit} and predicted T_g^{pred} values. T_g^{pred} for substrate mixtures is derived from the Gordon Taylor equation (Gordon and Taylor, 2007) assuming literature T_g values and no residual water present. The uncertainties in T_g^{pred} values are derived by Gaussian error propagation. Except for the GLU substrate film, we achieve agreement or close agreement with either T_g^{lit} or T_g^{pred}. Since T_g determination depends on cooling or drying rates, we do not expect agreement with literature values or predicted values. In addition, if 10%-16% residual water is considered while using Gordon-Taylor equation, T_g^{pred} would be roughly 30 K lower than T_g^{exp}, assuming the residual water is homogeneously distributed in the film. This discrepancy is very likely due to our substrate film preparation process where under slow drying (evaporation), the outermost layers of the film contain less water than the deeper layers. Thus, the substrate surface represents closer the experimental conditions. Furthermore, the microscope focus in our poke-flow experiments is on the substrate surface, thereby monitoring the substrate morphology that is governed by the film viscosity closest representing the desired conditions.

The temperature dependence of the substrate viscosity can be predicted by using the modified Vogel-Tammann-Fulcher (VTF) equation (Angell, 1991):

$$\log \eta = -5 + 0.434 \frac{T_0 D}{T - T_0} , \quad (1)$$

where T_0 is the Vogel temperature and T is the ambient temperature. The fragility parameter, D, is defined in terms of the deviation of the temperature dependence of the viscosity from the simple Arrhenius behavior. Assuming $T = T_g$, $\eta = 10^{12}$ Pa s, T_0 can be represented by T_g (DeRieux et al., 2018):

$$T_0 = \frac{39.17 T_g}{D + 39.17} . \quad (2)$$

Therefore, the temperature dependence of substrate viscosity can be predicted using our measured T_g^{exp} as illustrated in Fig. 4. For our calculations, we use literature *D* values for pure sugars and a mass-weighted interpolation of *D* values for the mixtures as shown in Table 1. In Fig. 4a, LEV maintains a relatively higher viscosity compared to the LEV/XYL mixture throughout the studied temperature. The poke-flow experiments indicate the presence of a liquid phase at 293 K and solid phase at 238 K. In contrast to our poke-flow experiments, Fig. 4a suggests that the LEV/XYL mixture does not show a liquid phase in the examined temperature regime. Capturing this phase transition with the modified VTF equation (Angell, 1991), can be only achieved when using lower *D* values of 5.7~7.6 (compared to the interpolated *D* value of the LEV/XYL mixture), a reasonable assumption when considering the presence of residual water in the substrate. The addition of water increases the steepness of the glass transition and decreases *D* values by potentially reducing the thermal energy necessary to promote the cooperative chain motions (Angell, 2002;Borde et al., 2002). Furthermore, a study of the trehalose/water system corroborates that the presence of water lowers *D* values to 3.32 - 4.85 as a lower limit (Elias and Elias, 1999). For GLU and the GLU/HEX mixture shown in Fig. 4b, adding HEX to GLU greatly lowers the T_g of the mixture, and thus decreases its viscosity. Also, in this case, the predicted substrate viscosity of GLU/HEX disagrees with our observations when interpolating the *D* values of the pure compounds. A *D* value between 4.3 and 5.7 better represents the observed phase transition of the GLU/HEX mixture.

3.2 Reactive uptake kinetics

The uptake coefficient is determined experimentally from the loss of the gas phase oxidant to the organic substrate as the substrate area or corresponding reaction time is changed. Figure 5 shows three exemplary uptakes of O_3 by the canola oil (CA) film, NO_3 by LEV film and OH radical by the GLU film, indicating the stepwise irreversible removal of the gas oxidants. Taking O_3 uptake as an example, the injector is pulled back in 2 cm increments until reaching 10 cm and is then pushed back to its original position (0 cm), with normalized O_3 signals recovering to unity.

From these data, the observed first-order wall loss rate, k_{obs}, is determined as the slope of the change in the natural logarithm of the oxidant signal as a function of reaction time, i.e., the residence time of the oxidants in the flow reactor (Knopf et al., 2011;Slade and Knopf, 2013). Figure 6 shows exemplary k_{obs} derived for uptakes of O_3, NO_3, and OH for various temperatures. k_{obs} is obtained from the slope of the linear fit to the data. The good linear regression indicates that the reported uncertainties for γ are likely due to the variability of organic substrates and uncertainty in the diffusion coefficient. In the case of O_3 uptake (Fig. 6a), we can identify two different regimes of k_{obs}, where the linear regression with a larger slope at higher temperatures indicates greater reactivity. As discussed in detail further below, the large difference in k_{obs} between these two temperature regimes coincides with the canola oil substrates being in a liquid and solid phase state, respectively. For the cases of NO_3 and OH (Figs. 6b and 6c), the gradual change of k_{obs} coincides with a phase transition for both substrates from a highly viscous liquid to a semi-solid and solid (glassy) phase.

The change in concentration of oxidant X along the flow tube due to reactive uptake can be expressed using the effective uptake coefficient

$$\gamma_{\mathrm{eff,X}} = \frac{D_{\mathrm{tube}}}{\omega_{\mathrm{X}}} \times \left[ln \left(\frac{[\mathrm{X}]_{\mathrm{g,0}}}{[\mathrm{X}]_{\mathrm{g}}} \right) / t \right] = \frac{D_{\mathrm{tube}}}{\omega_{\mathrm{X}}} \times k_{\mathrm{obs}} \quad . \tag{3}$$

Following the Knopf-Pöschl-Shiraiwa (KPS) method (Knopf et al., 2015), actual γ can be derived as:

$$\gamma = \frac{\gamma_{\mathrm{eff,X}}}{1 - \gamma_{\mathrm{eff,X}} \frac{3}{2 N_{\mathrm{shw}}^{\mathrm{eff}} Kn_{\mathrm{X}}}} \quad , \tag{4}$$

where D_{tube} is the diameter of the coated-wall tube and ω_{X} (X = O_3, NO_3 or OH radical) is the mean molecular velocity of the respective gas-phase oxidant. $N_{\mathrm{shw}}^{\mathrm{eff}}$ is the effective Sherwood number which represents an effective dimensionless mass-transfer coefficient to account for changes in the radial concentration profile of the entry region (Knopf et al., 2015;Davis, 2008), and Kn_{X} is the Knudsen number that characterizes the flow regime (Wutz, 1989;Fuchs and Sutugin, 1971). The Sherwood number departs from $N_{\mathrm{Shw}}^{\mathrm{eff}}$=3.66 under conditions of fast flows and short tubes. The KPS method is advantageous over the correction approach by Brown (1978) since it accounts for entrance effects that can result in the overestimation of reactive uptake coefficients as outlined by Davis (2008) and discussed in more detail in the Appendix. The Cooney-Kim-Davis (CKD) method (Cooney et al. 1974) also accounts for the flow entrance effects as discussed in Murphy and Fahey (1987). This is crucial for fast uptakes involving the OH radical, however, less so for the uptakes involving O_3 and NO_3 radicals. The uncertainty in derived γ values represents the greater value of either a 20% uncertainty in the diffusion coefficient or variation in measurements expressed as ±1σ.

The gas-phase diffusion coefficient of O_3 in He ($D_{\mathrm{O_3-He}}$) is taken as 394 Torr cm^2 s^{-1} at 298 K (Moise and Rudich, 2000). Diffusion coefficients of NO_3 in He and O_2 are taken as 345 and 80 Torr cm^2 s^{-1} at 273 K, respectively (Rudich et al., 1996). The method introduced by Fuller et al. (1966) was utilized for O_3 and NO_3 to derive the diffusion coefficients at other temperatures. The diffusion coefficients of OH in He and O_2 gas ($D_{\mathrm{OH-He}}$ and $D_{\mathrm{OH-O_2}}$) for different temperatures are theoretically calculated based on a method reported by Mason and Monchick (1962). A reference value of $D_{\mathrm{OH-He}}$ measured at room temperature is 662 ± 33 Torr cm^2 s^{-1} (Ivanov et al., 2007;Liu et al., 2009). To calculate the diffusion coefficient of an oxidant (D_{X}) in a mixture of He and O_2, we applied the following equation with P_{He} and $P_{\mathrm{O_2}}$ representing pressures derived from experimental flow rates and pressure measurements (Hanson and Ravishankara, 1991)

$$D_{\mathrm{X}} = \left(\frac{P_{\mathrm{He}}}{D_{\mathrm{X-He}}} + \frac{P_{\mathrm{O_2}}}{D_{\mathrm{X-O_2}}} \right)^{-1} \quad . \tag{5}$$

The pressure in the flow reactor is maintained at less than 2.5 hPa to avoid transport limitations by diffusion of OH radicals that undergo fast reactive uptake kinetics. Diffusion limitation can be estimated by using the additivity formula for kinetic resistances as (Gershenzon et al., 1995)

$$\frac{1}{k_{\mathrm{obs}}} = \frac{1}{k_{\mathrm{k}}} + \frac{1}{k_{\mathrm{d}}} \tag{6}$$

$$k_{\mathrm{k}} = \frac{\omega_{\mathrm{X}} \times \gamma}{R \times (2 - \gamma)} \tag{7}$$

$$k_{\mathrm{d}} = 3.66 \frac{D_{\mathrm{X}}}{R^2} \quad , \tag{8}$$

where k_{obs} (s^{-1}) is the observed wall loss rate of heterogeneous uptake, and k_k and k_d represent its kinetic and diffusion limits, respectively. R is the radius of the flow tube. Gershenzon et al. (1995) proposed that k_k/k_d should be < 3~5 to obtain an accurate γ value. Some of the highest temperature OH uptake experiments involving liquid canola oil were conducted under diffusion limitation with $k_k/k_d \cong 15$~30. However, for all the remaining experiments $k_k/k_d < 5$ and, thus, are not diffusion limited.

As outlined in Supplemental Text S4, for semi-solid and solid substrate films, the fraction of the unoxidized reaction sites is always larger than 90% due to short reaction time and low concentrations of gas oxidants (Bertram et al., 2001) implying no significant surface saturation effect on γ. In other words, during the typical duration of a reactive uptake experiment, the oxidant exposure does not lead to complete oxidation of the substrate surface.

3.3 Temperature modulated reactive O_3 uptake

Figure 7 shows γ of O_3 reacting with canola oil as a function of temperature. The reactive uptake is determined under dry conditions in the presence of O_2. Both Brown and KPS methods were used to derive γ (Brown, 1978;Knopf et al., 2015). Both methods yield the same results due to the slow uptake kinetics as further discussed in the Appendix. Around 90% of canola oil is made up of oleic acid, linoleic acid and α-linolenic acid (Ghazani and Marangoni, 2013), and it solidifies readily around its melting point (de Gouw and Lovejoy, 1998). γ decreases sharply by a factor of ~18 from $(5.65 \pm 0.89) \times 10^{-4}$ to $(3.23 \pm 0.74) \times 10^{-5}$ as the temperature decreases from 267 K to 258 K, a temperature range in which the canola oil experiences a phase transition from liquid to solid (Fasina et al., 2008). In this temperature regime, the bulk diffusion coefficients of both ozone and canola oil are expected to decrease by several orders of magnitude due to the transition from a viscous liquid to a solid (Koop et al., 2011). Our O_3 reactive uptake coefficients agree with previous literature data by de Gouw and Lovejoy (1998) and extend those to lower temperatures. A study by Berkemeier et al. (2016) showed that the uptake of O_3 by shikimic acid is $\sim 5 \times 10^{-6}$ at low RH conditions and increases by a factor of ~16 at higher RH due to a decrease in viscosity as a result of a RH-induced phase transition, similar to our observations. Our results are consistent with previous studies (Shiraiwa et al., 2009;Shiraiwa et al., 2010;Steimer et al., 2015), which showed that the O_3 uptake is slower and restricted to near the particle surface if the organic is in a solid phase, while the uptake is dominated by bulk reaction if the organic is in a liquid phase.

In the low temperature regime, from 213 K to 258 K, γ only increases by about a factor of 1.7 (Fig. 6). If we consider the gas-phase reaction kinetics of O_3 with an unsaturated bond having an activation energy of 15 kJ mol^{-1} (Atkinson et al., 2006), an increase of the reaction rate by a factor of 4.4 would be expected over a temperature of 45 K. This less than expected temperature dependency of γ may be due to the combined temperature effects on both the underlying reaction kinetics and the desorption lifetime (Pöschl et al., 2007). As the temperature decreases and reactivity decreases, the desorption lifetime increases, potentially resulting in a compensating effect on the overall uptake kinetics. In the temperature regime above the phase transition, between 267 K and 293 K, γ is significantly larger than when the canola oil substrate is solid, likely due to greater reaction rates and greater O_3 and condensed-phase diffusion coefficients.

3.4 Temperature modulated reactive NO_3 uptake

The uptake coefficient of NO_3 by levoglucosan (LEV) decreases from $(4.2\pm0.6) \times 10^{-4}$ to $(2.8 \pm 0.3) \times 10^{-4}$ as the temperature decreases from 293 K to 213 K, thus, displaying only a slight change in γ within the experimental temperature range (Fig. 8a). Based on our poke-flow experiment, LEV substrates maintained a semi-solid or solid phase state for all examined temperatures. The slight increase of γ with temperature may be due to the combined effects of changes in substrate viscosity (see Fig. 4), the counteracting effect of the temperature dependence of the reaction rate (Atkinson et al., 2006) and the desorption lifetime (Pöschl et al., 2007). Assessment of these various impacts on the observed uptake kinetics necessitates an in-depth analysis, e.g., by application of kinetic flux modeling (Shiraiwa et al., 2012;Arangio et al., 2015). Note, the γ of NO_3 by LEV in this experiment is smaller than the value of $(1.3 \pm 0.9) \times 10^{-3}$ determined in our previous study at 298 K, although the data agree within uncertainties (Knopf et al., 2011). A possible explanation for the lower γ value in this study is that the substrates have undergone longer drying to remove residual water. Presence of water would render the film less viscous thereby increasing reactivity.

For the mixture of LEV/XYL (Fig. 8b), γ at 293 K is 8.5×10^{-4}, about a factor of 2 larger than for pure LEV (see Table 2). As the temperature decreases, γ reaches a value of 3.1×10^{-4} at 213 K, similar to the γ value derived for solid LEV (Fig. 8a). Our poke-flow experiment yielded T_g = 238 K for the applied LEV/XYL film. The largest change of γ is observed above the expected T_g (Fig. 8b). Therefore, the significant change in NO_3 uptake reactivity in the investigated temperature range can be attributed to the transition of a solid or highly viscous to a liquid substrate film. As such, the underlying reaction mechanism changes, i.e., at higher temperatures, the kinetic uptake is likely governed by surface and bulk reactions and at lower temperatures only surface reaction dominates. As shown in Shiraiwa et al. (2012), for highly viscous/solid LEV films, the transport of bulk LEV towards the interface is strongly limited, slowing the reactive uptake kinetics. At higher temperatures, with decreasing viscosity of LEV, the diffusivity of LEV and NO_3 increases, likely facilitating transport and thus reaction.

Gross et al. (2009) reported that γ of NO_3 by liquid glycerol (GLY) is $(14\pm3) \times 10^{-4}$ at 293 K and decreases to 8.3×10^{-4} at 268 K, representing a decrease of 41% in γ over 25 K. The T_g of glycerol is 193 K, and the viscosity decreases from 20 Pa s at 268 K to 1.32 Pa s at 293 K (Schröter and Donth, 2000). For the same temperature difference of 25 K, γ for the viscous liquid LEV/XYL substrate decreases by about 24%. The viscosity of LEV/XYL film is around 10^1 to 10^2 Pa s based on our poke-flow experiments and viscosity prediction as outlined in section 3.1. We hypothesize that the lesser change in γ with temperature for the LEV/XYL substrate compared to a GLY substrate (Gross et al. 2009), may be due to the viscosity difference between both substrates. Moise et al. (2002) studied the uptake of NO_3 by a saturated alcohol, 1-octanol, in the liquid and solid-phase. They derived $\gamma = 7.1\times10^{-3}$ at 258 K for the liquid phase of 1-octanol and 4.1×10^{-3} at 248 K for the solid phase as shown in Table 2. The change in γ is a factor 1.73 over 10 K, mainly because of the rapid phase transition of 1-octanol. In our LEV/XYL uptake experiment, γ changes by a factor 2.74 over a temperature range of 80 K, however, γ measured here is about one order of magnitude lower. We suggest that the different sensitivity in γ over these different temperature ranges is

due to the continuous amorphous phase transition of the LEV/XYL mixture compared to the abrupt phase transition of 1-octanol.

At low temperatures, γ for NO_3 uptake by LEV and LEV/XYL films are similar within our experimental uncertainties, as shown in Table 2. This is in contrast to expectations derived from the gas-phase structure activity relationships (SARs) (Atkinson, 1987;Kerdouci et al., 2014), which predict that the reaction NO_3 + LEV occurs 6.7 times faster than the reaction of NO_3 + XYL. Also, γ of solid LEV and LEV/XYL is similar to NO_3 uptake by solid alkane substrates and monolayers, e.g. n-hexadecane given in Table 2 (Knopf et al., 2006;Knopf et al., 2011;Gross and Bertram, 2009;Moise et al., 2002). However, an alcohol is expected to be more reactive with NO_3 compared to an alkane, as the α-hydrogen atom at the OH group is more labile and thus facilitates the hydrogen abstraction. These measurements indicate that the presence of labile α-hydrogen atoms in solid substrate films do not significantly yield higher γ. A possible explanation may be that the number density of labile α-hydrogen atoms at the interface is not sufficiently different between LEV, the LEV/XYL mixture and alkane substrates films. Furthermore, considering that NO_3 concentrations are too low to saturate the substrate surface, the probability of collisions with the most reactive hydrogen may also be low. This may result in similar γ within our uncertainties, for both substrates. In conclusion, our study demonstrates a strong positive correlation between temperature, substrate phase state, and NO_3 uptake reactivity for saturated alcohols.

3.5 Temperature modulated reactive OH uptake

Figure 9a shows γ of OH reacting with GLU as a function of temperature indicating no significant change in reactivity over the examined temperature range. As the temperature increases from 250 K on, γ appears to slightly decrease from 0.11±0.03 to 0.09 ±0.03, although this change is within experimental uncertainties. GLU substrates maintain a solid or highly viscous phase state for all examined temperatures. The gas-phase structure activity relationship (SAR) predicts that the gas-phase reaction rate of OH radicals with GLU (k^{g}_{Glu}) decreases by a factor of 2.5 from 213 K to 298 K (Atkinson, 1987;Kwok and Atkinson, 1995). We also observe a decrease in reactivity (Fig. 9a), however, not as strong as during gas-phase reactions. This implies that other factors may also play a role in the observed heterogeneous reactivity. Since different chemical bonds have different reactivity and temperature dependence (Kwok and Atkinson, 1995), the reaction probability of OH radicals can be affected by the molecular orientation at the surface. SAR suggests that tertiary C-H bonds contribute to this negative temperature dependency of the reactivity. Hence, if more C-OH bonds are exposed to the surface compared to tertiary C-H bonds, this negative temperature dependency of reactivity weakens. A similar steric argument was given by Nah et al. (2014), who suggested that the increased surface density of C=C double bonds due to the formation of oleic acid dimers possibly leads to a faster surface reaction involving OH radicals. Also, the remaining amount of water in these substrates may impact the surface structure and the viscosity of the near-surface region, thereby potentially counteracting the decreasing reaction rate with increasing temperature predicted by SAR method.

For the GLU/HEX mixture (Fig. 9b), γ at 303 K is 0.13±0.03, ~1.5 times larger than that at 233 K. The larger γ at higher temperature can be attributed to the viscosity change of the substrate film with increasing temperature. T_g is estimated as (248

± 3) K by our poke-flow experiment. Judging by the morphology and the flow characteristics of the organic film, it experiences a glass phase transition within the investigated temperature range. The major change in γ occurs above the expected T_g of the GLU/HEX mixture. γ by GLU/HEX at low temperatures, i.e., between 213 K and 233 K, are lower than γ by GLU, and this is likely related to the lower reaction rate of HEX with OH radicals. For example, SAR predicts the reaction rate for HEX + OH to be 2.6 times slower than that for GLU + OH at 213 K.

Figure 9c shows that γ of CA increases by a factor of 5 within the experimental temperature range, from 0.13 ± 0.08 at 213 K to 0.66 ± 0.24 at 293 K. This increase of γ is particularly significant above the melting point of canola oil, T_m = 258 K (Fasina et al., 2008). Above the melting point, γ increases by a factor of ~2.4 between 273 K and 293 K, where the viscosity of canola oil changes from 0.185 to 0.079 Pa s (Fasina et al., 2006). Therefore, we attribute this large change in γ to the phase and viscosity change of the canola oil. We observed that as the canola oil is in a solid or viscous liquid (grease) state at temperatures between 213 and 253 K, γ is less sensitive to temperature changes compared to when the canola oil is in a liquid phase. γ by CA is larger than γ by GLU at low temperatures although both are in solid phase, thus implying that OH reacts faster with C=C bonds than with C-H bonds and OH groups present on solid surfaces. Waring et al. (2011) measured the reactive loss of gas-phase OH radicals on squalene surfaces at room temperature, reporting γ = 0.39 ± 0.07. These measurements suggest that γ by CA can be larger than γ by squalene although squalene has more double bonds compared to canola oil and both organics have similar viscosity (e.g., μ_{Sqe} is 0.012 Pa s at 298 K, Comunas et al. (2013)). Different accessibility of C=C bonds on the substrate surfaces could be one reason for different γ values. X-ray diffraction studies on liquid oleic acid showed that the unsaturated acid molecules exist primarily as dimers through hydrogen bonding of the carbonyl oxygen and the acidic hydrogen (Iwahashi and Kasahara, 2011;Iwahashi et al., 2000), and this possibly leads to more C=C double bonds at the substrate surface (Hearn et al., 2005). However, whether or not this phenomenon can compensate for the more numerous C=C double bonds present in squalene molecules is uncertain. Lastly, gas-phase reaction kinetics suggest that unsaturated oxygenated organics (e.g., acids, alcohols, ketones) are more reactive toward OH radicals than their alkene equivalents due to the formation of a hydrogen bonded complex that facilities the formation of stable reaction products via interactions between the OH radical and the oxygenated functional group of the molecule (Mellouki et al., 2003;Orlando et al., 2001).

4 Atmospheric implications

Temperature varies greatly in the troposphere, both in the latitudinal and altitudinal directions. The zonal average surface temperature changes approximately 0.86 K per latitude degree in the northern hemisphere (Gates et al., 1999), and the vertical temperature gradient is typically defined by the lapse rate of ~10 K km^{-1} for dry air and ~7 K km^{-1} for wet air (Wallace and Hobbs, 2006). Globally, the temperature will greatly influence the phase state and the heterogeneous oxidation of OA particles, especially for SOA particles that can exist a liquid phase state in the warmer planetary boundary layer but can be mostly solid in the colder middle and upper troposphere (Shiraiwa et al., 2017a).

The determined γ values can be used to estimate the oxidation lifetime for a solid organic surface with the following equation (Moise and Rudich, 2001):

$$\tau = \frac{4N_{\mathrm{tot}}}{\gamma \omega_{\mathrm{X}} [\mathrm{X}]_{\mathrm{g}}} \quad , \qquad (9)$$

where τ is the lifetime of one monolayer of coverage, i.e., how long it takes for 63% surface molecules to be oxidized. N_{tot} represents the concentration of reaction sites on the organic substrate surface. Here, we apply this idealized approach to assess the degree of surface oxidation of OA particles in a solid or highly viscous phase state and when the oxidation reactions are confined to the surface. However, given that the surface-active organics are ubiquitous in tropospheric aerosols and organic films can exist on aerosol surfaces with potentially significant effects on atmospheric chemistry and climate, e.g., heterogeneous reactions, particle hygroscopicity, optical properties, and cloud forming activity (Jimenez et al., 2009;Kroll et al., 2015;Katrib et al., 2005b;Knopf et al., 2018;Slade et al., 2017;Robinson et al., 2007;Shiraiwa et al., 2017a;Cosman and Bertram, 2008;McNeill et al., 2006;Knopf et al., 2007;Knopf and Forrester, 2011;Moise et al., 2015) , this approach can further our understanding of the chemical evolution of atmospheric OA. We assume $N_{\mathrm{tot}} = 10^{15}$ cm^{-2} (Bertram et al., 2001). The concentration of gas oxidants O_3, NO_3, and OH are based on ambient conditions as 1×10^{12}, 1.25×10^{9} and 1×10^{6} molecules cm^{-3}, respectively (Finlayson-Pitts and Pitts Jr, 1999). Figure 10 shows the effect of temperature on the surface species' lifetime for the different examined heterogeneous oxidation reactions. Oxidation of CA by O_3 proceeds within minutes to hours for typical tropospheric temperatures. Thus, degradation of unsaturated fatty acids is expected to proceed efficiently, even at colder temperatures. Despite the OH radical being the most effective oxidizer, Fig. 10 suggests that for middle and upper tropospheric conditions, oxidation of the particle surface by OH can take 1 to 2 weeks, emphasizing the slow physicochemical changes of the particle properties during transport at high altitudes. However, closer to the surface, degradation can proceed almost an order of magnitude faster. Degradation of the particle surface by NO_3 may proceed by about a factor 2 slower at the coldest tropospheric temperatures compared to boundary layer conditions. Clearly, these datasets indicate that the topmost organic layers for most of the investigated OA surrogates can be oxidized within 1 week for lower and middle tropospheric conditions. However, as soon as OA particles reach higher altitudes and lower temperatures by, e.g., pyro-convection (Andreae et al., 2004;Jost et al., 2004;Fromm and Servranckx, 2003), their atmospheric lifetime increases significantly. For example, aerosol particles originating from extreme wildfires like an Australia bushfire can circumnavigate the globe in weeks and can even reach the stratosphere existing for weeks or months (Ribeiro et al., 2020).

For OA particles, the lifetime (τ_{p}) and particle degraded fraction (*DF*) can be estimated by the equations below (George et al., 2007):

$$\tau_{\mathrm{p}} = \frac{4}{3} \frac{\rho R N_a}{\gamma \omega_{\mathrm{X}} [\mathrm{X}]_{\mathrm{g}} M} \qquad (10)$$

and

$$DF = 1 - \exp\left(-\frac{t}{\tau_{\mathrm{p}}}\right), \qquad (11)$$

where R is the radius of the particle, chosen here as 100 nm, N_a is Avagadro's number, M is the molecular weight of the condensed-phase species, and t is time. We derive *DF* as a function of temperature and oxidant exposure time for oxidant concentrations given above. However, we note that this *DF* estimate is a simplified approach, since we assume that measured oxidation kinetics proceed throughout the entire particle with the same rate. This ignores the slow gas diffusion in the condensed phase and the hindered internal mixing of organic species, particularly when the OA particle is in a solid or highly viscous phase state. For OH oxidation, previous studies indicate that the oxidation reaction is confined to near the surface of a liquid or solid organic substrate, even for longer OH exposure periods at lower OH concentrations (Slade and Knopf, 2014;George and Abbatt, 2010;Lee and Wilson, 2016;Shiraiwa et al., 2011). However, whether bulk processes may significantly change the reactivity under long oxidant exposure as encountered in the atmosphere still needs to be examined. In the case of O_3 and NO_3 oxidation of organic substrates, the results by Shiraiwa et al. (2011) and Shiraiwa et al. (2012) indicate that the reactive uptake coefficients decrease with increasing exposure. Therefore, we probably underestimate the chemical lifetime. As such, the *DF* values at lower temperatures likely represent upper limits. In other words, degradation in ambient particles is expected to be less. Keeping this limitation in mind, Fig. 11 displays the estimated *DF* for the examined oxidant-surrogate systems. As expected, for the lowest temperatures, the *DF* values are lowest, implying longest lifetimes. The stronger the particle viscosity change with temperature, the greater is the change in *DF*, e.g., viscosity of CA decreases from 10^{12} to 10^{-2} Pa s over 213 to 293 K. This yields the largest change in *DF* over this temperature range compared to the other investigated systems (considering the same exposure time period). Figures 11(c) and (d) display a small *DF* within one month for LEV/XYL and GLU/HEX mixtures in the upper troposphere. This is consistent with previous aircraft observations reporting a large amount of biomass burning aerosol particles in aged plumes at higher altitudes of the troposphere (Cubison et al., 2011). This also supports the hypothesis that aerosol particles originating from large wildfires (e.g., Australian bushfires) can be transported into the northern hemisphere from the stratosphere within a time period of one year (Deshler, 2008;Peterson et al., 2018). The presence of water vapor will significantly impact the phase state, in particular, of hygroscopic species such as LEV and GLU (Zobrist et al., 2008;Koop et al., 2011;Mikhailov et al., 2009), where increasing humidity yields lower condensed-phase viscosity and, in turn, faster reaction kinetics (Slade and Knopf, 2014;Slade et al., 2017;Davies and Wilson, 2015). Neglecting this effect will lead to an underestimation of *DF*. This discussion neglects the chemical complexity of ambient OA where different condensed-phase species can result in different reactivities and reaction pathways (Zhang et al., 2015;Surratt et al., 2010;Ziemann and Atkinson, 2012;Knopf et al., 2005;Davies and Wilson, 2015). Those in turn can change the multiphase kinetics and its dependency on temperature and particle phase state. Furthermore, heterogeneous particle composition and morphology can result in matrix effects or liquid-liquid phase separation, where, e.g., more reactive organic species are shielded by less reactive species (Lignell et al., 2014;Lee and Wilson, 2016;Charnawskas et al., 2017;Bertram et al., 2011). Those effects were not assessed in this study but necessitate additional experimental investigations.

5 Conclusions

In this study, we measured γ for several systems of oxidant and organic aerosol surrogate combinations including O_3 and OH + CA, NO_3 + LEV and LEV/XYL, OH + GLU and GLU/HEX, under dry conditions and for temperatures ranging from 213 K to 313 K. For the case of OH, this is the first low temperature reactive uptake study of which the authors are aware. The phase states of the organic substrate films were examined using the poke-flow technique allowing for an estimation of T_g and substrate flow characteristics to constrain the magnitude of the substrate viscosity at different temperatures using the VTF equation.

The strongest changes in heterogeneous reactivity observed for the examined oxidant-substrate systems correlates with the largest change in organic substrate viscosity with temperature associated with a solid-to-liquid phase transition. The largest reactivity occurs between O_3 and CA exhibiting a change by a factor of 34, due to the phase transition of CA. In general, we attribute the faster heterogeneous kinetics in the semi-solid and liquid phase state to surface and bulk reactions, the latter enabled by increased diffusion coefficients of gas and condensed species resulting from lower viscosity. Furthermore, once in the liquid phase, as temperature increases viscosity decreases and diffusivity increases, leading to potentially strong increases in reactivity. LEV and GLU substrates display a semi-solid and solid phase state over the entire probed temperature range, with estimated viscosities larger than 10^4 Pa s. As a result, the overall reactivity is lower compared to liquid substrate films and does not change significantly with temperature. Although viscosity in the semi-solid phase regime can change substantially with temperature, viscosity can still be too high to allow for significant bulk processes to play a role. In this case, surface reactions likely dominate and replenishment of unoxidized molecules to the surface is hindered. Application of organic substrate mixtures to control T_g to induce a solid-to-liquid phase transition as temperature increases, is accompanied with an increase in reactivity.

Our results are consistent with previous studies reporting the significance of particle phase state for the reactive uptake kinetics (Arangio et al., 2015;Knopf et al., 2005;Kolesar et al., 2014;Slade and Knopf, 2014;Davies and Wilson, 2015;Shiraiwa et al., 2012). To resolve the molecular processes of the measured heterogeneous kinetics, detailed modelling studies (Pöschl et al., 2007;Shiraiwa et al., 2010;Arangio et al., 2015;Houle et al., 2015;Houle et al., 2018a;Pöschl and Shiraiwa, 2015) extended to lower temperatures are needed. A crucial aspect of this study is the interplay between the temperature dependence of the reaction kinetics and the desorption lifetime. At lower temperatures when an organic substrate in the solid state, over a wide temperature range the reactivity does not change significantly. Desorption lifetime will likely increase significantly with decreasing temperature with subsequent effects on the reaction kinetics. Changes in substrate viscosity with temperature may also play a role in the overall heterogeneous kinetics when the substrate is in a semi-solid phase state. However, to what extent the particle viscosity will influence the diffusion and reaction kinetics is still not resolved. The comprehensive data set presented here will allow application of a more detailed kinetic multi-layer model to constrain the temperature dependency of reaction and transport parameters. This study did not address the role of water vapor acting as a plasticizer concurrent to phase changes induced by temperature changes (Zobrist et al., 2008;Koop et al., 2011;Mikhailov et al., 2009). The role of humidity

on amorphous phase state and resulting multiphase kinetics has been studied at room temperature (Shiraiwa et al., 2011;Slade and Knopf, 2014;Davies and Wilson, 2015;Li et al., 2018). Most of these studies suggest that increasing humidity leads to faster reactive uptake kinetics. However, at lower temperatures, diffusivity is slower leading to kinetically hindered adjustments of the condensed-phase state (Berkemeier et al., 2014;Knopf et al., 2018;Charnawskas et al., 2017;Wang et al., 2012). Future experimental studies should focus on how the coupled effects of ambient temperature and humidity on the amorphous phase state of OA particles modulate the multiphase oxidation kinetics.

Our study demonstrates unambiguously that the chemical reactivity of organic matter towards atmospheric oxidants can vary significantly in response to ambient temperature, which, in turn, modulates the organic phase state. Ambient OA, however, display greater chemical and morphological complexity (Laskin et al., 2016;Laskin et al., 2019), and as such we expect varying multiphase reaction pathways having different reactivity towards atmospheric gas-phase oxidants which will translate into different reactivity dependencies on temperature and phase state. Despite this caveat, due to lower temperatures at higher altitudes, we can expect OA particles during transport in the free troposphere to have significantly longer lifetimes with respect to chemical degradation. As a result, we can expect OA particles during transport in the free troposphere to have significantly longer lifetimes with respect to chemical degradation. This is important information for our understanding of the chemical evolution of OA particles and their impact on source apportionment, air quality, and climate.

6 Appendix: The impact of gas flow entrance effects and velocity profiles on the reactive uptake kinetics

The KPS method (Knopf et al., 2015), similar to the Cooney-Kim-Davis (CKD) method applied by Murphy and Fahey (1987) , accounts for gas flow entrance effects into the flow reactor, i.e., the establishment of concentration profiles, that impact the derivation of the reactive uptake coefficient as pointed out by Davis (2008). When considering the establishment of gas concentration profiles for correction of observed pseudo-first order wall loss rates, slower uptake reaction kinetics (e.g., the uptake of O_3), typically represent conditions of either having a slow gas flow or long flow tube, and thus the $N_{\mathrm{shw}}^{\mathrm{eff}} \approx 3.66$ as shown in Fig. A1 (Davis, 2008). In this case, the different approaches (Brown, CKD, and KPS) to correct observed wall loss rate for transport limitations by diffusion yield the same γ values as illustrated in Fig. 7 (CKD approach is not shown but yields same results as KPS). However, reactive OH uptake exerts faster reaction kinetics and thus resembles conditions of a fast gas flow or a short flow tube (Fig. A1) where $N_{\mathrm{shw}}^{\mathrm{eff}}$ can significantly depart from 3.66 (Knopf et al., 2015;Murphy and Fahey, 1987;Davis, 2008). In this case, γ values derived by the Brown method always yield larger values compared to those derived by the KPS method as illustrated in Fig. A2 for the uptake of OH by glucose. Hence, for fast uptake kinetics, we recommend using either the KPS or CKD methods to derive accurate uptake kinetics when using a coated-wall flow reactor.

The gas flow velocity ratio between mean flow velocities in the flow reactor ($u_{\mathrm{mean}}^{\mathrm{ann}}$) and the gas flow exiting the movable injector ($u_{\mathrm{mean}}^{\mathrm{inj}}$) also impacts the derivation of γ. If $u_{\mathrm{mean}}^{\mathrm{ann}} < u_{\mathrm{mean}}^{\mathrm{inj}}$, reactive uptake experiments are ambiguous, potentially resulting in an underestimation of the uptake kinetics, as pointed out by Davis (2008). This flow condition can lead to a jet-

like exit gas flow from the movable injector. Figure A2 displays this effect when $u_{\mathrm{mean}}^{\mathrm{ann}}/u_{\mathrm{mean}}^{\mathrm{inj}} < 1$, where the measured γ values can deviate by a factor of 3 from the actual value.

For all experimentally derived γ values, we set $u_{\mathrm{mean}}^{\mathrm{ann}}/u_{\mathrm{mean}}^{\mathrm{inj}} > 1.27$ for the flow tube with 1.758 cm inner diameter (ID) and $u_{\mathrm{mean}}^{\mathrm{ann}}/u_{\mathrm{mean}}^{\mathrm{inj}} > 1.33$ for the flow tube with an ID of 1.2 cm, based on the theoretical calculation below. The velocity profile and volume flow rate Q of a Poiseuille flow in the annular section can be described by the equations (Rosenhead, 1988)

$$u(r) = \frac{G}{4\mu}\left[(R_1^2 - r^2) + (R_2^2 - R_1^2)\frac{\ln(r/R_1)}{\ln(R_2/R_1)}\right] \quad \text{(A1)}$$

and

$$Q = \int_{R_1}^{R_2} 2\pi r u(r) dr = \frac{G\pi}{8\mu}\left[R_2^4 - R_1^4 - \frac{(R_2^2 - R_1^2)^2}{\ln(R_2/R_1)}\right], \quad \text{(A2)}$$

where $u(r)$ is the flow velocity profile as a function of the radius *r*. *G* is a constant pressure gradient, μ is the dynamic viscosity, R_1 is the inner cylinder radius, R_2 is the outer cylinder radius, and *r* is a radius value between R_1 and R_2. If R_1, R_2 and constant parameters (*G* and μ) are known, the maximum flow velocity $u_{\max}$ is obtained by setting $du(r)/dr = 0$, and the mean flow velocity in the annular section u_{mean} is derived from Q/A_{ann}, where A_{ann} is the cross-sectional area of the annular section.

Using the flow tube with a diameter of 1.758 cm as an example, and setting R_1= 0.325 cm and R_2=0.879 cm, the ratio of maximum flow velocity over the average flow velocity in the annular section is $u_{\max}^{\mathrm{ann}}/u_{\mathrm{mean}}^{\mathrm{annul}}$ = 1.575. The ratio of the mean flow velocity over the maximum velocity in a tubular injector is $u_{\max}^{\mathrm{inj}}/u_{\mathrm{mean}}^{\mathrm{inj}}$= 2 as the injector flow is laminar (Rogers, 1992). Therefore, even when adjusting the gas flows in the injector and flow reactor to yield the same mean flow velocities, the difference in the maximum flow velocities can still differ significantly. In this case, the difference can be up to 27%, potentially resulting in a jet-like gas flow profile. For this reason, we set $u_{\mathrm{mean}}^{\mathrm{ann}}/u_{\mathrm{mean}}^{\mathrm{inj}} > 1.27$ to avoid this effect. In the case of using a flow tube with a diameter of 1.2 cm, $u_{\mathrm{mean}}^{\mathrm{ann}}/u_{\mathrm{mean}}^{\mathrm{inj}} > 1.33$.

Data availability

Data and code generated from this study are available from the corresponding author upon request.

Author contributions

JL conducted O_3, NO_3, and OH uptake experiments. SF performed N_2O_5 synthesis and conducted NO_3 uptake experiments. JL conducted the poke-flow experiments. JL performed all analysis of data. SF conducted analysis of NO_3 uptake data and contributed to the writing of the manuscript. JL led the writing of the manuscript. DK oversaw the project, envisioned analysis, and contributed to the writing of the manuscript.

Competing interest

The authors declare no conflict of interest.

Acknowledgements

Support from the National Science Foundation grant AGS-1446286 is acknowledged. Partial support from the U.S. Department of Energy, Office of Science (BER), Atmospheric System Research (DE-SC0016370), is acknowledged.

References

Abbatt, J. P. D., Leaitch, W. R., Aliabadi, A. A., Bertram, A. K., Blanchet, J. P., Boivin-Rioux, A., Bozem, H., Burkart, J., Chang, R. Y. W., Charette, J., Chaubey, J. P., Christensen, R. J., Cirisan, A., Collins, D. B., Croft, B., Dionne, J., Evans, G. J., Fletcher, C. G., Gali, M., Ghahremaninezhad, R., Girard, E., Gong, W. M., Gosselin, M., Gourdal, M., Hanna, S. J., Hayashida, H., Herber, A. B., Hesaraki, S., Hoor, P., Huang, L., Hussherr, R., Irish, V. E., Keita, S. A., Kodros, J. K., Kollner, F., Kolonjari, F., Kunkel, D., Ladino, L. A., Law, K., Levasseur, M., Libois, Q., Liggio, J., Lizotte, M., Macdonald, K. M., Mahmood, R., Martin, R. V., Mason, R. H., Miller, L. A., Moravek, A., Mortenson, E., Mungall, E. L., Murphy, J. G., Namazi, M., Norman, A. L., O'Neill, N. T., Pierce, J. R., Russell, L. M., Schneider, J., Schulz, H., Sharma, S., Si, M., Staebler, R. M., Steiner, N. S., Thomas, J. L., von Salzen, K., Wentzell, J. J. B., Willis, M. D., Wentworth, G. R., Xu, J. W., and Yakobi-Hancock, J. D.: Overview paper: New insights into aerosol and climate in the Arctic, Atmos. Chem. Phys., 19, 2527-2560, http://doi.org/10.5194/acp-19-2527-2019, 2019.

Abramson, E., Imre, D., Beranek, J., Wilson, J., and Zelenyuk, A.: Experimental determination of chemical diffusion within secondary organic aerosol particles, Phys. Chem. Chem. Phys., 15, 2983-2991, http://doi.org/10.1039/c2cp44013j, 2013.

Andreae, M. O., Rosenfeld, D., Artaxo, P., Costa, A. A., Frank, G. P., Longo, K. M., and Silva-Dias, M. A.: Smoking rain clouds over the Amazon, Science, 303, 1337-1342, http://doi.org/10.1126/science.1092779, 2004.

Angell, C. A.: Relaxation in liquids, polymers and plastic crystals - strong fragile patterns and problems, J. Non-Cryst. Solids, 131, 13-31, http://doi.org/10.1016/0022-3093(91)90266-9, 1991.

Angell, C. A.: Formation of glasses from liquids and biopolymers, Science, 267, 1924-1935, http://doi.org/10.1126/science.267.5206.1924, 1995.

Angell, C. A.: Liquid fragility and the glass transition in water and aqueous solutions, Chem. Rev., 102, 2627-2650, http://doi.org/10.1021/cr000689q, 2002.

Arangio, A. M., Slade, J. H., Berkemeier, T., Pöschl, U., Knopf, D. A., and Shiraiwa, M.: Multiphase chemical kinetics of OH radical uptake by molecular organic markers of biomass burning aerosols: humidity and temperature dependence, surface reaction, and bulk diffusion, J. Phys. Chem. A, 119, 4533-4544, http://doi.org/10.1021/jp510489z, 2015.

Atkinson, R.: A structure-activity relationship for the estimation of rate constants for the gas-phase reactions of OH radicals with organic compounds, Int. J. Chem. Kinet., 19, 799-828, http://doi.org/10.1002/kin.550190903, 1987.

Atkinson, R., Baulch, D. L., Cox, R. A., Crowley, J. N., Hampson, R. F., Hynes, R. G., Jenkin, M. E., Rossi, M. J., and Troe, J.: Evaluated kinetic and photochemical data for atmospheric chemistry: Volume I - gas phase reactions of O_x, HO_x, NO_x and SO_x species, Atmos. Chem. Phys., 4, 1461-1738, http://doi.org/10.5194/acp-4-1461-2004, 2004.

Atkinson, R., Baulch, D. L., Cox, R. A., Crowley, J. N., Hampson, R. F., Hynes, R. G., Jenkin, M. E., Rossi, M. J., and Troe, J.: Evaluated kinetic and photochemical data for atmospheric chemistry: Volume II - gas phase reactions of organic species, Atmos. Chem. Phys., 6, 3625-4055, http://doi.org/10.5194/acp-6-3625-2006, 2006.

Baetzold, R., and Somorjai, G. A.: Preexponential factors in surface reactions, J. Catal., 45, 94-105, http://doi.org/10.1016/0021-9517(76)90059-2, 1976.

Bai, J., Sun, X., Zhang, C., Xu, Y., and Qi, C.: The OH-initiated atmospheric reaction mechanism and kinetics for levoglucosan emitted in biomass burning, Chemosphere, 93, 2004-2010, http://doi.org/10.1016/j.chemosphere.2013.07.021, 2013.

Berkemeier, T., Shiraiwa, M., Pöschl, U., and Koop, T.: Competition between water uptake and ice nucleation by glassy organic aerosol particles, Atmos. Chem. Phys., 14, 12513-12531, http://doi.org/10.5194/acp-14-12513-2014, 2014.

Berkemeier, T., Steimer, S. S., Krieger, U. K., Peter, T., Pöschl, U., Ammann, M., and Shiraiwa, M.: Ozone uptake on glassy, semi-solid and liquid organic matter and the role of reactive oxygen intermediates in atmospheric aerosol chemistry, Phys. Chem. Chem. Phys., 18, 12662-12674, http://doi.org/10.1039/c6cp00634e, 2016.

Bertram, A. K., Ivanov, A. V., Hunter, M., Molina, L. T., and Molina, M. J.: The reaction probability of OH on organic surfaces of tropospheric interest, J. Phys. Chem. A, 105, 9415-9421, http://doi.org/10.1021/jp0114034, 2001.

Bertram, A. K., Martin, S. T., Hanna, S. J., Smith, M. L., Bodsworth, A., Chen, Q., Kuwata, M., Liu, A., You, Y., and Zorn, S. R.: Predicting the relative humidities of liquid-liquid phase separation, efflorescence, and deliquescence of mixed particles of ammonium sulfate, organic material, and water using the organic-to-sulfate mass ratio of the particle and the oxygen-to-carbon elemental ratio of the organic component, Atmos. Chem. Phys., 11, 10995-11006, http://doi.org/10.5194/acp-11-10995-2011, 2011.

Borde, B., Bizot, H., Vigier, G., and Buleon, A.: Calorimetric analysis of the structural relaxation in partially hydrated amorphous polysaccharides. I. Glass transition and fragility, Carbohyd. Polym., 48, 83-96, http://doi.org/10.1016/s0144-8617(01)00217-x, 2002.

Brown, R.: Tubular flow reactors with first-order kinetics, J. Res. Natl. Bur. Stand, 83, 1-8, 1978.

Brown, S. S., Ryerson, T. B., Wollny, A. G., Brock, C. A., Peltier, R., Sullivan, A. P., Weber, R. J., Dube, W. P., Trainer, M., Meagher, J. F., Fehsenfeld, F. C., and Ravishankara, A. R.: Variability in nocturnal nitrogen oxide processing and its role in regional air quality, Science, 311, 67-70, http://doi.org/10.1126/science.1120120, 2006.

Charnawskas, J. C., Alpert, P. A., Lambe, A. T., Berkemeier, T., O'Brien, R. E., Massoli, P., Onasch, T. B., Shiraiwa, M., Moffet, R. C., Gilles, M. K., Davidovits, P., Worsnop, D. R., and Knopf, D. A.: Condensed-phase biogenic-anthropogenic interactions with implications for cold cloud formation, Faraday Discuss., 200, 165-194, http://doi.org/10.1039/c7fd00010c, 2017.

Chenyakin, Y., Ullmann, D. A., Evoy, E., Renbaum-Wolff, L., Kamal, S., and Bertram, A. K.: Diffusion coefficients of organic molecules in sucrose-water solutions and comparison with Stokes-Einstein predictions, Atmos. Chem. Phys., 17, 2423-2435, http://doi.org/10.5194/acp-17-2423-2017, 2017.

Comunas, M. J. P., Paredes, X., Gacino, F. M., Fernandez, J., Bazile, J. P., Boned, C., Daridon, J. L., Galliero, G., Pauly, J., Harris, K. R., Assael, M. J., and Mylona, S. K.: Reference Correlation of the Viscosity of Squalane from 273 to 373 K at 0.1 MPa, J. Phys. Chem. Ref. Data, 42, http://doi.org/10.1063/1.4812573, 2013.

Cosman, L. M., and Bertram, A. K.: Reactive uptake of N_2O_5 on aqueous H_2SO_4 solutions coated with 1-component and 2-component monolayers, J. Phys. Chem. A, 112, 4625-4635, http://doi.org/10.1021/jp8005469, 2008.

Cubison, M. J., Ortega, A. M., Hayes, P. L., Farmer, D. K., Day, D., Lechner, M. J., Brune, W. H., Apel, E., Diskin, G. S., Fisher, J. A., Fuelberg, H. E., Hecobian, A., Knapp, D. J., Mikoviny, T., Riemer, D., Sachse, G. W., Sessions, W., Weber, R. J., Weinheimer, A. J., Wisthaler, A., and Jimenez, J. L.: Effects of aging on organic aerosol from open biomass burning smoke in aircraft and laboratory studies, Atmos. Chem. Phys., 11, 12049-12064, http://doi.org/10.5194/acp-11-12049-2011, 2011.

Davies, J. F., and Wilson, K. R.: Nanoscale interfacial gradients formed by the reactive uptake of OH radicals onto viscous aerosol surfaces, Chem. Sci., 6, 7020-7027, http://doi.org/10.1039/c5sc02326b, 2015.

Davies, J. F., and Wilson, K. R.: Raman Spectroscopy of Isotopic Water Diffusion in Ultraviscous, Glassy, and Gel States in Aerosol by Use of Optical Tweezers, Anal. Chem., 88, 2361-2366, http://doi.org/10.1021/acs.analchem.5b04315, 2016.

Davis, E. J.: Interpretation of uptake coefficient data obtained with flow tubes, J. Phys. Chem. A, 112, 1922-1932, http://doi.org/10.1021/jp074939j, 2008.

de Gouw, J. A., and Lovejoy, E. R.: Reactive uptake of ozone by liquid organic compounds, Geophys. Res. Lett., 25, 931-934, http://doi.org/10.1029/98gl00515, 1998.

DeRieux, W.-S. W., Li, Y., Lin, P., Laskin, J., Laskin, A., Bertram, A. K., Nizkorodov, S. A., and Shiraiwa, M.: Predicting the glass transition temperature and viscosity of secondary organic material using molecular composition, Atmos. Chem. Phys., 18, 6331-6351, http://doi.org/10.5194/acp-18-6331-2018, 2018.

Deshler, T.: A review of global stratospheric aerosol: Measurements, importance, life cycle, and local stratospheric aerosol, Atmos. Res., 90, 223-232, http://doi.org/10.1016/j.atmosres.2008.03.016, 2008.

Dette, H. P., and Koop, T.: Glass Formation Processes in Mixed Inorganic/Organic Aerosol Particles, J. Phys. Chem. A, 119, 4552-4561, http://doi.org/10.1021/jp5106967, 2015.

Diogo, H. P., and Ramos, J. J. M.: Slow molecular mobility in the crystalline and amorphous solid states of glucose as studied by thermally stimulated depolarization currents (TSDC), Carbohydr. Res., 343, 2797-2803, http://doi.org/10.1016/j.carres.2008.07.002, 2008.

Dorfmüller, T., Dux, H., Fytas, G., and Mersch, W.: A light scattering study of the molecular motion in hexanetriol 1,2,6, J. Chem. Phys., 71, 366-375, http://doi.org/10.1063/1.438079, 1979.

Edebeli, J., Ammann, M., and Bartels-Rausch, T.: Microphysics of the aqueous bulk counters the water activity driven rate acceleration of bromide oxidation by ozone from 289-245 K, Environ. Sci-Proc. Imp., 21, 63-73, http://doi.org/10.1039/c8em00417j, 2019.

Elias, M. E., and Elias, A. M.: Trehalose plus water fragile system: properties and glass transition, J. Mol. Liq., 83, 303-310, http://doi.org/10.1016/s0167-7322(99)00094-x, 1999.

Ervens, B., Turpin, B. J., and Weber, R. J.: Secondary organic aerosol formation in cloud droplets and aqueous particles (aqSOA): a review of laboratory, field and model studies, Atmos. Chem. Phys., 11, 11069-11102, http://doi.org/10.5194/acp-11-11069-2011, 2011.

Fasina, O. O., Hallman, H., Craig-Schmidt, M., and Clements, C.: Predicting temperature-dependence viscosity of vegetable oils from fatty acid composition, J. Am. Oil Chem. Soc., 83, 899-903, http://doi.org/10.1007/s11746-006-5044-8, 2006.

Fasina, O. O., Craig-Schmidt, M., Colley, Z., and Hallman, H.: Predicting melting characteristics of vegetable oils from fatty acid composition, LWT-Food Sci. Technol., 41, 1501-1505, http://doi.org/10.1016/j.lwt.2007.09.012, 2008.

Finlayson-Pitts, B. J., and Pitts Jr, J. N.: Chemistry of the upper and lower atmosphere: theory, experiments, and applications, Academic, San Diego, 969 pp., 1999.

Fromm, M. D., and Servranckx, R.: Transport of forest fire smoke above the tropopause by supercell convection, Geophys. Res. Lett., 30, 1542, http://doi.org/10.1029/2002gl016820, 2003.

Fuchs, N., and Sutugin, A. G.: High-dispersed aerosols, in: Topics in current aerosol research, Pergamon Press, Oxford, 1, http://doi.org/10.1016/B978-0-08-016674-2.50006-6, 1971.

Fuller, E. N., Schettler, P. D., and Giddings, J. C.: New Method for Prediction of Binary Gas-Phase Diffusion Coefficients, Ind. Eng. Chem., 58, 18-27, http://doi.org/10.1021/ie50677a007, 1966.

Gaston, C. J., Thornton, J. A., and Ng, N. L.: Reactive uptake of N_2O_5 to internally mixed inorganic and organic particles: the role of organic carbon oxidation state and inferred organic phase separations, Atmos. Chem. Phys, 14, 5693-5707, 2014.

Gates, W. L., Boyle, J. S., Covey, C., Dease, C. G., Doutriaux, C. M., Drach, R. S., Fiorino, M., Gleckler, P. J., Hnilo, J. J., Marlais, S. M., Phillips, T. J., Potter, G. L., Santer, B. D., Sperber, K. R., Taylor, K. E., and Williams, D. N.: An Overview of the Results of the Atmospheric Model Intercomparison Project (AMIP I), Bull. Am. Meteorol. Soc., 80, 29-55, http://doi.org/10.1175/1520-0477(1999)080<0029:Aootro>2.0.Co;2, 1999.

George, I. J., Vlasenko, A., Slowik, J. G., Broekhuizen, K., and Abbatt, J. P. D.: Heterogeneous oxidation of saturated organic aerosols by hydroxyl radicals: uptake kinetics, condensed-phase products, and particle size change, Atmos. Chem. Phys., 7, 4187-4201, http://doi.org/10.5194/acp-7-4187-2007, 2007.
George, I. J., and Abbatt, J. P.: Heterogeneous oxidation of atmospheric aerosol particles by gas-phase radicals, Nat. Chem., 2, 713-722, http://doi.org/10.1038/nchem.806, 2010.
Gershenzon, Y. M., Grigorieva, V. M., Ivanov, A. V., and Remorov, R. G.: O_3 and OH sensitivity to heterogeneous sinks of HO_x and CH_3O_2 on aerosol particles, Faraday Discuss., 100, 83-100, http://doi.org/10.1039/fd9950000083, 1995.
Ghazani, S. M., and Marangoni, A. G.: Minor Components in Canola Oil and Effects of Refining on These Constituents: A Review, J. Am. Oil Chem. Soc., 90, 923-932, http://doi.org/10.1007/s11746-013-2254-8, 2013.
Gordon, M., and Taylor, J. S.: Ideal copolymers and the second-order transitions of synthetic rubbers. i. non-crystalline copolymers, J. Appl. Chem., 2, 493-500, http://doi.org/10.1002/jctb.5010020901, 2007.
Gross, S., and Bertram, A. K.: Products and kinetics of the reactions of an alkane monolayer and a terminal alkene monolayer with NO_3 radicals, J. Geophys. Res., 114, http://doi.org/10.1029/2008jd010987, 2009.
Gross, S., Iannone, R., Xiao, S., and Bertram, A. K.: Reactive uptake studies of NO3 and N2O5 on alkenoic acid, alkanoate, and polyalcohol substrates to probe nighttime aerosol chemistry, Phys. Chem. Chem. Phys., 11, 7792-7803, http://doi.org/10.1039/b904741g, 2009.
Hallquist, M., Wenger, J. C., Baltensperger, U., Rudich, Y., Simpson, D., Claeys, M., Dommen, J., Donahue, N. M., George, C., Goldstein, A. H., Hamilton, J. F., Herrmann, H., Hoffmann, T., Iinuma, Y., Jang, M., Jenkin, M. E., Jimenez, J. L., Kiendler-Scharr, A., Maenhaut, W., McFiggans, G., Mentel, T. F., Monod, A., Prévôt, A. S. H., Seinfeld, J. H., Surratt, J. D., Szmigielski, R., and Wildt, J.: The formation, properties and impact of secondary organic aerosol: current and emerging issues, Atmos. Chem. Phys., 9, 5155-5236, http://doi.org/10.5194/acp-9-5155-2009, 2009.
Hanson, D. R., and Ravishankara, A. R.: The reaction probabilities of $ClONO_2$and N_2O_5on polar stratospheric cloud materials, J. Geophys. Res., 96, 5081-5090, http://doi.org/10.1029/90jd02613, 1991.
Hearn, J. D., Lovett, A. J., and Smith, G. D.: Ozonolysis of oleic acid particles: evidence for a surface reaction and secondary reactions involving Criegee intermediates, Phys. Chem. Chem. Phys., 7, 501-511, http://doi.org/10.1039/b414472d, 2005.
Hopke, P. K.: Review of receptor modeling methods for source apportionment, J. Air Waste Manage., 66, 237-259, http://doi.org/10.1080/10962247.2016.1140693, 2016.
Houle, F. A., Hinsberg, W. D., and Wilson, K. R.: Oxidation of a model alkane aerosol by OH radical: the emergent nature of reactive uptake, Phys. Chem. Chem. Phys., 17, 4412-4423, http://doi.org/10.1039/c4cp05093b, 2015.
Houle, F. A., Wiegel, A. A., and Wilson, K. R.: Predicting Aerosol Reactivity Across Scales: from the Laboratory to the Atmosphere, Environ. Sci. Technol., 52, 13774-13781, http://doi.org/10.1021/acs.est.8b04688, 2018a.
Houle, F. A., Wiegel, A. A., and Wilson, K. R.: Changes in Reactivity as Chemistry Becomes Confined to an Interface. The Case of Free Radical Oxidation of C30H62 Alkane by OH, J. Phys. Chem. Lett., 9, 1053-1057, http://doi.org/10.1021/acs.jpclett.8b00172, 2018b.
Hu, W. W., Palm, B. B., Day, D. A., Campuzano-Jost, P., Krechmer, J. E., Peng, Z., de Sa, S. S., Martin, S. T., Alexander, M. L., Baumann, K., Hacker, L., Kiendler-Scharr, A., Koss, A. R., de Gouw, J. A., Goldstein, A. H., Seco, R., Sjostedt, S. J., Park, J. H., Guenther, A. B., Kim, S., Canonaco, F., Prevot, A. S. H., Brune, W. H., and Jimenez, J. L.: Volatility and lifetime against OH heterogeneous reaction of ambient isoprene-epoxydiols-derived secondary organic aerosol (IEPOX-SOA), Atmos. Chem. Phys., 16, 11563-11580, http://doi.org/10.5194/acp-16-11563-2016, 2016.
Iinuma, Y., Bruggemann, E., Gnauk, T., Muller, K., Andreae, M. O., Helas, G., Parmar, R., and Herrmann, H.: Source characterization of biomass burning particles: The combustion of selected European conifers, African hardwood, savanna grass, and German and Indonesian peat, J. Geophys. Res., 112, http://doi.org/10.1029/2006jd007120, 2007.
Ivanov, A. V., Trakhtenberg, S., Bertram, A. K., Gershenzon, Y. M., and Molina, M. J.: OH, HO_2, and ozone gaseous diffusion coefficients, J. Phys. Chem. A, 111, 1632-1637, http://doi.org/10.1021/jp066558w, 2007.
Iwahashi, M., Kasahara, Y., Matsuzawa, H., Yagi, K., Nomura, K., Terauchi, H., Ozaki, Y., and Suzuki, M.: Self-Diffusion, Dynamical Molecular Conformation, and Liquid Structures of n-Saturated and Unsaturated Fatty Acids, J. Phys. Chem. B, 104, 6186-6194, http://doi.org/10.1021/jp000610l, 2000.
Iwahashi, M., and Kasahara, Y.: Dynamic molecular movements and aggregation structures of lipids in a liquid state, Curr. Opin. Colloid In., 16, 359-366, http://doi.org/10.1016/j.cocis.2011.06.005, 2011.
Jimenez, J. L., Canagaratna, M. R., Donahue, N. M., Prevot, A. S., Zhang, Q., Kroll, J. H., DeCarlo, P. F., Allan, J. D., Coe, H., Ng, N. L., Aiken, A. C., Docherty, K. S., Ulbrich, I. M., Grieshop, A. P., Robinson, A. L., Duplissy, J., Smith, J. D., Wilson, K. R., Lanz, V. A., Hueglin, C., Sun, Y. L., Tian, J., Laaksonen, A., Raatikainen, T., Rautiainen, J., Vaattovaara, P., Ehn, M., Kulmala, M., Tomlinson, J. M., Collins, D. R., Cubison, M. J., Dunlea, E. J., Huffman, J. A., Onasch, T. B., Alfarra, M. R., Williams, P. I., Bower, K., Kondo, Y., Schneider, J., Drewnick, F., Borrmann, S., Weimer, S., Demerjian, K., Salcedo, D., Cottrell, L., Griffin, R., Takami, A., Miyoshi, T., Hatakeyama, S., Shimono, A., Sun, J. Y., Zhang, Y. M., Dzepina, K., Kimmel, J. R., Sueper, D., Jayne, J. T., Herndon, S. C., Trimborn, A. M., Williams, L. R., Wood, E. C., Middlebrook, A. M., Kolb, C. E., Baltensperger, U., and Worsnop, D. R.: Evolution of organic aerosols in the atmosphere, Science, 326, 1525-1529, http://doi.org/10.1126/science.1180353, 2009.

Jost, H. J., Drdla, K., Stohl, A., Pfister, L., Loewenstein, M., Lopez, J. P., Hudson, P. K., Murphy, D. M., Cziczo, D. J., Fromm, M., Bui, T. P., Dean-Day, J., Gerbig, C., Mahoney, M. J., Richard, E. C., Spichtinger, N., Pittman, J. V., Weinstock, E. M., Wilson, J. C., and Xueref, I.: In-situ observations of mid-latitude forest fire plumes deep in the stratosphere, Geophys. Res. Lett., 31, L11101, http://doi.org/10.1029/2003gl019253, 2004.

Kaiser, J. C., Riemer, N., and Knopf, D. A.: Detailed heterogeneous oxidation of soot surfaces in a particle-resolved aerosol model, Atmos. Chem. Phys., 11, 4505-4520, http://doi.org/10.5194/acp-11-4505-2011, 2011.

Kanakidou, M., Seinfeld, J. H., Pandis, S. N., Barnes, I., Dentener, F. J., Facchini, M. C., Van Dingenen, R., Ervens, B., Nenes, A., Nielsen, C. J., Swietlicki, E., Putaud, J. P., Balkanski, Y., Fuzzi, S., Horth, J., Moortgat, G. K., Winterhalter, R., Myhre, C. E. L., Tsigaridis, K., Vignati, E., Stephanou, E. G., and Wilson, J.: Organic aerosol and global climate modelling: a review, Atmos. Chem. Phys., 5, 1053-1123, http://doi.org/10.5194/acp-5-1053-2005, 2005.

Katrib, Y., Biskos, G., Buseck, P. R., Davidovits, P., Jayne, J. T., Mochida, M., Wise, M. E., Worsnop, D. R., and Martin, S. T.: Ozonolysis of mixed oleic-acid/stearic-acid particles: reaction kinetics and chemical morphology, J. Phys. Chem. A, 109, 10910-10919, http://doi.org/10.1021/jp054714d, 2005a.

Katrib, Y., Martin, S. T., Rudich, Y., Davidovits, P., Jayne, J. T., and Worsnop, D. R.: Density changes of aerosol particles as a result of chemical reaction, Atmos. Chem. Phys., 5, 275-291, http://doi.org/10.5194/acp-5-275-2005, 2005b.

Kawamura, K., Ishimura, Y., and Yamazaki, K.: Four years' observations of terrestrial lipid class compounds in marine aerosols from the western North Pacific, Global Biogeochem. Cycles, 17, http://doi.org/10.1029/2001gb001810, 2003.

Kerdouci, J., Picquet-Varrault, B., and Doussin, J.-F.: Structure–activity relationship for the gas-phase reactions of NO_3 radical with organic compounds: Update and extension to aldehydes, Atmos. Environ., 84, 363-372, http://doi.org/10.1016/j.atmosenv.2013.11.024, 2014.

Kessler, S. H., Smith, J. D., Che, D. L., Worsnop, D. R., Wilson, K. R., and Kroll, J. H.: Chemical sinks of organic aerosol: kinetics and products of the heterogeneous oxidation of erythritol and levoglucosan, Environ. Sci. Technol., 44, 7005-7010, http://doi.org/10.1021/es101465m, 2010.

Kidd, C., Perraud, V., Wingen, L. M., and Finlayson-Pitts, B. J.: Integrating phase and composition of secondary organic aerosol from the ozonolysis of alpha-pinene, Proc. Nat. Acad. Sci. U.S.A., 111, 7552-7557, http://doi.org/10.1073/pnas.1322558111, 2014.

Kiland, K. J., Maclean, A. M., Kamal, S., and Bertram, A. K.: Diffusion of Organic Molecules as a Function of Temperature in a Sucrose Matrix (a Proxy for Secondary Organic Aerosol), J. Phys. Chem. Lett., 10, 5902-+, http://doi.org/10.1021/acs.jpclett.9b02182, 2019.

Knopf, D. A., Anthony, L. M., and Bertram, A. K.: Reactive uptake of O_3 by multicomponent and multiphase mixtures containing oleic acid, J. Phys. Chem. A, 109, 5579-5589, http://doi.org/10.1021/jp0512513, 2005.

Knopf, D. A., Mak, J., Gross, S., and Bertram, A. K.: Does atmospheric processing of saturated hydrocarbon surfaces by NO_3 lead to volatilization?, Geophys. Res. Lett., 33, L17816, http://doi.org/10.1029/2006gl026884, 2006.

Knopf, D. A., Cosman, L. M., Mousavi, P., Mokamati, S., and Bertram, A. K.: A novel flow reactor for studying reactions on liquid surfaces coated by organic monolayers: methods, validation, and initial results, J. Phys. Chem. A, 111, 11021-11032, http://doi.org/10.1021/jp075724c, 2007.

Knopf, D. A., and Forrester, S. M.: Freezing of water and aqueous NaCl droplets coated by organic monolayers as a function of surfactant properties and water activity, J. Phys. Chem. A, 115, 5579-5591, http://doi.org/10.1021/jp2014644, 2011.

Knopf, D. A., Forrester, S. M., and Slade, J. H.: Heterogeneous oxidation kinetics of organic biomass burning aerosol surrogates by O_3, NO_2, N_2O_5, and NO_3, Phys. Chem. Chem. Phys., 13, 21050-21062, http://doi.org/10.1039/c1cp22478f, 2011.

Knopf, D. A., Pöschl, U., and Shiraiwa, M.: Radial diffusion and penetration of gas molecules and aerosol particles through laminar flow reactors, denuders, and sampling tubes, Anal. Chem., 87, 3746-3754, http://doi.org/10.1021/ac5042395, 2015.

Knopf, D. A., Alpert, P. A., and Wang, B.: The Role of Organic Aerosol in Atmospheric Ice Nucleation: A Review, ACS Earth Space Chem., 2, 168-202, http://doi.org/10.1021/acsearthspacechem.7b00120, 2018.

Kolesar, K. R., Buffaloe, G., Wilson, K. R., and Cappa, C. D.: OH-initiated heterogeneous oxidation of internally-mixed squalane and secondary organic aerosol, Environ. Sci. Technol., 48, 3196-3202, http://doi.org/10.1021/es405177d, 2014.

Koop, T., Bookhold, J., Shiraiwa, M., and Pöschl, U.: Glass transition and phase state of organic compounds: dependency on molecular properties and implications for secondary organic aerosols in the atmosphere, Phys. Chem. Chem. Phys., 13, 19238-19255, http://doi.org/10.1039/c1cp22617g, 2011.

Kroll, J. H., Lim, C. Y., Kessler, S. H., and Wilson, K. R.: Heterogeneous Oxidation of Atmospheric Organic Aerosol: Kinetics of Changes to the Amount and Oxidation State of Particle-Phase Organic Carbon, J. Phys. Chem. A, 119, 10767-10783, http://doi.org/10.1021/acs.jpca.5b06946, 2015.

Kwok, E., and Atkinson, R.: Estimation of hydroxyl radical reaction rate constants for gas-phase organic compounds using a structure-reactivity relationship: An update, Atmos. Environ., 29, 1685-1695, http://doi.org/10.1016/1352-2310(95)00069-b, 1995.

Laidler, K. J., Glasstone, S., and Eyring, H.: Application of the Theory of Absolute Reaction Rates to Heterogeneous Processes I. The Adsorption and Desorption of Gases, J. Chem. Phys., 8, 659-667, http://doi.org/10.1063/1.1750736, 1940.

Laskin, A., Laskin, J., and Nizkorodov, S. A.: Chemistry of atmospheric brown carbon, Chem. Rev., 115, 4335-4382, http://doi.org/10.1021/cr5006167, 2015.

Laskin, A., Gilles, M. K., Knopf, D. A., Wang, B. B., and China, S.: Progress in the Analysis of Complex Atmospheric Particles, in: Annual Review of Analytical Chemistry, Vol 9, edited by: Bohn, P. W., and Pemberton, J. E., Annu. Rev. Anal. Chem., 117-143, http://doi.org/10.1146/annurev-anchem-071015-041521, 2016.

Laskin, A., Moffet, R. C., and Gilles, M. K.: Chemical Imaging of Atmospheric Particles, Acc. Chem. Res., 52, 3419-3431, http://doi.org/10.1021/acs.accounts.9b00396, 2019.

Lee, L., and Wilson, K.: The Reactive-Diffusive Length of OH and Ozone in Model Organic Aerosols, J. Phys. Chem. A, 120, 6800-6812, http://doi.org/10.1021/acs.jpca.6b05285, 2016.

Li, Z., Smith, K. A., and Cappa, C. D.: Influence of relative humidity on the heterogeneous oxidation of secondary organic aerosol, Atmos. Chem. Phys., 18, 14585-14608, http://doi.org/10.5194/acp-18-14585-2018, 2018.

Lienhard, D. M., Huisman, A. J., Krieger, U. K., Rudich, Y., Marcolli, C., Luo, B. P., Bones, D. L., Reid, J. P., Lambe, A. T., Canagaratna, M. R., Davidovits, P., Onasch, T. B., Worsnop, D. R., Steimer, S. S., Koop, T., and Peter, T.: Viscous organic aerosol particles in the upper troposphere: diffusivity-controlled water uptake and ice nucleation?, Atmos. Chem. Phys., 15, 13599-13613, http://doi.org/10.5194/acp-15-13599-2015, 2015.

Lignell, H., Hinks, M. L., and Nizkorodov, S. A.: Exploring matrix effects on photochemistry of organic aerosols, Proc. Nat. Acad. Sci. U.S.A., 111, 13780-13785, http://doi.org/10.1073/pnas.1322106111, 2014.

Limbeck, A., and Puxbaum, H.: Organic acids in continental background aerosols, Atmos. Environ., 33, 1847-1852, http://doi.org/10.1016/s1352-2310(98)00347-1, 1999.

Liu, T. Y., Li, Z. J., Chan, M. N., and Chan, C. K.: Formation of secondary organic aerosols from gas-phase emissions of heated cooking oils, Atmos. Chem. Phys., 17, 7333-7344, http://doi.org/10.5194/acp-17-7333-2017, 2017.

Liu, Y., Ivanov, A. V., and Molina, M. J.: Temperature dependence of OH diffusion in air and He, Geophys. Res. Lett., 36, L03816, http://doi.org/10.1029/2008gl036170, 2009.

Marsh, A., Petters, S. S., Rothfuss, N. E., Rovelli, G., Song, Y. C., Reid, J. P., and Petters, M. D.: Amorphous phase state diagrams and viscosity of ternary aqueous organic/organic and inorganic/organic mixtures, Phys. Chem. Chem. Phys., 20, 15086-15097, http://doi.org/10.1039/c8cp00760h, 2018.

Marshall, F. H., Berkemeier, T., Shiraiwa, M., Nandy, L., Ohm, P. B., Dutcher, C. S., and Reid, J. P.: Influence of particle viscosity on mass transfer and heterogeneous ozonolysis kinetics in aqueous-sucrose-maleic acid aerosol, Phys. Chem. Chem. Phys., 20, 15560-15573, http://doi.org/10.1039/c8cp01666f, 2018.

Mason, E. A., and Monchick, L.: Transport Properties of Polar-Gas Mixtures, J. Chem. Phys., 36, 2746-2757, http://doi.org/10.1063/1.1732363, 1962.

McFiggans, G., Mentel, T. F., Wildt, J., Pullinen, I., Kang, S., Kleist, E., Schmitt, S., Springer, M., Tillmann, R., Wu, C., Zhao, D., Hallquist, M., Faxon, C., Le Breton, M., Hallquist, A. M., Simpson, D., Bergstrom, R., Jenkin, M. E., Ehn, M., Thornton, J. A., Alfarra, M. R., Bannan, T. J., Percival, C. J., Priestley, M., Topping, D., and Kiendler-Scharr, A.: Secondary organic aerosol reduced by mixture of atmospheric vapours, Nature, 565, 587-593, http://doi.org/10.1038/s41586-018-0871-y, 2019.

McNeill, V. F., Patterson, J., Wolfe, G. M., and Thornton, J. A.: The effect of varying levels of surfactant on the reactive uptake of N_2O_5 to aqueous aerosol, Atmos. Chem. Phys., 6, 1635-1644, http://doi.org/10.5194/acp-6-1635-2006, 2006.

Mellouki, A., Le Bras, G., and Sidebottom, H.: Kinetics and mechanisms of the oxidation of oxygenated organic compounds in the gas phase, Chem. Rev., 103, 5077-5096, http://doi.org/10.1021/cr020526x, 2003.

Mikhailov, E., Vlasenko, S., Martin, S. T., Koop, T., and Pöschl, U.: Amorphous and crystalline aerosol particles interacting with water vapor: conceptual framework and experimental evidence for restructuring, phase transitions and kinetic limitations, Atmos. Chem. Phys., 9, 9491-9522, http://doi.org/10.5194/acp-9-9491-2009, 2009.

Moise, T., and Rudich, Y.: Reactive uptake of ozone by proxies for organic aerosols: Surface versus bulk processes, J. Geophys. Res., 105, 14667-14676, http://doi.org/10.1029/2000jd900071, 2000.

Moise, T., and Rudich, Y.: Uptake of Cl and Br by organic surfaces-A perspective on organic aerosols processing by tropospheric oxidants, Geophys. Res. Lett., 28, 4083-4086, http://doi.org/10.1029/2001gl013583, 2001.

Moise, T., and Rudich, Y.: Reactive Uptake of Ozone by Aerosol-Associated Unsaturated Fatty Acids: Kinetics, Mechanism, and Products, J. Phys. Chem. A, 106, 6469-6476, http://doi.org/10.1021/jp025597e, 2002.

Moise, T., Talukdar, R. K., Frost, G. J., Fox, R. W., and Rudich, Y.: Reactive uptake of NO_3 by liquid and frozen organics, J. Geophys. Res., 107, http://doi.org/10.1029/2001jd000334, 2002.

Moise, T., Flores, J. M., and Rudich, Y.: Optical properties of secondary organic aerosols and their changes by chemical processes, Chem. Rev., 115, 4400-4439, http://doi.org/10.1021/cr5005259, 2015.

Moridnejad, A., and Preston, T. C.: Models of Isotopic Water Diffusion in Spherical Aerosol Particles, J. Phys. Chem. A, 120, 9759-9766, http://doi.org/10.1021/acs.jpca.6b11241, 2016.

Mu, Q., Shiraiwa, M., Octaviani, M., Ma, N., Ding, A. J., Su, H., Lammel, G., Pöschl, U., and Cheng, Y. F.: Temperature effect on phase state and reactivity controls atmospheric multiphase chemistry and transport of PAHs, Science Advances, 4, UNSP eaap7314, http://doi.org/10.1126/sciadv.aap7314, 2018.

Murphy, D. M., and Fahey, D. W.: Mathematical treatment of the wall loss of a trace species in denuder and catalytic converter tubes, Anal. Chem., 59, 2753-2759, http://doi.org/10.1021/ac00150a006, 1987.
Murray, B. J., Wilson, T. W., Dobbie, S., Cui, Z. Q., Al-Jumur, S., Mohler, O., Schnaiter, M., Wagner, R., Benz, S., Niemand, M., Saathoff, H., Ebert, V., Wagner, S., and Karcher, B.: Heterogeneous nucleation of ice particles on glassy aerosols under cirrus conditions, Nat. Geosci., 3, 233-237, http://doi.org/10.1038/ngeo817, 2010.
Murray, B. J., Haddrell, A. E., Peppe, S., Davies, J. F., Reid, J. P., amp, apos, Sullivan, D., Price, H. C., Kumar, R., Saunders, R. W., Plane, J. M. C., Umo, N. S., and Wilson, T. W.: Glass formation and unusual hygroscopic growth of iodic acid solution droplets with relevance for iodine mediated particle formation in the marine boundary layer, Atmos. Chem. Phys., 12, 8575-8587, http://doi.org/10.5194/acp-12-8575-2012, 2012.
Nah, T., Kessler, S. H., Daumit, K. E., Kroll, J. H., Leone, S. R., and Wilson, K. R.: Influence of molecular structure and chemical functionality on the heterogeneous OH-initiated oxidation of unsaturated organic particles, J. Phys. Chem. A, 118, 4106-4119, http://doi.org/10.1021/jp502666g, 2014.
Orlando, J. J., Tyndall, G. S., and Ceazan, N.: Rate Coefficients and Product Yields from Reaction of OH with 1-Penten-3-ol, (Z)-2-Penten-1-ol, and Allyl Alcohol (2-Propen-1-ol), J. Phys. Chem. A, 105, 3564-3569, http://doi.org/10.1021/jp0041712, 2001.
Pachauri, R. K., Allen, M. R., Barros, V. R., Broome, J., Cramer, W., Christ, R., Church, J. A., Clarke, L., Dahe, Q., and Dasgupta, P.: Climate change 2014: synthesis report. Contribution of Working Groups I, II and III to the fifth assessment report of the Intergovernmental Panel on Climate Change, IPCC, Geneva, 151 pp., 2014.
Pajunoja, A., Hu, W. W., Leong, Y. J., Taylor, N. F., Miettinen, P., Palm, B. B., Mikkonen, S., Collins, D. R., Jimenez, J. L., and Virtanen, A.: Phase state of ambient aerosol linked with water uptake and chemical aging in the southeastern US, Atmos. Chem. Phys., 16, 11163-11176, http://doi.org/10.5194/acp-16-11163-2016, 2016.
Peterson, D. A., Campbell, J. R., Hyer, E. J., Fromm, M. D., Kablick, G. P., Cossuth, J. H., and DeLand, M. T.: Wildfire-driven thunderstorms cause a volcano-like stratospheric injection of smoke, NPJ Clim. Atmos. Sci., 1, 30, http://doi.org/10.1038/s41612-018-0039-3, 2018.
Petters, S. S., Kreidenweis, S. M., Grieshop, A. P., Ziemann, P. J., and Petters, M. D.: Temperature- and Humidity-Dependent Phase States of Secondary Organic Aerosols, Geophys. Res. Lett., 46, 1005-1013, http://doi.org/10.1029/2018gl080563, 2019.
Pöschl, U., Rudich, Y., and Ammann, M.: Kinetic model framework for aerosol and cloud surface chemistry and gas-particle interactions–Part 1: General equations, parameters, and terminology, Atmos. Chem. Phys., 7, 5989-6023, http://doi.org/acp-7-5989-2007, 2007.
Pöschl, U., and Shiraiwa, M.: Multiphase chemistry at the atmosphere-biosphere interface influencing climate and public health in the anthropocene, Chem Rev, 115, 4440-4475, http://doi.org/10.1021/cr500487s, 2015.
Price, H. C., Mattsson, J., Zhang, Y., Bertram, A. K., Davies, J. F., Grayson, J. W., Martin, S. T., O'Sullivan, D., Reid, J. P., Rickards, A. M. J., and Murray, B. J.: Water diffusion in atmospherically relevant alpha-pinene secondary organic material, Chem. Sci., 6, 4876-4883, http://doi.org/10.1039/c5sc00685f, 2015.
Reid, J. P., Bertram, A. K., Topping, D. O., Laskin, A., Martin, S. T., Petters, M. D., Pope, F. D., and Rovelli, G.: The viscosity of atmospherically relevant organic particles, Nat. Commun., 9, 956, http://doi.org/10.1038/s41467-018-03027-z, 2018.
Renbaum-Wolff, L., Grayson, J. W., Bateman, A. P., Kuwata, M., Sellier, M., Murray, B. J., Shilling, J. E., Martin, S. T., and Bertram, A. K.: Viscosity of alpha-pinene secondary organic material and implications for particle growth and reactivity, Proc. Nat. Acad. Sci. U.S.A., 110, 8014-8019, http://doi.org/10.1073/pnas.1219548110, 2013.
Riemer, N., Ault, A. P., West, M., Craig, R. L., and Curtis, J. H.: Aerosol Mixing State: Measurements, Modeling, and Impacts, Rev. Geophys., 57, 187-249, http://doi.org/10.1029/2018rg000615, 2019.
Robinson, A. L., Subramanian, R., Donahue, N. M., Bernardo-Bricker, A., and Rogge, W. F.: Source apportionment of molecular markers and organic aerosol. 2. Biomass smoke, Environ. Sci. Technol., 40, 7811-7819, http://doi.org/10.1021/es060782h, 2006.
Robinson, A. L., Donahue, N. M., Shrivastava, M. K., Weitkamp, E. A., Sage, A. M., Grieshop, A. P., Lane, T. E., Pierce, J. R., and Pandis, S. N.: Rethinking organic aerosols: semivolatile emissions and photochemical aging, Science, 315, 1259-1262, http://doi.org/10.1126/science.1133061, 2007.
Rogers, D. F.: Laminar flow analysis, Cambridge University Press, Edinburgh Building, Cambridge, 422 pp., 1992.
Rogge, W. F., Hildemann, L. M., Mazurek, M. A., Cass, G. R., and Simonelt, B. R. T.: Souces of fine organic aerosol. 1. Charbroilers and meat cooking operations, Environ. Sci. Technol., 25, 1112-1125, http://doi.org/10.1021/es00018a015, 1991.
Rothfuss, N. E., and Petters, M. D.: Characterization of the temperature and humidity-dependent phase diagram of amorphous nanoscale organic aerosols, Phys. Chem. Chem. Phys., 19, 6532-6545, http://doi.org/10.1039/c6cp08593h, 2017.
Rothfuss, N. E.: Toward Better Characterization of the Viscosity of Organic Aerosol, 2019.
Rudich, Y., Talukdar, R. K., Imamura, T., Fox, R. W., and Ravishankara, A. R.: Uptake of NO_3 on KI solutions: rate coefficient for the NO3 + I− reaction and gas-phase diffusion coefficients for NO3, Chem. Phys. Lett., 261, 467-473, http://doi.org/10.1016/0009-2614(96)00980-3, 1996.
Rudich, Y., Donahue, N. M., and Mentel, T. F.: Aging of organic aerosol: bridging the gap between laboratory and field studies, Annu. Rev. Phys. Chem., 58, 321-352, http://doi.org/10.1146/annurev.physchem.58.032806.104432, 2007.
Samaké, A., Jaffrezo, J. L., Favez, O., Weber, S., Jacob, V., Albinet, A., Riffault, V., Perdrix, E., Waked, A., Golly, B., Salameh, D., Chevrier, F., Oliveira, D. M., Bonnaire, N., Besombes, J. L., Martins, J. M. F., Conil, S., Guillaud, G., Mesbah, B., Rocq, B., Robic, P. Y.,

Hulin, A., Le Meur, S., Descheemaecker, M., Chretien, E., Marchand, N., and Uzu, G.: Polyols and glucose particulate species as tracers of primary biogenic organic aerosols at 28 French sites, Atmos. Chem. Phys., 19, 3357-3374, http://doi.org/10.5194/acp-19-3357-2019, 2019.
Schauer, J. J., Kleeman, M. J., Cass, G. R., and Simoneit, B. R. T.: Measurement of emissions from air pollution sources. 3. C-1-C-29 organic compounds from fireplace combustion of wood, Environ. Sci. Technol., 35, 1716-1728, http://doi.org/10.1021/es001331e, 2001.
Schauer, J. J., Kleeman, M. J., Cass, G. R., and Simoneit, B. R. T.: Measurement of emissions from air pollution sources. 5. C-1-C-32 organic compounds from gasoline-powered motor vehicles, Environ. Sci. Technol., 36, 1169-1180, http://doi.org/10.1021/es0108077, 2002.
Schröter, K., and Donth, E.: Viscosity and shear response at the dynamic glass transition of glycerol, J. Chem. Phys., 113, 9101-9108, http://doi.org/10.1063/1.1319616, 2000.
Schwartz, S. E.: Mass-transport considerations pertinent to aqueous phase reactions of gases in liquid-water clouds, in: Chemistry of multiphase atmospheric systems, Springer, Berlin, Heidelberg, Germany, 415-471, http://doi.org/10.1007/978-3-642-70627-1, 1986.
Seinfeld, J. H., and Pandis, S. N.: Atmospheric chemistry and physics: from air pollution to climate change, 3rd ed., John Wiley & Sons, Hoboken, New Jersey, 1152 pp., 2016.
Shiraiwa, M., Garland, R. M., and Pöschl, U.: Kinetic double-layer model of aerosol surface chemistry and gas-particle interactions (K2-SURF): Degradation of polycyclic aromatic hydrocarbons exposed to O_3, NO_2, H_2O, OH and NO_3, Atmos. Chem. Phys., 9, 9571-9586, http://doi.org/10.5194/acp-9-9571-2009, 2009.
Shiraiwa, M., Pfrang, C., and Pöschl, U.: Kinetic multi-layer model of aerosol surface and bulk chemistry (KM-SUB): the influence of interfacial transport and bulk diffusion on the oxidation of oleic acid by ozone, Atmos. Chem. Phys., 10, 3673-3691, http://doi.org/10.5194/acp-10-3673-2010, 2010.
Shiraiwa, M., Ammann, M., Koop, T., and Pöschl, U.: Gas uptake and chemical aging of semisolid organic aerosol particles, Proc. Nat. Acad. Sci. U.S.A., 108, 11003-11008, http://doi.org/10.1073/pnas.1103045108, 2011.
Shiraiwa, M., Pöschl, U., and Knopf, D. A.: Multiphase Chemical Kinetics of NO_3 Radicals Reacting with Organic Aerosol Components from Biomass Burning, Environ. Sci. Technol., 46, 6630-6636, http://doi.org/10.1021/es300677a, 2012.
Shiraiwa, M., and Seinfeld, J. H.: Equilibration timescale of atmospheric secondary organic aerosol partitioning, Geophys. Res. Lett., 39, L24801 http://doi.org/10.1029/2012gl054008, 2012.
Shiraiwa, M., Li, Y., Tsimpidi, A. P., Karydis, V. A., Berkemeier, T., Pandis, S. N., Lelieveld, J., Koop, T., and Pöschl, U.: Global distribution of particle phase state in atmospheric secondary organic aerosols, Nat. Commun., 8, 15002, http://doi.org/10.1038/ncomms15002, 2017a.
Shiraiwa, M., Ueda, K., Pozzer, A., Lammel, G., Kampf, C. J., Fushimi, A., Enami, S., Arangio, A. M., Frohlich-Nowoisky, J., Fujitani, Y., Furuyama, A., Lakey, P. S. J., Lelieveld, J., Lucas, K., Morino, Y., Pöschl, U., Takaharna, S., Takami, A., Tong, H. J., Weber, B., Yoshino, A., and Sato, K.: Aerosol Health Effects from Molecular to Global Scales, Environ. Sci. Technol., 51, 13545-13567, http://doi.org/10.1021/acs.est.7b04417, 2017b.
Slade, J. H., and Knopf, D. A.: Heterogeneous OH oxidation of biomass burning organic aerosol surrogate compounds: assessment of volatilisation products and the role of OH concentration on the reactive uptake kinetics, Phys. Chem. Chem. Phys., 15, 5898-5915, http://doi.org/10.1039/c3cp44695f, 2013.
Slade, J. H., and Knopf, D. A.: Multiphase OH oxidation kinetics of organic aerosol: The role of particle phase state and relative humidity, Geophys. Res. Lett., 41, 5297-5306, http://doi.org/10.1002/2014gl060582, 2014.
Slade, J. H., Shiraiwa, M., Arangio, A., Su, H., Pöschl, U., Wang, J., and Knopf, D. A.: Cloud droplet activation through oxidation of organic aerosol influenced by temperature and particle phase state, Geophys. Res. Lett., 44, 1583-1591, http://doi.org/10.1002/2016gl072424, 2017.
Springmann, M., Knopf, D. A., and Riemer, N.: Detailed heterogeneous chemistry in an urban plume box model: reversible co-adsorption of O_3, NO_2, and H_2O on soot coated with benzo[a]pyrene, Atmos. Chem. Phys., 9, 7461-7479, http://doi.org/10.5194/acp-9-7461-2009, 2009.
Steimer, S. S., Berkemeier, T., Gilgen, A., Krieger, U. K., Peter, T., Shiraiwa, M., and Ammann, M.: Shikimic acid ozonolysis kinetics of the transition from liquid aqueous solution to highly viscous glass, Phys. Chem. Chem. Phys., 17, 31101-31109, http://doi.org/10.1039/c5cp04544d, 2015.
Surratt, J. D., Chan, A. W. H., Eddingsaas, N. C., Chan, M. N., Loza, C. L., Kwan, A. J., Hersey, S. P., Flagan, R. C., Wennberg, P. O., and Seinfeld, J. H.: Reactive intermediates revealed in secondary organic aerosol formation from isoprene, Proc. Nat. Acad. Sci. U.S.A., 107, 6640-6645, http://doi.org/10.1073/pnas.0911114107, 2010.
Tombari, E., and Johari, G. P.: Structural fluctuations and orientational glass of levoglucosan-High stability against ordering and absence of structural glass, J. Chem. Phys., 142, http://doi.org/10.1063/1.4913759, 2015.
Virtanen, A., Joutsensaari, J., Koop, T., Kannosto, J., Yli-Pirila, P., Leskinen, J., Makela, J. M., Holopainen, J. K., Pöschl, U., Kulmala, M., Worsnop, D. R., and Laaksonen, A.: An amorphous solid state of biogenic secondary organic aerosol particles, Nature, 467, 824-827, http://doi.org/10.1038/nature09455, 2010.
Wallace, J. M., and Hobbs, P. V.: Atmospheric science: an introductory survey, 2nd ed., Elsevier, 504 pp., 2006.
Wang, B. B., Lambe, A. T., Massoli, P., Onasch, T. B., Davidovits, P., Worsnop, D. R., and Knopf, D. A.: The deposition ice nucleation and immersion freezing potential of amorphous secondary organic aerosol: Pathways for ice and mixed-phase cloud formation, J. Geophys. Res., 117, http://doi.org/10.1029/2012jd018063, 2012.

Waring, C., King, K. L., Bagot, P. A., Costen, M. L., and McKendrick, K. G.: Collision dynamics and reactive uptake of OH radicals at liquid surfaces of atmospheric interest, Phys. Chem. Chem. Phys., 13, 8457-8469, http://doi.org/10.1039/C0CP02734K, 2011.
Wutz, M.: Theory and practice of vacuum technology, Vieweg, Braunschweig, Germany, 667 pp., 1989.
Yang, Z., Liu, X., Yang, Z., Zhuang, G., Bai, Z., Zhang, H., and Guo, Y.: Preparation and formation mechanism of levoglucosan from starch using a tubular furnace pyrolysis reactor, J. Anal. Appl. Pyrol., 102, 83-88, http://doi.org/10.1016/j.jaap.2013.03.012, 2013.
Zasypkin, A. Y., Grigor'eva, V. M., Korchak, V. N., and Gershenson, Y. M.: A formula for summing of kinetic resistances for mobile and stationary media: I. Cylindrical reactor, Kinet. Catal+. 38, 772-781, 1997.
Zhang, X., McVay, R. C., Huang, D. D., Dalleska, N. F., Aumont, B., Flagan, R. C., and Seinfeld, J. H.: Formation and evolution of molecular products in alpha-pinene secondary organic aerosol, Proc. Nat. Acad. Sci. U.S.A., 112, 14168-14173, http://doi.org/10.1073/pnas.1517742112, 2015.
Zhang, Y., Chen, Y. Z., Lambe, A. T., Olson, N. E., Lei, Z. Y., Craig, R. L., Zhang, Z. F., Gold, A., Onasch, T. B., Jayne, J. T., Worsnop, D. R., Gaston, C. J., Thornton, J. A., Vizuete, W., Ault, A. P., and Surratt, J. D.: Effect of the Aerosol-Phase State on Secondary Organic Aerosol Formation from the Reactive Uptake of Isoprene-Derived Epoxydiols (IEPDX), Environ. Sci. Tech. Let., 5, 167-174, http://doi.org/10.1021/acs.estlett.8b00044, 2018.
Zhang, Y., Nichman, L., Spencer, P., Jung, J. I., Lee, A., Heffernan, B. K., Gold, A., Zhang, Z. F., Chen, Y. Z., Canagaratna, M. R., Jayne, J. T., Worsnop, D. R., Onasch, T. B., Surratt, J. D., Chandler, D., Davidovits, P., and Kolb, C. E.: The Cooling Rate- and Volatility-Dependent Glass-Forming Properties of Organic Aerosols Measured by Broadband Dielectric Spectroscopy, Environ. Sci. Technol., 53, 12366-12378, http://doi.org/10.1021/acs.est.9b03317, 2019.
Zhou, S., Hwang, B. C. H., Lakey, P. S. J., Zuend, A., Abbatt, J. P. D., and Shiraiwa, M.: Multiphase reactivity of polycyclic aromatic hydrocarbons is driven by phase separation and diffusion limitations, Proc. Nat. Acad. Sci. U.S.A., 116, 11658-11663, http://doi.org/10.1073/pnas.1902517116, 2019.
Zhu, C. M., Kawamura, K., and Kunwar, B.: Organic tracers of primary biological aerosol particles at subtropical Okinawa Island in the western North Pacific Rim, J. Geophys. Res., 120, 5504-5523, http://doi.org/10.1002/2015jd023611, 2015.
Ziemann, P. J.: Aerosol products, mechanisms, and kinetics of heterogeneous reactions of ozone with oleic acid in pure and mixed particles, Faraday Discuss., 130, 469-490, http://doi.org/10.1039/b417502f, 2005.
Ziemann, P. J., and Atkinson, R.: Kinetics, products, and mechanisms of secondary organic aerosol formation, Chem. Soc. Rev., 41, 6582-6605, http://doi.org/10.1039/c2cs35122f, 2012.
Zobrist, B., Marcolli, C., Pedernera, D. A., and Koop, T.: Do atmospheric aerosols form glasses?, Atmos. Chem. Phys., 8, 5221-5244, http://doi.org/10.5194/acp-8-5221-2008, 2008.
Zobrist, B., Soonsin, V., Luo, B. P., Krieger, U. K., Marcolli, C., Peter, T., and Koop, T.: Ultra-slow water diffusion in aqueous sucrose glasses, Phys. Chem. Chem. Phys., 13, 3514-3526, http://doi.org/10.1039/c0cp01273d, 2011.

Table 1. Estimated T_g of the applied substrate films. T_g^{exp} is the measured T_g using the poke-flow technique. T_g^{lit} is the literature reported T_g. T_g^{pred} is predicted T_g for mixtures by Gordon-Taylor equation using T_g^{lit} and k_{GT}. k_{GT} is solute specific constant in the Gordon-Taylor equation. D is fragility.

Substrate	T_g^{exp} / K	T_g^{pred} / K	T_g^{lit} / K	k_{GT}	D
Levoglucosan (LEV)	243 ± 4		248 ± 2 [a,h,g]	3.26 [a]	14.1 [b]
Xylitol (XYL)			249 ± 7 [f,g,i]	2.1 [c]	8.65 [b]
LEV/XYL	238 ± 3	249 ± 5			11.3 [d]
Glucose (GLU)	273 ± 3		305 ± 13 [e,g,j]	3.95 [e]	12.1 [b]
1,2,6-Hexanetriol (HEX)			204 ± 6 [f,g,i]	0.88 [e]	13.16 [f]
GLU/HEX	248 ± 3	252 ± 7			12.3 [d]

[a] Lienhard et al. (2012). [b] DeRieux et al. (2018). [c] Elamin et al. (2012). [d] Interpolated values based on mass fraction. [e] Zobrist et al. (2008). [f] Nakanishi et al. (2011). [g] Rothfuss (2019). [h] Tombari and Johari (2015). [i] Dorfmüller et al. (1979). [j] Diogo and Ramos (2008).

Table 2. Comparison of uptake coefficients of NO_3 on liquid and solid substrates of saturated and unsaturated organics.

Surface	Liquid surface		Solid surface	
	T / K	γ_{liquid}	T / K	γ_{solid}
LEV			293	$(4.2\pm0.6)\times10^{-4}$ [a]
LEV			213	$(2.8\pm0.3)\times10^{-4}$ [a]
LEV/XYL	293	$(8\pm2)\times10^{-4}$ [a]	213	$(3.10\pm0.9)\times10^{-4}$ [a]
Glycerol	293	$(1.4\pm0.3)\times10^{-3}$ [b]		
Glycerol	268	$(8.3\pm0.5)\times10^{-4}$ [b]		
1-octanol	258	$(7.1\pm1.6)\times10^{-3}$ [c]	248	$(4.1\pm1.0)\times10^{-3}$ [c]
DES	298	$(4.1\pm0.3)\times10^{-3}$ [b]	263	$(2.5\pm0.2)\times10^{-4}$ [b]
n-Hexadecane	293	$(2.6\pm0.8)\times10^{-3}$ [c]	283-289	$(3.8\pm1.0)\times10^{-4}$ [c]

[a]This study. [b]Gross et al. (2009). [c]Moise et al. (2002).

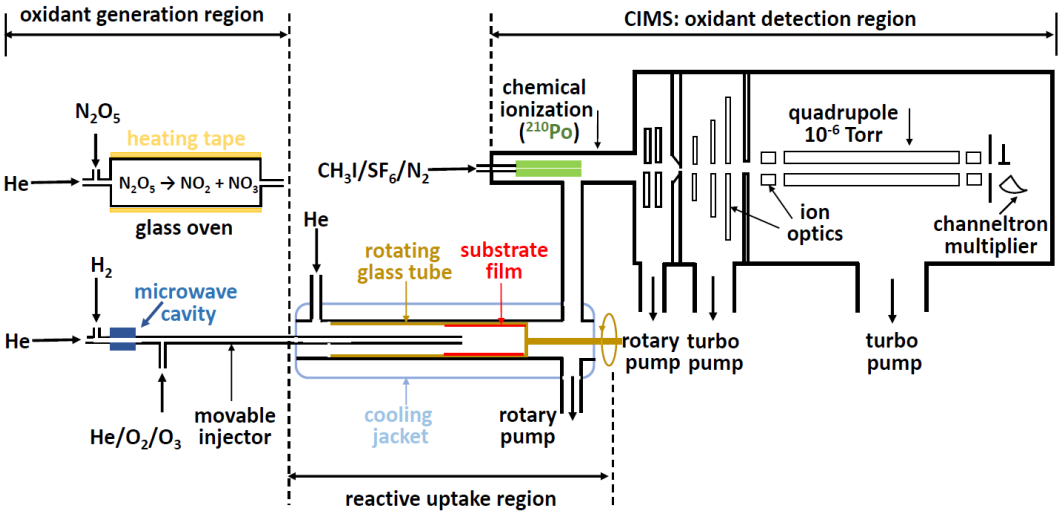

Figure 1: Schematic of the low-temperature coated-wall flow reactor coupled to the chemical ionization mass spectrometer (CIMS). The oxidant generation region displays the generation methods for NO_3 and OH radicals.

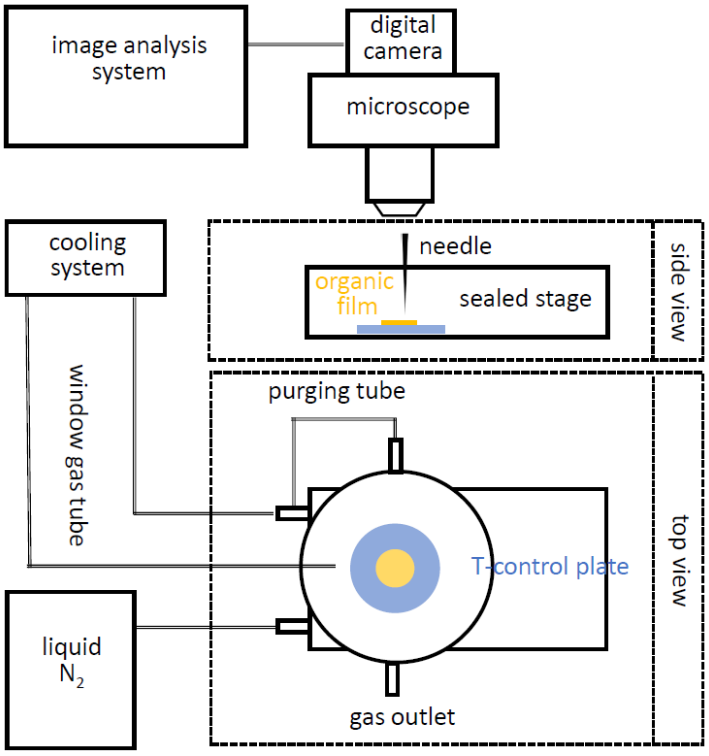

Figure 2. Schematic of the experimental poke-flow setup. This includes a temperature controlled Linkam cooling stage coupled to a microscope equipped with a digital camera and an image analysis system.

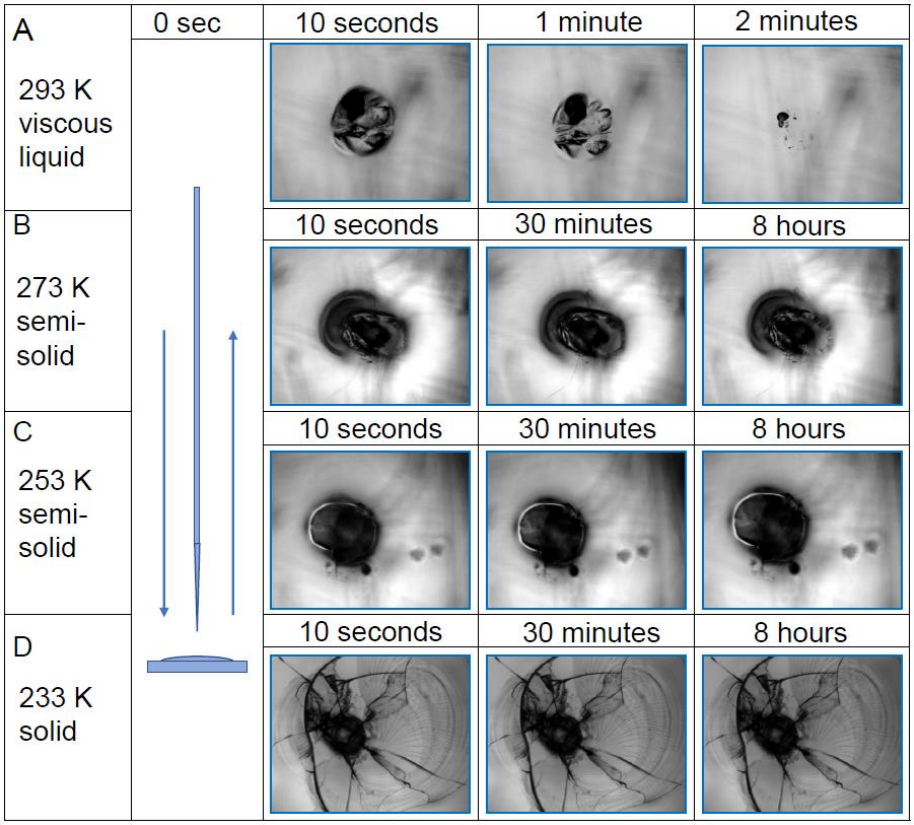

Figure 3. Estimation of the phase state of the film substrate as shown for a GLU/HEX mixture (mass ratio of 4:1). Deformation and recovery were monitored for different time periods due to the poking of the substrate at different temperatures. The microscope images are 200 µm wide.

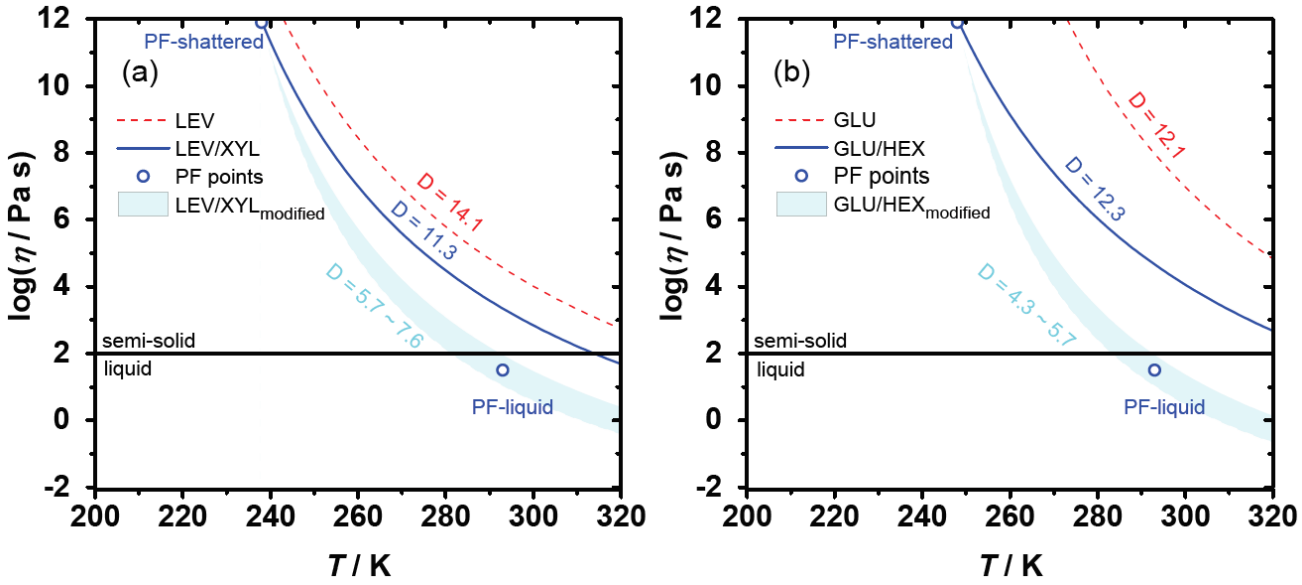

Figure 4. The Angell plot of viscosity as a function of temperature for LEV, LEV/XYL, GLU and GLU/HEX substrates. The lines represent predicted viscosities as a function of T_g^{exp} and applied D values (see Table 1). PF-shattered and PF-liquid (blue circles) indicate the conditions for which the poke-flow (PF) experiment detected a solid (glassy) and liquid phase state of the substrate, respectively. The shaded areas represent predicted viscosities by using the VTF equation with modified D values as indicated in the panels based on the estimated viscosities derived from the poke-flow experiment. The horizontal black line at $\eta = 10^2$ Pa s indicates the threshold of liquid and semi-solid phase states.

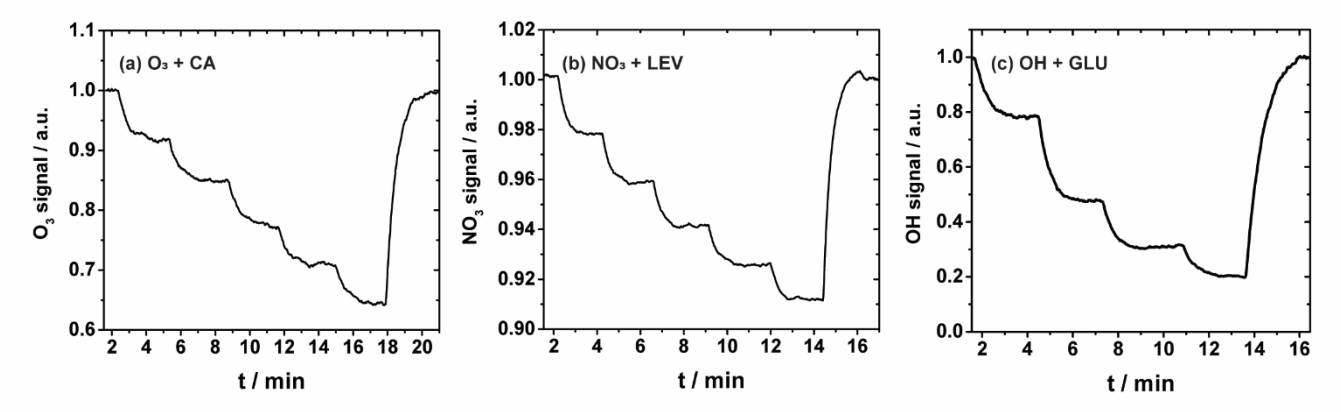

Figure 5. Reactive uptake experiments showing the change in the normalized gas-phase oxidant signal as the reaction time is changed by pulling back the injector incrementally. (a) uptake of O_3 by canola oil (CA); (b) uptake of NO_3 by levoglucosan (LEV); (c) uptake of OH radical by glucose (GLU).

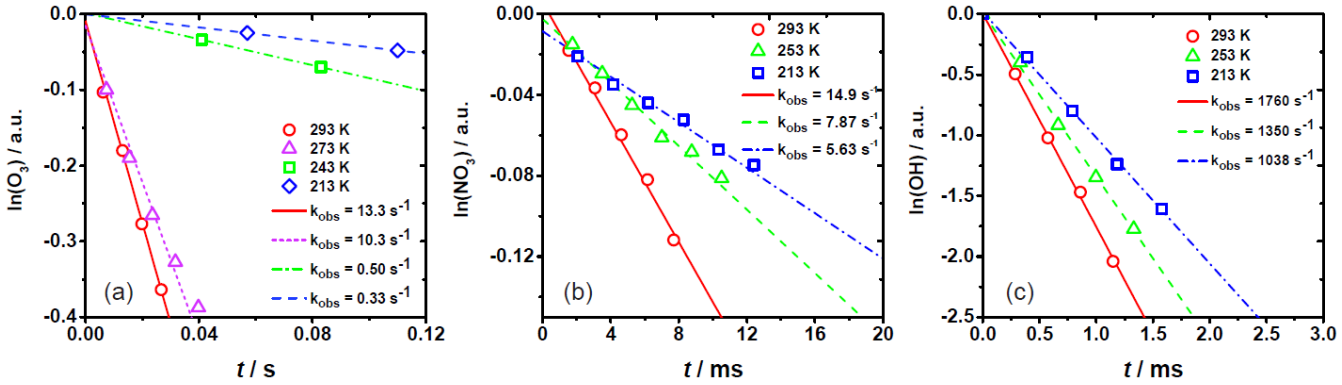

Figure 6. Natural logarithm of the change in gas-phase oxidant signal as a function of reaction time for (a) O_3 uptake by CA, (b) NO_3 uptake by LEV/XYL mixture, and (c) OH uptake by GLU/HEX mixture. Open circles, triangles, squares, and diamonds correspond to uptake measurements at different temperatures. Lines represent the corresponding linear fits to the data and corresponding slopes. k_{obs} values are given in legend.

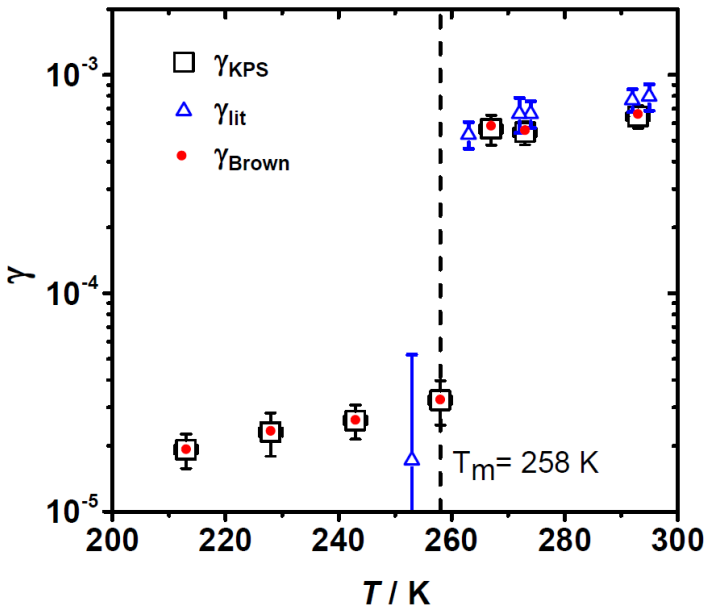

Figure 7. Reactive uptake coefficients of O_3 by canola oil as a function of temperature. Squares and red circles represent γ values derived using the KPS and Brown method, respectively. See text for more details. γ_{lit} represents values reported by de Gouw et al. (1998).

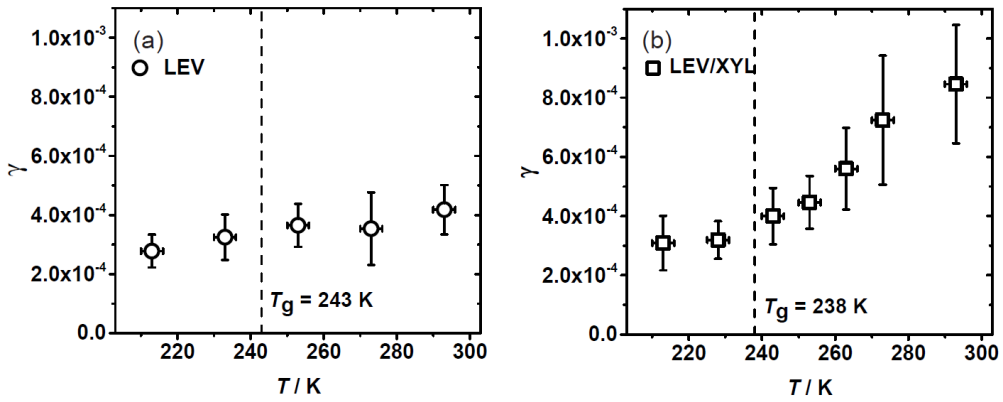

Figure 8. Reactive uptake coefficients, γ, of NO_3 reacting with (a) levoglucosan (LEV) and (b) 1:1 by mass LEV and xylitol (XYL) mixture as a function of temperature. The dashed line represents the glass transition temperature (T_g) measured in the poke-flow experiment.

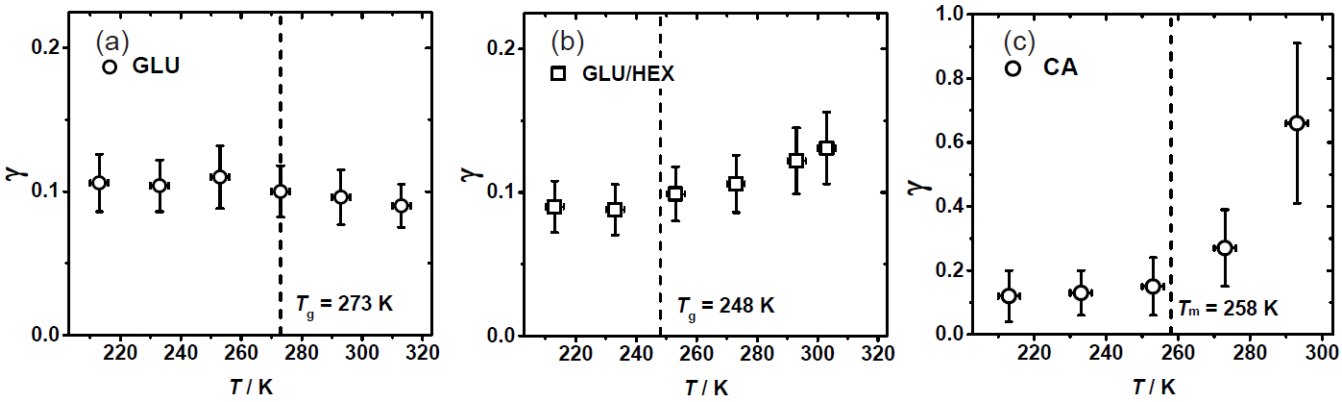

Figure 9. Reactive uptake coefficients, γ, of OH radicals reacting with (a) glucose (GLU), (b) 1:4 by mass glucose and 1,2,6-hexanetriol (GLU/HEX) mixture and (c) canola oil (CA) as a function of temperature. T_g is the glass transition temperature determined in the poke-flow experiment.

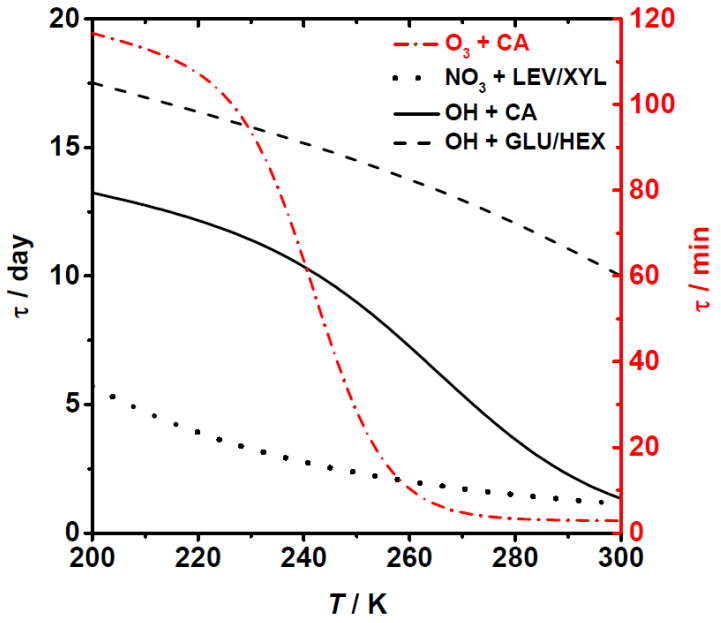

Figure 10. Lifetime estimates of one monolayer of examined OA surrogates for typical background concentrations of O_3, NO_3, and OH. See text for more details.

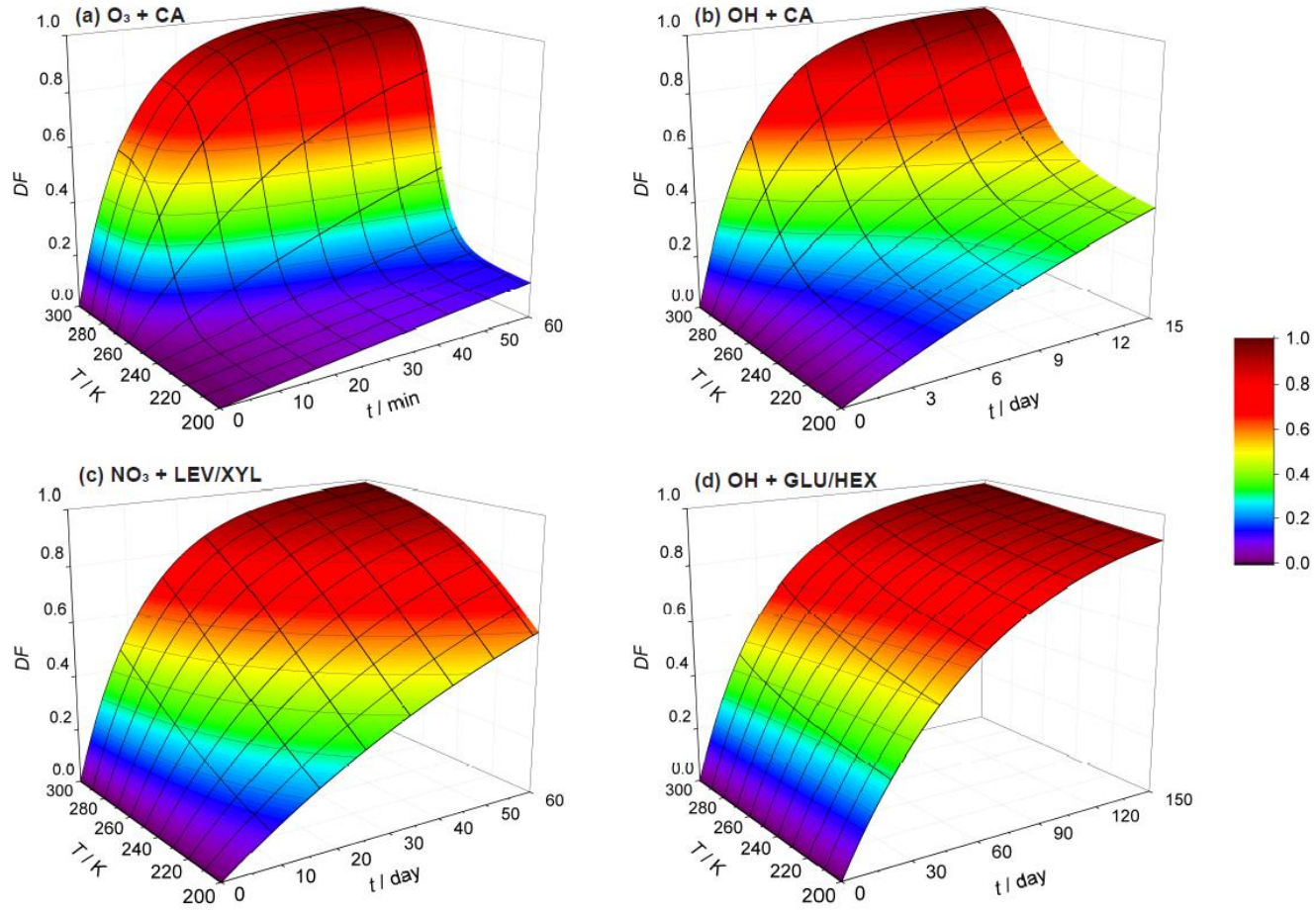

Figure 11. Exposure and temperature dependent particle degraded fraction (DF) for particles 200 nm in diameter for (a) O_3 oxidation of canola oil, (b) OH oxidation of canola oil, (c) NO_3 oxidation of LEV/XYL mixture, and (d) OH oxidation of GLU/HEX mixture. Note the different scales on the time axis.

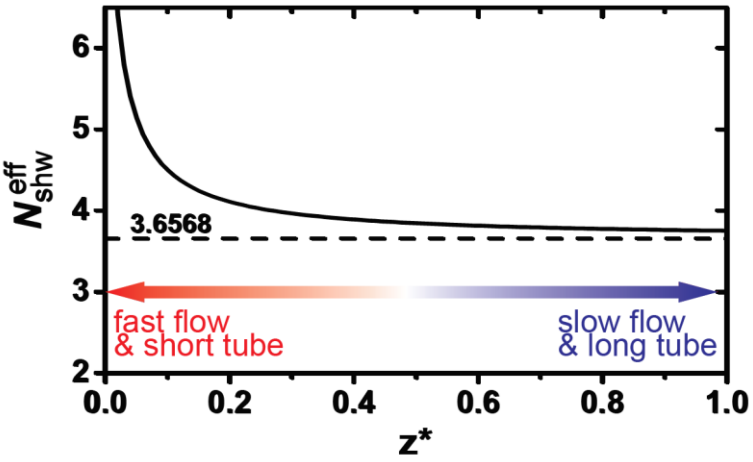

Figure A1. Dependence of the effective Sherwood number ($N_{\mathrm{shw}}^{\mathrm{eff}}$) on the dimensionless axial distance of the flow reactor. Smaller dimensionless axial distance represents the scenario of a fast flow or short tube. Adapted from Davies (2008) and Knopf et al. (2015).

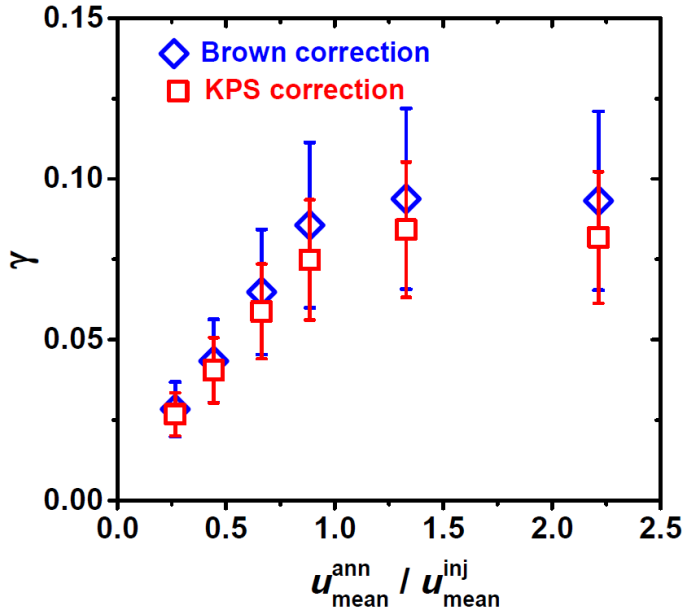

Figure A2. Differences in reactive uptake coefficient (γ) derived from two gas transport correction methods for fast heterogeneous kinetics involving OH uptake by glucose as a function of flow velocity ratio between mean gas flow velocity in the annular section of the flow reactor ($u^{\mathrm{ann}}_{\mathrm{mean}}$) and the gas flow exiting the movable injector ($u^{\mathrm{inj}}_{\mathrm{mean}}$). Red squares and blue diamonds represent KPS and Brown methods, respectively.

Supplemental information

Heterogeneous oxidation of amorphous organic aerosol surrogates by O_3, NO_3, and OH at typical tropospheric temperatures

Jienan Li, Seanna M. Forrester, Daniel A. Knopf

School of Marine and Atmospheric Sciences, Stony Brook University, Stony Brook, NY 11794-5000, USA

Correspondence to: Daniel A. Knopf (Daniel.knopf@stonybrook.edu)

S1. Axial temperature profile in flow reactor

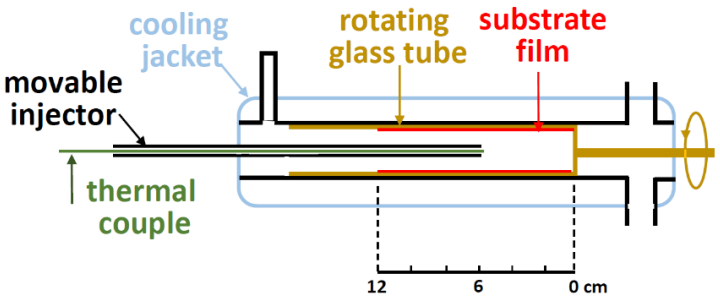

Figure S1. Measurement of the axial temperature in the flow reactor.

The flow reactor is designed to conduct uptake experiments in the temperature range of 313. 15 K to 213.15 K. To ensure minimal axial temperature gradients, we measured the temperature along the flow reactor using a thermocouple wire at the tip of the injector. As the thermocouple is moved in tandem with the movable injector, the temperature along the flow tube axis is recorded. We measured the temperature profile for different flow rates (50, 200, 500, 1000 and 2000 cm^{-3} min^{-1}, STP) at ~293 K, 273 K, 243 K and 213 K. Table A1 shows the temperature values at different distances for the coldest applied temperature (211 K) and corresponding pressures under different flow conditions. As can be seen, for the first 6 cm of the reactive substrate, the temperature is equal within 0.5 K including the fastest applied flows of 2000 cm^{-3} min^{-1} (STP). Significant deviation from desired temperature occurs only beyond 10 cm. For slower flow rates, the flow reactor exhibits uniform temperature. In most of the presented uptake experiments, the total flowrate in the flow reactor is below 1000 cm^{-3} min^{-1} (STP), and thus the temperature change is smaller than 1 K within 10 cm of the reactive film length. Therefore, no significant effects of the temperature gradient on substrate phase state and reaction kinetics are expected.

Table S1. Axial temperature measurements for various flow conditions at T = 211 K. The temperature accuracy is ±0.2 K with a resolution of 0.1 K for all measurements. P_{FR} represents pressure in the flow reactor.

Distance	50 sccm	200 sccm	500 sccm	1000 sccm	2000 sccm
2 cm	211 K	210.9 K	211 K	210.9 K	211 K
4 cm	211 K	211 K	211 K	210.9 K	211.3 K
6 cm	211 K	211 K	211 K	211 K	211.7 K
8 cm	211 K	211 K	211 K	211.1 K	212.5 K
10 cm	211 K	211 K	211 K	211.5 K	215 K
12 cm	211 K	211.1 K	211.5 K	213.8 K	222.1 K
P_{FR}	2.16 hPa	1.7 hPa	2.32 hPa	3.54 hPa	5.44 Pa

S2. Measurement of the water content in the organic substrate films

The water content in the organic film substrate was determined using an ultra-microbalance with an accuracy of 0.2 µg (Mettler Toledo XP2U). Six drops of water/organic solution are applied to a glass slide with a 2 µL pipette. After drying the droplets following the same procedure as film preparation in the uptake experiments, the thickness of the resulting films is about 50-100 µm, like the film substrates in the uptake experiments. The film thickness can be measured using a microscope. The water content is derived by the mass difference before and after the drying procedure, expressed by the following equation:

$$w\% = \frac{m_{\text{final}} - m_{\text{initial}} \times R_{\text{org}}}{m_{\text{final}}} \times 100\% \,, \qquad \text{(S1)}$$

where m_{final} is the mass of the substrate film after the drying procedure, m_{initial} is the initial mass of the solution drops, and R_{org} is the initial mass ratio of the organic component to water in the solution. Levoglucosan, glucose and xylitol are non-volatile. The vapor pressure of 1,2,6 hexanetriol is ~ $(3.82 \pm 1.16) \times 10^{-4}$ Pa (Lv et al., 2019) and thus can be ignored compared to water with a vapor pressure of 2.34 kPa at 293.15 K. As shown in Table S2, the water content of applied films ranges from (10.33±0.54) % to (16.02±0.79) % at room temperature, indicating that water molecules can still be trapped in the substrate films after the drying process.

Table S2. Estimated water concentration in the applied substrate films.

substrate	Initial solute concentration / wt%	Organic mass ratio	Estimated water content / wt%
LEV	5	1	13.6±0.3
LEV/XYL	5	1:1	16.0±0.8
GLU	10	1	13.2±1.6
GLU/HEX	10	4:1	13.8±1.2

Table S3. Water concentration in the levoglucosan film substrates. Five samples are evaluated resulting in an average water content of 13.56 wt% and standard deviation σ = 0.33 wt%.

#	m_{final} / mg	m_{initial} / mg	R_{org}	Concentration / wt%
	0.6766	11.6577	0.05	13.85
2	0.7105	12.2391	0.05	13.87
3	0.7259	12.5564	0.05	13.51
4	0.7009	12.1216	0.05	13.52
5	0.6864	11.9375	0.05	13.04

Table S4. Water concentration in LEV/XYL film substrates with mass ratio of 1:1. Five samples evaluated resulting in an average water content of 16.02 wt% and standard deviation σ = 0.79 wt%.

#	m_{final} / mg	$m_{initial}$ / mg	R_{org}	Concentration / wt%
1	0.7262	12.0218	0.05	17.22
2	0.6929	11.6323	0.05	16.06
3	0.7028	11.9386	0.05	15.06
4	0.7229	12.1855	0.05	15.72
5	0.7114	11.9457	0.05	16.04

Table S5. Water concentration in film substrates of glucose. Six samples are evaluated resulting in an average water content of 13.17 wt% and standard deviation σ = 1.58 wt%.

#	m_{final} / mg	$m_{initial}$ / mg	R_{org}	Concentration / wt%
1	1.4208	12.0855	0.1	14.94
2	1.4000	12.2318	0.1	12.63
3	1.4599	12.4411	0.1	14.78
4	1.4371	12.3182	0.1	14.28
5	1.3754	12.1838	0.1	11.42
6	1.3738	12.2300	0.1	10.98

Table S6. Water concentration in substrate films of GLU/HEX with mass ratio of 1:4. Five samples are evaluated resulting in an average water content of 13.84 wt% and standard deviation σ = 1.24 wt%.

#	m_{final} / mg	$m_{initial}$ / mg	R_{org}	Concentration / wt%
1	1.4837	12.4658	0.0999	15.98
2	1.4070	12.1748	0.0999	13.47
3	1.4224	12.3041	0.0999	13.50
4	1.4757	12.5525	0.0999	14.94
5	1.4701	12.8476	0.0999	12.61
6	1.4634	12.8002	0.0999	12.53

S3. Glass transition estimation using the poke-flow technique

T_g can be estimated by monitoring the flowing and shattering of the substrate films while lowering the temperature of the substrate. From a starting temperature T which is slightly higher (e.g., 10 K) than the predicted T_g, we poke the film to determine its phase. If the film does not shatter, the temperature of the cell is lowered by 3 K. After 5 mins at this new temperature, the substrate is poked again to monitor potential shattering. For each substrate, we examined the phase state at least six times and calculated the average to yield the estimated T_g value. Structures in Figs. S2-S7 that are not in focus are from minor superficial scratches of the silver sample holder within the temperature-controlled cooling stage. Figures S2 and S3 show images of shattering substrates and corresponding T_g estimates for GLU and GLU/HEX substrate mixtures.

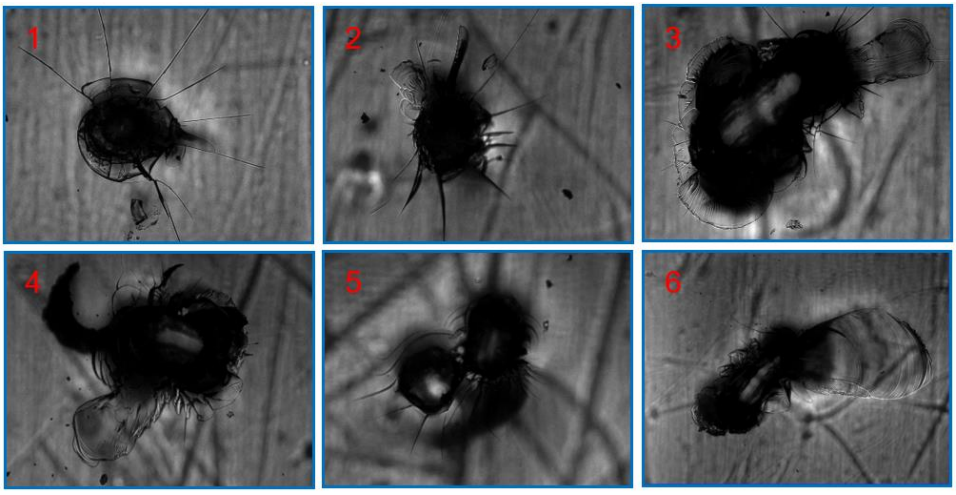

Figure S2. T_g estimation using poke-flow technique. Shattering of GLU films. The shattering temperatures are 277 K, 273 K, 271 K, 272 K, 275 K, 270 K. The average is (273 ± 2) K.

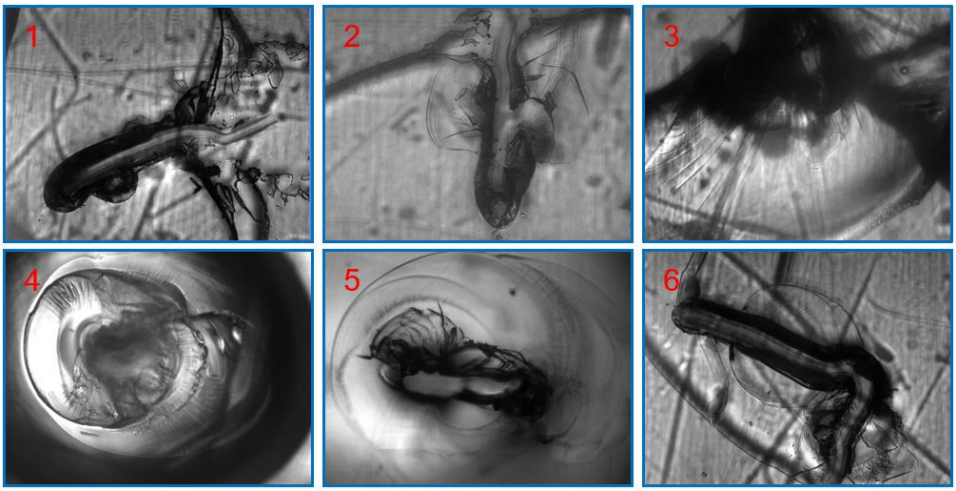

Figure S3. T_g estimation using poke-flow technique. Shattering of GLU/HEX mixture with a mass ratio of 4:1. The shattering temperatures are 247 K, 247 K, 244 K, 253 K, 248 K, 249 K. The average is (248 ± 3) K.

The LEV substrates exhibit more complicated morphological and solidification characteristics. In Fig. S4, in image 1 the film surface is in focus whereas in image 2 the bottom of the substrate is in focus. Those two images demonstrate that the film is transparent. In Fig. S4, image 3, the film was poked and displays semi-solid properties at 293 K. One hour later (much longer than the duration of the uptake experiments), the dent is still unchanged as is visible in image 4. Figure S4, image 5, displays crystallization while being poked at 260 K. The crystallization proceeds into the surrounding substrate as displayed in image 6 (10 seconds later). In summary, the LEV substrates exhibit a semi-solid or solid phase state in our studied temperature range from 213 K to 293 K. The glass transition mechanism of LEV is beyond the scope of this study and is thoroughly discussed by (Tombari and Johari, 2015) and Lienhard et al. (2012).

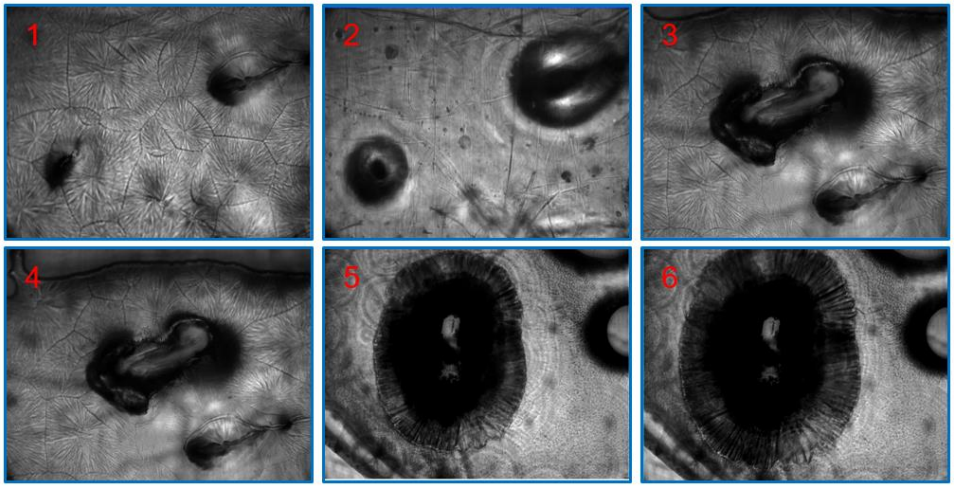

Figure S4. Morphology of LEV at 293 K. Image 1 focuses on film top and image 2 focuses on film bottom. Image 3: substrate poked at 293 K, image 4: the same substrate as image 3 after 1 hour. Image 5: crystallization occurred after poking, image 6: the same substrate as image 5 after 10 s.

Figure S5 displays the highest temperatures under which we observed the shattering of the LEV substrate film yielding T_g = (243 ± 4) K. Figure S5, image 6, shows crystallization of the glassy film presented in image 5 upon warming. Figures S6 and S7 show the poke-flow experiments for LEV/XYL substrate mixtures. In Fig. S6 at 293 K, the LEV/XYL substrate film recovers quickly within 1 min, exhibiting enhanced flow characteristics compared to GLU/HEX films. Figure S7 displays the shattering of the LEV/XYL substrate at temperatures around T_g = (238 ± 3) K.

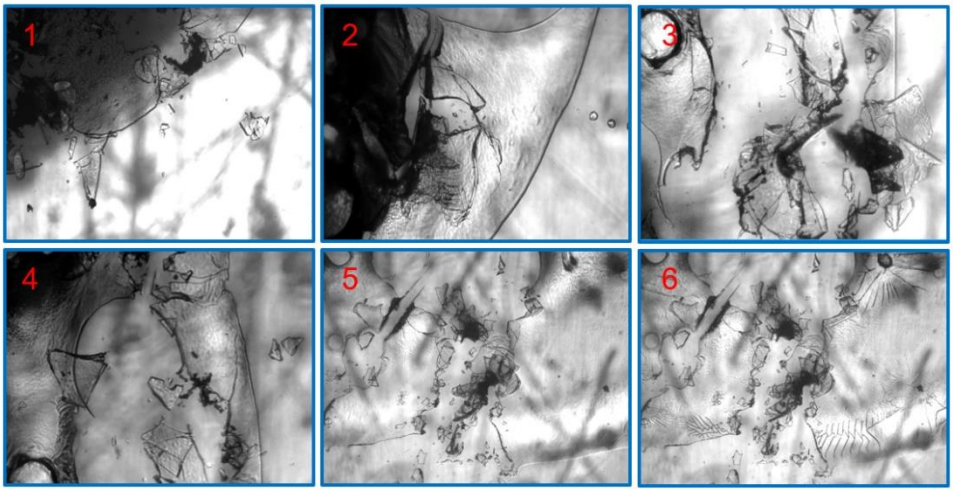

Figure S5. T_g estimation using poke-flow technique. Shattering of LEV in images 1-5. The shattering temperatures are 244 K, 239 K, 237 K, 245 K, 248 K. The average is (243 ± 4) K. Image 6 shows crystallization of substrate film in image 5 upon warming.

140

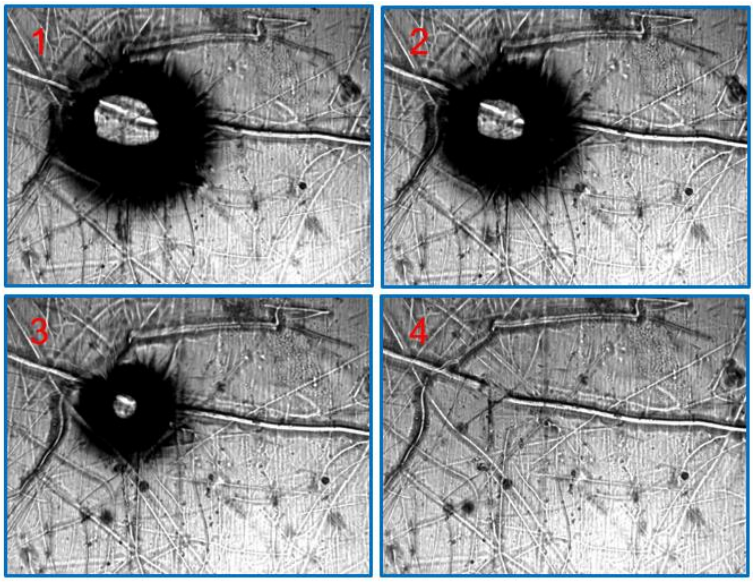

Figure S6. Morphology of LEV/XYL at 293 K. After poking by a needle, the film recovered quickly within about 1 min, indicating that the film was in a liquid phase state.

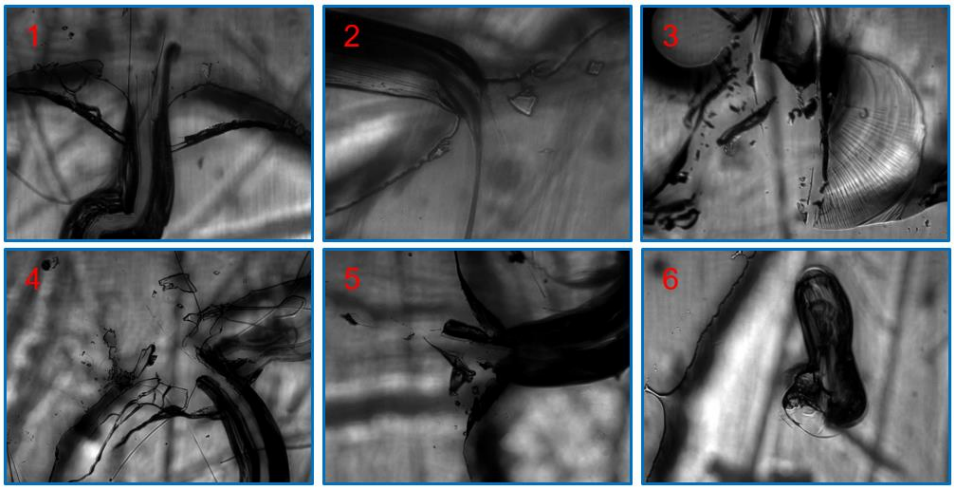

Figure S7. T_g estimation using the poke-flow technique. Shattering of LEV/XYL mixture with a mass ratio of 1:1. The shattering temperatures are 237 K, 236 K, 233 K, 237 K, 240 K, 243 K. The average is (238 ± 3) K.

S4 Surface coverage fraction of unoxidized reaction sites

The fraction of the unoxidized reaction sites (F) on the film surface can be estimated by using the equation below (Bertram et al., 2001):

$$F = \exp\left(\frac{\gamma Z t}{N_{\mathrm{tot}}}\right), \qquad \text{(S2)}$$

where γ represents the uptake coefficient, Z is the collision frequency of the gas oxidant with the surface (molecules $\mathrm{cm^{-2}s^{-1}}$) defined as $Z = [\mathrm{X}]_g \cdot \frac{\omega_X}{4}$, (Pöschl et al., 2007). t is reaction time and N_{tot} is the number concentration of reactive sites ($\mathrm{cm^{-2}}$).

When the substrate films are liquid, the surface can be assumed to be always replenished under our experimental conditions. However, when the substrate films are solid or semi-solid, γ may be affected by surface saturation effects, i.e., during the experiment time a significant fraction of the surface reactants are lost. This effect can be avoided either by lowering the oxidant concentration or by shortening the exposure time. A typical reaction time in uptake experiments ranges from 5 to 18 min. As shown in Table S7 below, under the experimental conditions, the substrate surfaces can be considered as fresh surfaces during the reactive uptake kinetics studies. The number concentration of reactive sites is assumed to be 1×10^{15} $\mathrm{cm^{-2}}$ based on the average number of surface reactive sites (Bertram et al., 2001;Shiraiwa et al., 2012). Less than 5% of the substrate

surface area will be oxidized in presented uptake experiments, thus, implying negligible impact of surface saturation effects on the derived kinetics.

Table S7. Estimation of the degree of substrate surface oxidation under typical experimental conditions. Reactive uptake coefficient (γ), gas-phase oxidant concentration $[X]_g$ exposure time (t), number concentration of reactive sites (N_{tot}) and fraction of unoxidized reaction sites (F) are given.

oxidant	γ	$[X]_g$ / molecules cm^{-3}	t / min	N_{tot} / cm^{-2}	F / %
O_3	3×10^{-5}	3×10^{11}	18	1×10^{15}	91.6
NO_3	8×10^{-4}	1×10^{10}	18	1×10^{15}	93.4
OH	0.2	3×10^{7}	18	1×10^{15}	90.6

References

Bertram, A. K., Ivanov, A. V., Hunter, M., Molina, L. T., and Molina, M. J.: The reaction probability of OH on organic surfaces of tropospheric interest, J. Phys. Chem. A, 105, 9415-9421, http://doi.org/10.1021/jp0114034, 2001.

Lienhard, D. M., Bones, D. L., Zuend, A., Krieger, U. K., Reid, J. P., and Peter, T.: Measurements of thermodynamic and optical properties of selected aqueous organic and organic-inorganic mixtures of atmospheric relevance, J. Phys. Chem. A, 116, 9954-9968, http://doi.org/10.1021/jp3055872, 2012.

Lv, X. J., Chen, Z., Ma, J. B., and Zhang, Y. H.: Volatility measurements of 1, 2, 6-hexanetriol in levitated viscous aerosol particles, J. Aerosol Sci, 138, http://doi.org/10.1016/j.jaerosci.2019.105449, 2019.

Pöschl, U., Rudich, Y., and Ammann, M.: Kinetic model framework for aerosol and cloud surface chemistry and gas-particle interactions–Part 1: General equations, parameters, and terminology, Atmos. Chem. Phys., 7, 5989-6023, http://doi.org/acp-7-5989-2007, 2007.

Shiraiwa, M., Poschl, U., and Knopf, D. A.: Multiphase Chemical Kinetics of NO_3 Radicals Reacting with Organic Aerosol Components from Biomass Burning, Environ. Sci. Technol., 46, 6630-6636, http://doi.org/10.1021/es300677a, 2012.

Tombari, E., and Johari, G. P.: Structural fluctuations and orientational glass of levoglucosan-High stability against ordering and absence of structural glass, J. Chem. Phys., 142, http://doi.org/10.1063/1.4913759, 2015.